國立臺灣大學醫學院暨工學院醫學工程研究所

博士論文

Institute of Biomedical Engineering

College of Medicine and College of Engineering

National Taiwan University

Doctoral Dissertation

利用質譜技術研究毛囊幹細胞的磷酸化蛋白質體

Investigation of phosphoproteome of hair follicle stem cells via mass spectrometry technique

王維宏

Wei-Hung Wang

指導老師：林頌然 博士

Advisor：Dr. Sung-Jan Lin

中華民國 107 年 2 月

February, 2018

doi:10.6342/NTU201800580

中文摘要

對再生醫學而言，如何調控器官其內的幹細胞以維持器官的恆定或是快速修復受損的組織，是非常重要的課題。成體幹細胞廣泛分佈人體各個器官，這些幹細胞往往分佈於組織器官的某個特定環境或部位(niche)，以利接受外來環境所給予的訊號並做出反應。目前已知同一個器官內的幹細胞，可以是具備不同的性質，根據組織恆定或受傷後再生修補的需要，做出適當的反應。毛囊是一個迷你器官，在一生中不斷週期性再生，目前已知其內具有性質不同的幹細胞且具有其特殊的活化及再生能力。裝備態幹細胞(primed stem cell)以及靜態幹細胞(quiescent stem cell) ，分別座落於毛囊內的次級毛胚(secondary hair germ)及突部(bulge)。相較於靜態幹細胞，裝備態幹細胞較容易快速活化，以加速毛囊再生，並負責分化出生長期毛囊的結構。而靜態幹細胞則較不容易活化及分化，主要負責維持幹細胞數量上的恆定。這樣的特性使毛囊成為研究不同族群幹細胞調控的重要模型。而蛋白質分子的磷酸化是調控細胞活性的重要途徑，這種磷酸化的過程(phosphorylation cascade)最後將會影響到細胞核內表觀遺傳學(epigenetics)或是轉錄(transcription)上的變化。

在我們的研究當中，我們先利用毛囊幹細胞中特異性表現之表面抗原分選並純化出裝備態幹細胞以及靜態幹細胞，再透過蛋白質譜與磷酸化蛋白質譜的方法分析在休止期和生長期早期的毛囊幹細胞的表現量與磷酸化程度。透過這些蛋白質分子表現量與磷酸化程度之差異，我們可以得知這兩群細胞在休止及活化時，是否因其訊息調控的不同，而造成這兩群細胞在行為上的差異。我們發現裝備態幹細胞在從休止期到活化期的過程當中，蛋白質表現量與磷酸化差異的程度比靜態幹細胞大。藉由分析這些磷酸化分子之間的交互作用，我們發現促使毛囊生長的Wnt signaling其下游分子與mTORC1之間可能有所關聯。而從組織染色上來看，

doi:10.6342/NTU201800580

mTORC1 的活化與毛囊幹細胞的動態在時間上之重疊性非常的高。因此我們假設 mTORC1 可能是調控毛囊幹細胞活化的重要途徑。

為了證實 mTORC1 在毛囊幹細胞活化之角色，我們利用 mTORC1 的小分子抑制劑進行功能性的分析，結果發現在毛囊幹細胞活化前抑制 mTORC1 的活性會延後毛囊幹細胞活化的時程，若是在毛囊幹細胞活化了之後再給予 mTORC1 的抑制劑則不會對於毛髮的生長產生結構性的影響。利用基因剃除鼠進行功能性分析時也可以得到延遲毛囊幹細胞活化的效果。因此我們證實 mTORC1 在活化毛囊幹細胞扮演一個很重要的角色，讓毛囊幹細胞可以在適當的時間上活化。這個功能性的分析也同時證實了磷酸化蛋白體可以為幹細胞研究提供更多有用的資訊。

雖然 mTORC1 並不會抑制進入生長期的毛髮生長，但我們發現 mTORC1 的抑制會增強 γ 射線對生長期毛囊所造成的輻射傷害。使得生長期內的毛囊發生更大量的細胞凋亡，並且對於修復性的增生也有抑制的作用。在這雙重影響之下，造成毛囊分化結構的破壞以及生長期落髮。因此 mTORC1 在毛囊中扮演著非常重要的角色: 1. 調控毛囊幹細胞的活化 2. 調控細胞對於輻射傷害的修復。

關鍵字：毛髮週期、裝備態幹細胞、磷酸化蛋白質體、mTORC1、輻射傷害

doi:10.6342/NTU201800580

ABSTRACT

How an organ regulates its stem cells to maintain homeostasis or to quickly regenerate damaged tissues is vital to the maintenance of organ functions. Adult stem cells are often located in designated niches and their behavior is tightly regulated by the niche environment. It has been demonstrated that stem cells of an organ are not identical and can be composed of heterogeneous cellular populations of cells to meet to specific needs for homeostasis maintenance or for repair of damaged tissues. Hair follicle, a miniorgan with life-long cyclic regeneration, provides an excellent model to study the behaviors of stem cells during tissue regeneration. Specifically, it harbors primed stem cells and quiescent stem cells in secondary hair germ and bulge, respectively. Compared with quiescent stem cells, primed stem cells are activated faster and they regenerate the most part of the growing follicles. In contrast, quiescent stem cells are shown to be activated slowly and are responsible for the long-term maintenance of stem cells. There properties make HF as an important model for investigating the regulation of HFSC heterogeneity. The modulation of instructive or repressive signals is depended on protein phosphorylation toward downstream targets, and the phosphorylation cascade would finally affect the epigenetics or transcription.

In our study, we sorted out the pSCs and qSCs by the specific expressed surface

doi:10.6342/NTU201800580

marker by FACS. Then, with the help of mass spectrometry technique, we can analyze the degree of protein abundance and protein phosphorylation in different HFSC populations and in different hair cycle stages. Via the proteome and phosphoproteome analysis, we can reveal if the signaling molecules could lead to the difference in behavior during the activation of the two HFSCs population. We found that the difference in protein abundance and phosphorylation were dramatically increased in pSCs, and the downstream of wnt signaling might have the correlation with mTORC1 signaling. From histology, the activation of mTORC1 is correlated with the dynamic of activation of HFSCs. Thus, we hypothesize mTORC1 might play an important role in regulating the activation of HFSCs.

To address the possible role of mTORC1 in HFSCs, we use the mTORC1 inhibitor for further investigation. Activation of HFSCs could be hampered and delayed with mTORC1 inhibition. Once HFSCs were activated and the HF entered the growing phase, the mTORC1 inhibitor was unable to affect hair growth in this stage. The genetic ablation of *raptor* gene yielded to similar results. Thus, we can concluded that mTORC1 has an influence on activation of HFSCs in a timely dependent manner. Besides, our data showed that the proteome and phosphoproteome analysis could shed light on further stem cell research.

doi:10.6342/NTU201800580

Although the inactivation of mTORC1 did not perturb the hair growth in anagen, but we found that the mTORC1 inhibition increased the sensitivity of damage form r-ray irradiation, leading to more extensive apoptosis and less regenerative proliferation. Therefore, mTORC1 suppression aggravated radiation-induced anagen effluvium. Taken together, our study revealed that mTORC1 plays an important role in activating HFSCs and attenuating irradiation-induced follicular damage.

Keywords: hair cycle, primed stem cells, phosphoproteome, mTORC1, radiation damage

doi:10.6342/NTU201800580

LIST OF ABBREVIATIONS

1.	ASC	Adult stem cell
2.	HF	Hair follicle
3.	HS	Hair shaft
4.	IFE	Interfollicular epidermis
5.	BgSC	Bulge stem cell
6.	2^{nd} HG	Secondary hair germ
7.	DPC	Dermal papilla cell
8.	IRS	Inner root sheath
9.	ORS	Outer root sheath
10.	TAC	Transit amplifying Cell
11.	LRC	Label retaining cell
12.	iTRAQ	Isobaric tags for relative and absolute quantification
13.	SILAC	Stable isotope labeling with amino acids in cell culture
14.	TMT	Tandem mass tag
15.	mTORC1	Mammalian target of rapamycin complex 1
16.	IR	Ionizing radiation
17.	PTM	Post-translational modification

doi:10.6342/NTU201800580

18. DSB Double-strand break

19. HR Homologous recombination

20. NHEJ Non-homologous end joining

21. TAM Tamoxifen

doi:10.6342/NTU201800580

CONTENTS

doi:10.6342/NTU201800580

doi:10.6342/NTU201800580

doi:10.6342/NTU201800580

doi:10.6342/NTU201800580

LIST OF FIGURES

doi:10.6342/NTU201800580

doi:10.6342/NTU201800580

doi:10.6342/NTU201800580

Chapter 1 Introduction

Adult stem cells (ASCs) often reside in specified niches where stem cell activity is tightly controlled to maintain physiological homeostasis and to regenerate lost tissue after injury (Tumbar, Guasch et al. 2004, Wagers and Weissman 2004, Moore and Lemischka 2006, Lin, Foley et al. 2013). Recent studies suggest that ASCs might exist in two distinct status: the less active, quiescent stem cells (qSCs) and the relative active, primed stem cells (pSCs) (Li and Clevers 2010, Blanpain and Fuchs 2014). Understanding how stem cell activities are controlled is pivotal to decipher how stem cell activity is coordinated to meet local tissue needs as well as to developing therapeutic strategies to facilitate tissue regeneration from injuries. Hair follicle stem cells (HFSCs) provide an excellent model for investigating the differences between pSCs and qSCs due to its distinct behavior between activated and inactivated state. The profile of transcriptome, epigenetic modification, and super-enhancer of HFSCs were analyzed by microarray or ChIP-sequencing (Tumbar, Guasch et al. 2004, Lien, Guo et al. 2011, Genander, Cook et al. 2014, Adam, Yang et al. 2015). However, the information of protein expression and post-translational modification (PTM) has not been validated. Proteomic and phosphoproteomic analysis of tissue stem cells has been widely employed in cultured stem cells (Olsen, Blagoev et al. 2006, Brill, Xiong et al.

doi:10.6342/NTU201800580

2009, Hutchins and Robson 2009, Van Hoof, Munoz et al. 2009). Though such analysis has helped to gain new knowledge about the complicated regulatory network in stem cells, it might not represent the *in vivo* profile of the proteome and phosphoproteome of stem cells. To investigate the dynamic change of proteome and phosphoproteome in HFSCs, we must start from the dynamics of anatomy of hair cycle.

1.1 Hair follicle structure and hair cycle

HFs can undergo life-long cyclic growth including growing phase (anagen), dystrophic phase (catagen), and resting phase (telogen) (Chase, Montagna et al. 1953, Chase 1954). In murine model, the hair cycle remained synchronized throughout the dorsal skin in the first two cycles, but then the hair cycle develops the un-synchronized hair domain (Muller-Rover, Handjiski et al. 2001, Plikus and Chuong 2008). The structure of HFs varied from different hair cycle stage (Muller-Rover, Handjiski et al. 2001, Stenn and Paus 2001, Paus and Foitzik 2004) , so we can tell the hair cycle from the structure of HFs.

1.1.1 Structure of the hair follicle

The HF presents a concentric cylinder structure from the cross-section, but from the longitudinal sections, the pilo-sebaceous unit is constituted of sebaceous gland, bulge, outer root sheath (ORS), inner root sheath (IRS), medulla,, hair bulb, and dermal

doi:10.6342/NTU201800580

papilla cells (DPCs) (Chase, Montagna et al. 1953, Chase 1954). The infundibulum and isthmus connect the interfollicullar epidermis (IFE) and the HFs, and provide the canal for hair shaft to protrude out of the skin.

1.1.1.1 Interfollicullar epidermis

The interfollicullar epidermis (IFE) is consisted by basal keratinocyte that can differentiate into the transient-amplifying suprabasal layer and terminal differentiated cornified layer. The IFE can not only precede skin barrier function to hinder the physical and chemical stimuli, but also prevent the water and temperature loss from the body. The histology shows that the basal cells reside in the IFE, infundibulum, isthmus, and HFs. The basal cells in IEF, infundibulum and isthmus can be characterized as integrin alph6^{+} and Sca-1^{+} population, which can be separated with follicular cells (Jensen, Yan et al. 2008, Chang, Pasolli et al. 2013).

1.1.1.2 Bulge: the niche of quiescent HFSCs

The bulge region is an anatomical protrusion portion located in the lower part of dermis which is the permanent portion during the hair cycle. The label-retaining cells (LRCs), or the so called bulge stem cells (BgSCs) reside in this bulge region (Cotsarelis, Sun et al. 1990, Tumbar, Guasch et al. 2004). In murine skin, the arretor pili muscle attach to the bulge region due to the expression of nephronectin which guides the

doi:10.6342/NTU201800580

smooth muscle precursor cell to attach to the bulge region (Fujiwara, Ferreira et al. 2011). In the telogen HFs, a small group of cells between bulge and dermal papilla cells, term "secondary hair germ" (2nd HG), can contribute to the TACs to regenerate a mature HFs (Rompolas, Mesa et al. 2013). In physiological condition, the BgSCs remain slow cycling and undifferentiated, even in the anagen (Greco, Chen et al. 2009). Bulge cells are endowed with multipotency and can differentiate into sebocytes, outer-root sheath (ORS), and interfollicular epidermal keratinocytes (Morris, Liu et al. 2004).

1.1.1.3 Hair bulb

The lowermost portion of anagen HF is termed "hair bulb", which is the most important part for generating hair fibers. According to the traffic light model, the basal cells in the ORS can contribute to the hair bulb and become the matrix cells, which are composed by TACs (Ma, Liu et al. 2003, Hsu, Pasolli et al. 2011, Hsu, Li et al. 2014). These TACs can undergo rapid proliferation and differentiate into IRS, and make the mature hair shaft (HS) protruding out of the epidermis.

1.1.1.4 Dermal papilla cells

DPCs reside in the lowermost portion in the telogen, and are encompassed by the matrix cell in the anagen. The DPCs are considered as a group of specialized fibroblast cells that can interact with HFSCs (in telogen) or matrix cells (in anagen) to develop the

doi:10.6342/NTU201800580

mature HFs (Jahoda, Horne et al. 1984, Rompolas, Mesa et al. 2013). It is believed that the inductive signals were secreted by DPCs to activate HFSCs, such as Wnt and TGF-β (Shimizu and Morgan 2004, Rendl, Lewis et al. 2005, Greco, Chen et al. 2009, Oshimori and Fuchs 2012). By laser ablation of DPCs, the proliferation of HFSCs ceased (Rompolas, Deschene et al. 2012), which demonstrated the inductive effect of DPCs.

doi:10.6342/NTU201800580

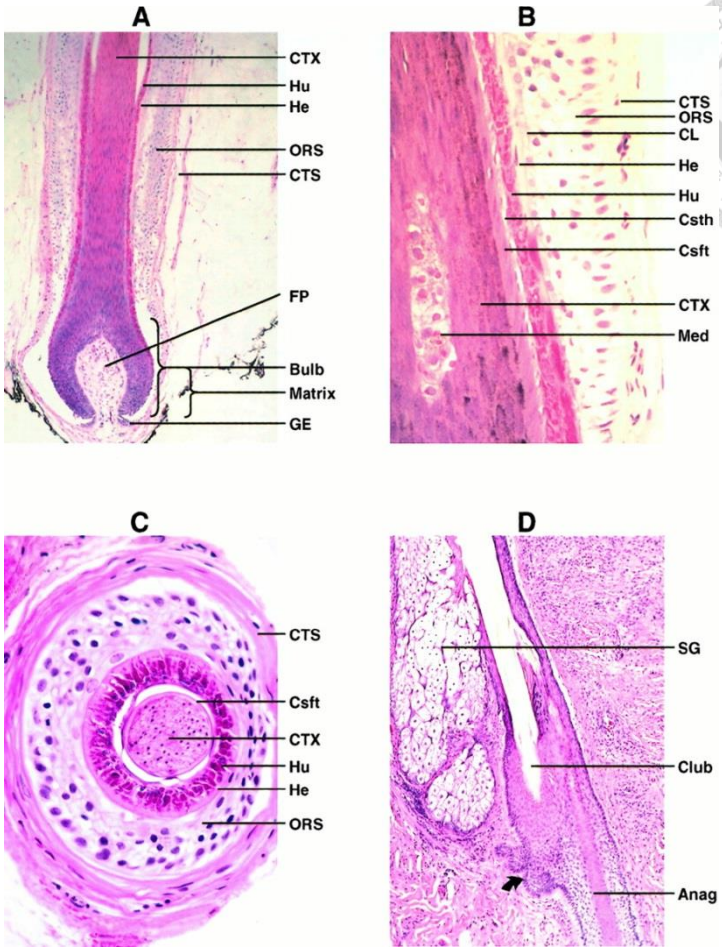

Figure 1. Histology of human HFs (Stenn and Paus 2001).

The concentric cylinder HFs are lined layer by layer starting from outermost the outer root sheath (ORS), the companion layer (CL), the inner root sheath Henle's layer (He), inner root sheath Huxley's layer (Hu), the cuticle of the inner root sheath (Csth), the cuticle of the hair shaft (Csft), the cortex of the shaft (CTX), and the medulla of the shaft (Med). IRS falls from the shaft just below the sebaceous gland duct. CTS, connective tissue sheath; SG, sebaceous gland; Club, telogen shaft base; Anag, proximal anagen follicle; FP, follicular papilla; GE, germinative epithelium.

doi:10.6342/NTU201800580

1.1.2 Hair Cycling

HFs can undergo eternal cyclic growth throughout one's life time, and this periodic growth of HFs is called the "hair cycle" which consist of the growing phase (anagen), the dystrophic phase (catagen), and the resting phase (telogen) (Chase 1954, Stenn and Paus 2001, Alonso and Fuchs 2006). In mice, the first two cycles of pelage hair remained synchronized, but in the later timepoint, the hair domain would be established (Plikus and Chuong 2008). Except for the physiological cycling, several chemical reagents, such as cyclosporine A and phorboester, can also induce the anagen entry (Gafter-Gvili, Sredni et al. 2003, Lan, Liu et al. 2015). Besides, the physical stimuli, like hair plucking and low-level light, can also stimulation the quiescent HFSCs (Avci, Gupta et al. 2014, Chen, Wang et al. 2015). The morphogenic signals and growth factors also induce the hair cycle entry by the ligand-receptors interaction to activate HFSCs.

1.1.2.1 Anagen

Anagen is the growing phase of HFs that the activated bulge stem cells and the 2nd HG cells start proliferation and differentiation into the concentric cylinder structure of hair trunk and hair bulb (Leblond 1951). The period of anagen varied from different species. For example, the anagen of mouse pelage HFs persists for 18 days

doi:10.6342/NTU201800580

(Muller-Rover, Handjiski et al. 2001). By the features of HF anatomy, the anagen can be divided into 6 subphases (Muller-Rover, Handjiski et al. 2001).

1.1.2.2 Catagen

At the end of anagen, the matrix cells stop proliferation and enter into the next dystrophic phase, catagen (Paus 1998). The distinct property of catagen is the massive apoptosis in the matrix cells. Thus, the cyclic portion of lower HF is shrinks and leaves the regressing structure called “epithelial strand”. In the meantime, the DPCs migrate upward with the epithelial strand and finally reach the HFSC niche.

1.1.2.3 Telogen

When the ORS cells in the upper epithelial strand retract and form the new bulge/ 2nd HG, these cells enter into a resting state, named telogen. During the telogen, the HFSCs remained quiescent, waiting for inductive cues to regenerate the next mature HFs (Greco, Chen et al. 2009).

doi:10.6342/NTU201800580

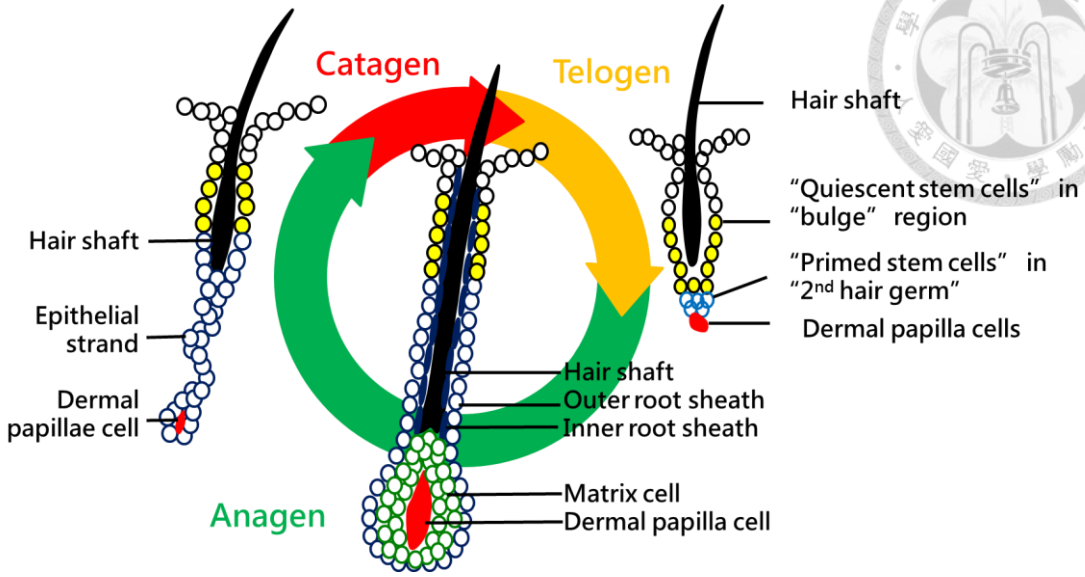

Figure 2. The illustration of three stages of hair cycle.

In telogen, the BgSCs and 2nd HG are relatively quiescent and no proliferation in this stage. When in early anagen, the cells in 2nd HG are activated prior than BgSCs. The cells can undergo rapid proliferation and differentiation for constructing a new HF. The HS is generated from matrix cells, and gradually protrudes out of the skin through the canal made by IRS. When the anagen goes into an end, the HF structures derived from BgSCs and 2nd HG would be destroyed by massive apoptosis. The epithelial strand would keep regressing, and the DPCs would migrate upward to reach the dermal part. When DPCs reach the 2nd HG, the telogen begins and waits for the next cycle.

doi:10.6342/NTU201800580

The quiescent stem cells and primed stem cells in HFs

Recently, it has been considered that there exist two distinct populations of SCs in the adult tissue (Tumbar, Guasch et al. 2004, Wagers and Weissman 2004, Moore and Lemischka 2006, Lin, Foley et al. 2013). In the early stage of anagen, the pSCs would respond to the inductive signals from DPCs prior to the qSCs, in a two-step manner (Greco, Chen et al. 2009). By life lineage tracing using two-photon technique, it is suggested the pSCs would give rise to the short-lived transient amplifying cells (TACs), and the qSCs would contribute to the ORS in the regenerating HFs (Rompolas, Deschene et al. 2012). The qSCs also showed its multipotency to replenish the conditional depletion of pSCs in the onset of anagen (Hoeck, Biehs et al. 2017). At the end of hair cycle, the remaining cells in ORS would become the new qSCs and pSCs, which implied the high similarity between each other (Hsu, Pasolli et al. 2011). HFSCs provide an excellent model for our purpose. First, the well-defined cyclic growth provides the clear-cut activated/ inactivated state, so we can isolate HFSCs at specific hair cycle stage. Second, the differential expression of SC markers allows us to separate the two populations for analysis (Greco, Chen et al. 2009, Chang, Pasolli et al. 2013). Besides, HFSCs provide enough quantity of cell source for the system-wide proteomic/ phosphoproteomic screening. Thus, it is worth to find out what makes the similar

doi:10.6342/NTU201800580

population been different during the early event of HFSC activation. Several identities are described below.

1.1.3 Label retention properties

Slow-cycling is considered as the basic properties of HFSCs for maintaining the tissue homeostasis. The label retaining cell (LRCs) has been found to incorporate nucleotide analog in the postnatal Day3 to Day5, and can be kept in the chromosome in a long time, even with the phorboester to accelerate cell proliferation (Cotsarelis, Sun et al. 1990). These LRCs are located in the bulge region. Another way to identify the LRCs is by using K5tTA/ TetO-H2BGFP mice with doxicyclin administration (Tumbar, Guasch et al. 2004). With doxycycline administration, the H2BGFP signal can be diluted by cell proliferation; thus, the remaining GFP^+ cells also represent the LRCs. By these two methods, the LRCs are both identified in the bulge region.

1.1.4 Differential expression of surface marker

By sorting out the LRCs, it becomes possible to analyze transcriptome (Tumbar, Guasch et al. 2004, Greco, Chen et al. 2009). The expression of certain surface proteins and cytokeratin could be further revealed by antibodies, such as CD34, CD200, integrin β1 (Trempus, Morris et al. 2003, Ohyama, Terunuma et al. 2006)

Thus, these proteins were found to be highly expressed in the bulge region. CD34

doi:10.6342/NTU201800580

is more specifically located in the bulge region (Trempus, Morris et al. 2003), and CD200 is found to be expressed in both bulge region and 2nd HG (Ohyama, Terunuma et al. 2006). By loxP-Cre system, it can further trace the linage from the origin of cre-expressing cells (Renninger, Schonthaler et al. 2011). Therefore, we can also observe the lineage commitment to study fate determination. In our study, we took advantage of the differential expression of surface markers to isolate and separate the qSCs and pSCs.

1.1.5 Clonogenicity and trichogenic capacity

By *in vitro* study of the differences between pSCs and qSCs, these two populations were isolated and plated on the feeder layer (Greco, Chen et al. 2009). The qSCs could generate more "holoclones" than pSCs, and the passage times for qSCs could be much longer than pSCs (Claudinot, Nicolas et al. 2005, Greco, Chen et al. 2009). The differences in trichogenecity performed by chamber assay also showed that qSCs retained better hair producing ability than pSCs (Greco, Chen et al. 2009). These functional assays indicated the hierarchy between pSC and qSCs, and these results suggested the qSCs could retain better clonogenecity and trichogenicity. By *in vivo* two-photon imaging, the activation of pSCs were recorded to encompass the DPCs for the following differentiation process (Rompolas, Deschene et al. 2012). The qSCs and

doi:10.6342/NTU201800580

pSCs could take place for each other after the pSCs or qSCs were ablated (Ito, Kizawa et al. 2002, Hoeck, Biehs et al. 2017). Thus, the two populations might also be interconvertible under the physiological environment.

1.1.6 Transcription factors play important roles in maintaining HFSCs

Over the past decade, the regulation of HFSC is mostly investigated through analysis of the transcriptomes of FACS freshly isolated stem cells (Blanpain, Lowry et al. 2004, Morris, Liu et al. 2004, Tumbar, Guasch et al. 2004, Greco, Chen et al. 2009). Several surface markers and transcription factors are identified to play an important role in regulating HFSCs, such as Sox9, Tcf3/4, and Lhx2 (Rhee, Polak et al. 2006, Nowak, Polak et al. 2008, Nguyen, Merrill et al. 2009). The transcriptome data provide a reasonable tool to investigate the status of selected populations, such as the increased BMP and FGF in telogen (Hsu, Pasolli et al. 2011). The transcriptome of BuSCs and 2nd HG shares a similar trend, but the cell cycle related genes are highly increased in 2nd HG, such as CDKs and cyclinD1 (Greco, Chen et al. 2009). Thus, the transcriptome result supports the two-step activation hypothesis.

Additionally, DPCs, the unique mesenchymal cells of HF, are able to regulate HFSC activity by secreting TGF-β2 and FGF-7 in early anagen (Greco, Chen et al. 2009, Oshimori and Fuchs 2012), which stimulate HFSC activity and thereby initiate a new

doi:10.6342/NTU201800580

hair cycle.

doi:10.6342/NTU201800580

1.2 The response of hair follicle cells toward genotoxic stress

Radiotherapy are wildly employed in cancer treatment (Delaney, Jacob et al. 2005). Despite the advance in modes of beam delivery and dose fracination, injury to normal tissues is still inevitable, leading to side effects in respective organs (Bentzen 2006). HFs are one of the most sensitive organs that are susceptible the genotoxic injuries induced by ionizing radiation (IR) (Malkinson, Griem et al. 1973). Clinically, hair loss is a common side effect of radiotherapy and, currently, there is no effective treatment. Understanding how HFs respond to and regenerate from IR injuries can help to develop strategies to mitigate hair loss from radiotherapy. In human scalp, at any time, about 90% of the HFs are in the anagen (Krause and Foitzik 2006). The matrix cells of anagen hair bulbs are one of the most actively proliferating cells in the body (Vanscott, Ekel et al. 1963). Due to this proliferative nature, human scalp HFs are highly susceptible to genotoxic injury from IR. Thus, to understand the pathology of the response of HFs toward radiation is extremely important. Two major responsive pathways have been characterized: the mild to moderate injury caused dystrophic anagen, and the severe injury induced dystrophic catagen (Paus, Haslam et al. 2013). However, the underlying mechanisms of the two responsive pathways remain unclear.

In the past decades, more and more studies focused on the mechanism of HF repair

doi:10.6342/NTU201800580

followed by genotoxic stress (Botchkarev, Komarova et al. 2000, Sharov, Li et al. 2003). IR induces genotoxic stress by direct DNA damage and indirect reactive oxygen species (ROS) formation (Tominaga, Kodama et al. 2004), leading to apoptosis of matrix cells with resultant HF dystrophy and hair loss (Malkinson and Keane 1981). It has been suggested that p53 plays the central role for the DNA damage repair or inducing apoptosis (Kastan, Onyekwere et al. 1991). Loss of p53 can attenuate the genotoxic stress to HFs (Botchkarev, Komarova et al. 2000). The stability of p53 is depend on Mdm2, which is an E3 ligase for p53 degradation (Lai, Leong et al. 2010). Therefore, understanding the molecular mechanisms of HF regeneration following IR injury would be helpful to develop a strategy to improve the management of hair loss.

doi:10.6342/NTU201800580

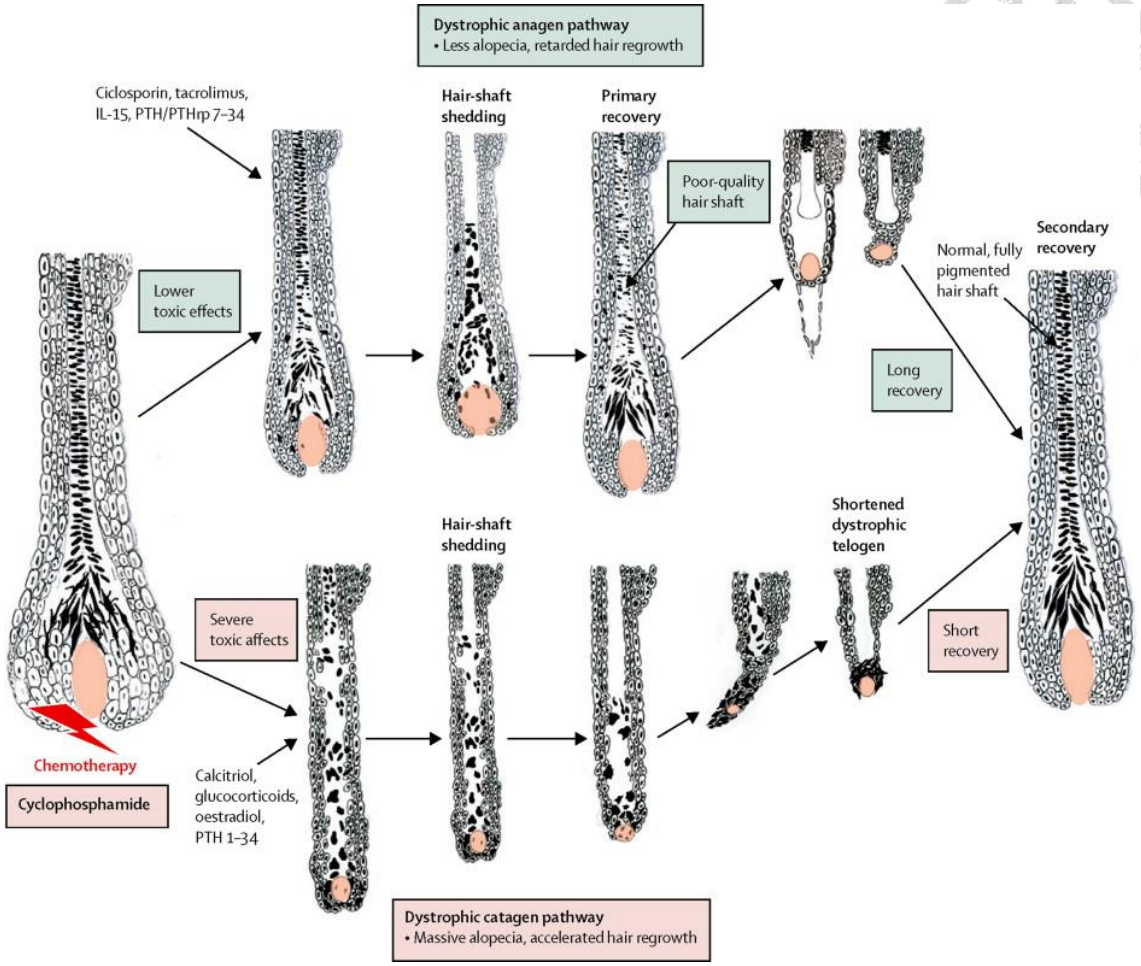

Figure 3. Two pathways for regenerate HFs after cyclophosphamide. (Paus, Haslam et al. 2013)

Depends on the dosage of cyclophosphamide, the HFs might show different response to repair HFs. The dystrophic anagen is caused by lower dose of cyclophosphamide, and the HFs retain in anagen with rapid regeneration. The higher dose of cyclophosphamide would lead to massive apoptosis in the matrix cells, and the severe atrophy occurs in the HFs which finally goes into telogen. The gross hair loss would be shown in pelage HFs.

doi:10.6342/NTU201800580

1.3 The phosphoproteome research in stem cells biology

Protein phosphorylation, the most common form of post-translational modification (PTM), is involved in various biological events. Protein phosphorylation and de-phosphorylation can switch the protein activity between different states without changing the amount of the protein. For example, phosphorylation of key transcription factors in embryonic stem cells modulates their pluripotency and differentiation (Van Hoof, Munoz et al. 2009). Additionally, protein phosphorylation also plays a key role in relaying extrinsic environmental message to the intracellular regulatory networks. Ligand-receptor interaction can lead to signal transduction through protein phosphorylation to transduce biological message to the downstream target. Recently, technical advance of mass spectrometry (MS) has enabled the exploration of phosphoproteome in cells and associated researches have provided useful clues to map the signaling network (Brill, Xiong et al. 2009, Hutchins and Robson 2009, Van Hoof, Munoz et al. 2009). Phosphoproteomic analysis of tissue stem cells has been widely employed in cultured stem cells. Though such analysis has helped to gain new knowledge about the complicated regulatory network in stem cells, it might not represent the profile of the phosphoproteome of stem cells *in vivo.* A method that allows the mapping of tissue stem cells in different states will be helpful in dissecting the

doi:10.6342/NTU201800580

dynamics of phosphoproteomes in vivo.

We started from a phosphoproteomic approach to screen for candidate signaling pathways. Mass spectrometry has gained popularity in proteomic research in the past decade. In recent years, several labeling strategies have been developed for biological research, including label-free, isobaric tags for relative and absolute quantitation (iTRAQ), stable isotope labeling using amino acids in cell culture (SILAC), and tandem mass tag (TMT) (Brewis and Brennan 2010, Perez-Riverol, Wang et al. 2014, Chang, Kim et al. 2016). The label-free strategy requires considerable amount of protein. This limits its use for the study of freshly isolated tissue SCs due to the relatively small numbers. The SILAC strategy depends on isotope replacement and is an ideal method for screening the *in vitro* proteomic or phosphoproteome profiles (Chen, Wei et al. 2015). However, it is not suitable for labeling stem cells *in vivo*. The iTRAQ and TMT strategy are similar methods to labeling the samples, but TMT requires much less amount of proteins (Rauniyar and Yates 2014). Additionally, TMT labeling can provides robust protein identification, flexible numbers of sample, and semi-quantitative result for analysis. Based on these advantages, TMT labeling would be a powerful tool for studying the dynamic changes of proteomes in HFSCs.

The *in vivo* molecular signaling of HFSCs during hair cycles has been rarely

doi:10.6342/NTU201800580

explored. The investigation of molecular signaling of HFSCs from a proteomic approach has been limited due to the scanty amounts of HFSCs obtained by cell sorting. The advance of mass spectrometry has come to a point for exploring the regulation of HFSCs through phosphoproteomic approaches. Although the small molecules are available for targeting specific signaling pathways, understanding the system-wide protein phosphorylation in HFSC can help to develop a new way to control the behavior of HFSC, either to promote or to perturb the hair cycle.

Another reason for phosphoproteomic research in stem cell is the lack of large screening profile from live animals. In previous studies, scientists focus on the transcription profiles of HFSCs (Tumbar, Guasch et al. 2004). However, protein molecules play the most important roles for processing the instruction from genome. To understand how the signals are delivered in to HFSCs, we must depict the profile of post-translational modification (PTM) of protein molecules. HFSCs exhibit distinct activated states and inactivated states. Hence, we speculate that there will be notable difference in proteomes/ phosphoproteomes analysis between the two states. Dissecting the proteome/ phosphoproteome profile will provide more information to discuss the dermal-epidermal interaction.

doi:10.6342/NTU201800580

1.4 mTORC1 signaling and its function

The mammalian target of rapamycin, mTOR, is the core protein of mTOR complex, which can be characterized as mTORC1 and mTORC2 (Saxton and Sabatini 2017). The macrolide of *Streptomyces hygroscopicus*, rapamycin, can specifically inhibit mTORC1 activity by allosteric inhibition of the adaptor protein, raptor (Chang and Sehgal 1991, Hara, Maruki et al. 2002, Kim, Sarbassov et al. 2002). In clinical application, rapamycin is now used as the immunosuppressant for solid organ transplant, and the commercial product name is “Sirolimus” (Calne, Collier et al. 1989, Zuckermann, Osorio-Jamillio et al. 2018). The mTORC1 signaling pathway regulates many cellular processes, including cell proliferation, survival, metabolism, etc (Mills, Hippo et al. 2008, Dowling, Topisirovic et al. 2010). Besides, the mTORC1 is considered to regulate cancer cell proliferation. Therefore, it is also a potent therapeutic target for cancer. In recent study, mTORC1 has been suggested to play an important role in development and homeostasis (Gangloff, Mueller et al. 2004, Guertin, Stevens et al. 2006, Bentzinger, Romanino et al. 2008, Polak, Cybulski et al. 2008, Ding, Bloch et al. 2016).

1.4.1 mTORC1 signaling

mTORC1 activity can be activated by various signaling pathways, such as Wnt, BMP, TGF-β, and PI3K/AKT pathway etc. (van der Poel 2004, Langenfeld, Kong et al.

doi:10.6342/NTU201800580

2005, Inoki, Ouyang et al. 2006). In the immortal cancer cell lines, the PI3K/Akt can activate S6K and the subsequent downstream target by mTORC1 to enhance the translational control for abundant protein synthesis and proliferation (Holz, Ballif et al. 2005, Balcazar, Sathyamurthy et al. 2009). Wnt signaling pathway, which is crucial for hair cycle regulation, can cross-talk with mTORC1 through the interaction between GSK3-β and TSC1/2 (Inoki, Ouyang et al. 2006). Additionally, the mTORC1 activity also regulate the DNA damage response by stabilizing p53 in the nucleus by phosphorylating Mdm2, which is known as the E3 ligase for p53 degradation (Lai, Leong et al. 2010). These findings suggest that the various function of mTORC1 might play certain role in HF cycling or traumatic regeneration.

1.4.2 mTORC1 function in development, tissue homeostasis, and repair in HFs

Due to the development of conditional knockout system, mTOR has now been discovered in tissue level (Guertin, Stevens et al. 2006, Bentzinger, Romanino et al. 2008, Polak, Cybulski et al. 2008, Ding, Bloch et al. 2016. It is shown that mTOR is highly phosphorylated in serine 2448 in HFSCs (Affara, Trempus et al. 2006). It has been reported that mTORC1 inhibition can rescue Wnt-1-induced replicative senescence, and prevents stem cell exhaustion (Castilho, Squarize et al. 2009). mTORC1 has long

doi:10.6342/NTU201800580

been reported as downstream of Wnt, and Wnt is also required for stem cell activation (Van Mater, Kolligs et al. 2003). Thus, we suspect that mTORC1 may play a crucial role in HFSC activation. Another interesting investigation indicated that mixing the newborn epidermis and enhanced mTORC1 fibroblast would regenerate HFs (Li, Thangapazham et al. 2011). By pharmaceutical inhibition of mTORC1, the anagen entry could be postponed (Kellenberger and Tauchi 2013), and similar result could be obtained in *K14cre; mTOR*$^{flox/flox}$ mice (Deng, Lei et al. 2015).

In physiological states, loss of mTORC1 activity can disrupt normal tissue homeostasis, leading to atrophic changes in muscle, intestinal crypt, adipocytes (Polak, Cybulski et al. 2008, Rodgers, King et al. 2014, Sampson, Davis et al. 2016). These results suggest that mTORC1 also plays a critical role in the homeostasis in their SCs and TACs. In tissue regeneration, several lines of evidence indicated that mTORC1 might play an important role to regulate the repairing process, including in intestine stem cell, muscle stem cell, and hematopoietic stem cells (Ghosh, Kobayashi et al. 2016, Sampson, Davis et al. 2016)(Gan and DePinho 2009).

1.4.3 The role of mTORC1 in genotoxic stress

Chromosomal stability is very important for descending genetic information to daughter cells (Coschi and Dick 2012). Thus, the mechanism of DNA repair following

doi:10.6342/NTU201800580

genotoxic injury important. There exist many kinds of chemical reagents and physical radiation that can cause DNA damage. Clinically, DNA damage treatment targenting DNA has great therapeutic value in cancer therapy, but, in the meant time, these reagents also damage normal cells as well. Alopecia and dry desquamentation are most common side effects (Metri, Bhargav et al. 2013). Radiation treatment usually induced DNA double-strand break (DSB) (Vignard, Mirey et al. 2013). When DSB happened, the homologous recombination (HR) and non-homologous end joining (NHEJ) mechanisms would repair the broken DNA, and p53 would decide to undergo cell cycle arrest or apoptosis (Kastan, Zhan et al. 1992, Chen, Ko et al. 1996). In ATM-deficient mice, the alopecia phenotype would get stronger after constitutively applied hair-plucking (Ruzankina, Pinzon-Guzman et al. 2007). More and more study indicated that mTORC1 may be involved in DNA damage response, but the mechanism is still remained unknown (Alexander, Cai et al. 2010, Dennis, McGhee et al. 2013, Shortt, Martin et al. 2013). In this study, we would present the importance of mTOR activity after hair follicle cells receiving radiation treatment.

doi:10.6342/NTU201800580

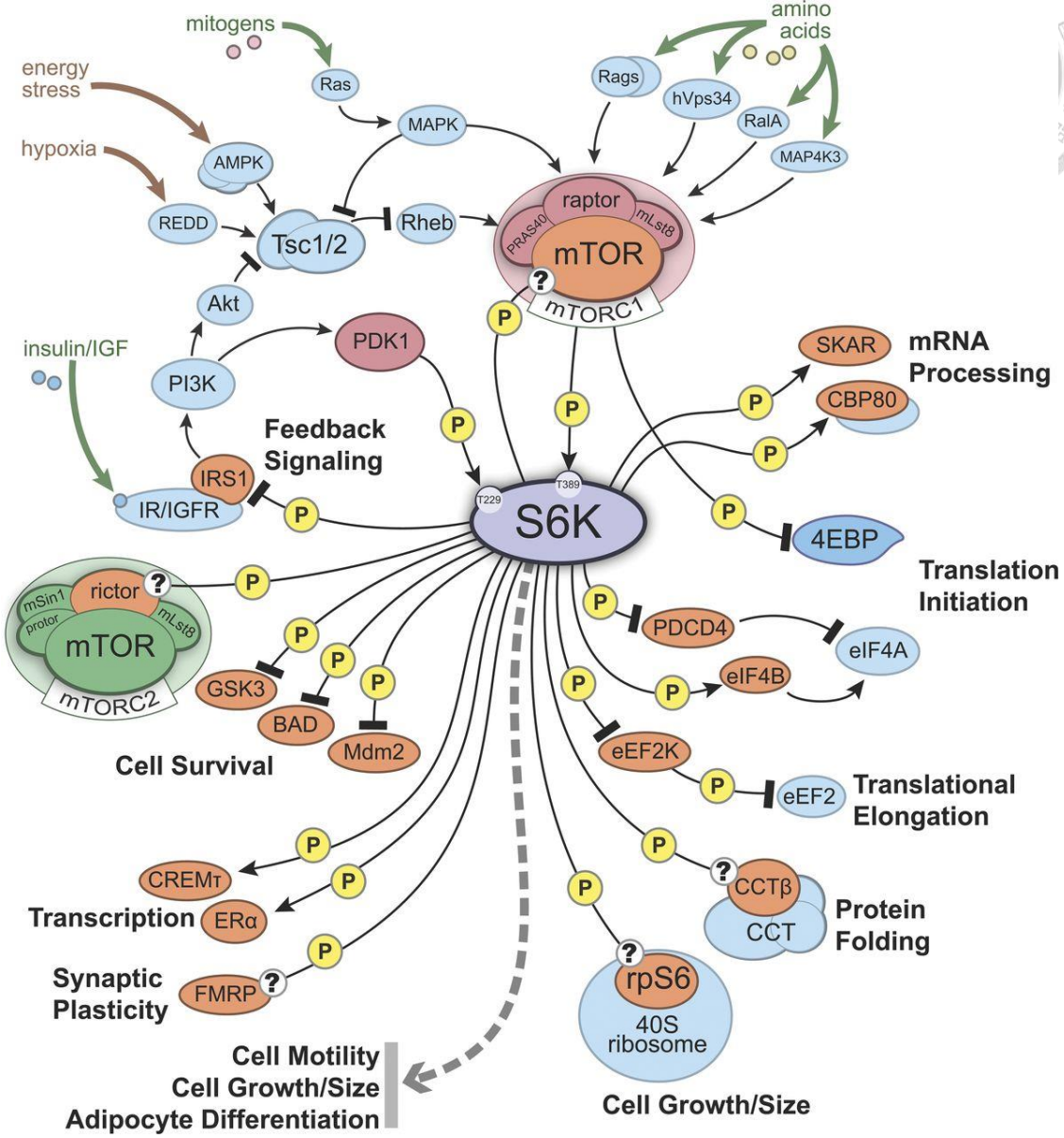

Figure 4. mTOR signaling and its downstream targets (Magnuson, Ekim et al. 2012)

doi:10.6342/NTU201800580

Chapter 2 Materials and Methods

2.1 Animals

All animal experiments were approved by our Institutional Animal Care and Use Committee. All mice were housed and maintained in the animal facility of National Taiwan University. Mice strain FVB and ICR used for fluorescence activating cell sorter (FACS), histology, and IHC staining were purchased from Taiwan National Laboratory Animal Center. For conditional knockout animals, *Rptor*$^{flox/flox}$ and *Lgr5-creERT2-IRES-EGFP* mice were purchased from Jackson lab. For animal anesthetizing process, the mixture of zolazepam (Zoletil vet, Virbac Laboratories) and xylazine (Rompun, Bayer) with the ratio of 4:1(v/v) were used for intramuscular injection. For induction of Cre activity, Tamoxifen was dissolved in sesame oil by the concentration of 20mg/ml. To ablate *raptor* gene, tamoxifen (Sigma) was administrated 1mg/mouse by intraperitoneal injection for consecutive 5 days in certain hair cycle stages. For pulse-chase experiment, 1mg of 5-bromo-20-deoxyuridine (BrdU) (Sigma) was administrated per mouse by intraperitoneal injection, and the skin specimens were collected at 1hr after BrdU injection.

doi:10.6342/NTU201800580

2.2 HFSCs isolation by FACs

To prepare single cell suspension for sorting, the subcutaneous fat was scraped off by scalpel. The skin was placed on trypsin (Gibco) with dermal site down at 37℃ for 35 mins. To obtain the epithelial cell suspension, the epidermal cells and HFSCs could be scraped off after the treatment of trypsin. Then the suspension was neutralized with 5% decalcium feral bovin serum (Bio-Rad chelexed) in PBS, and was filtered through 70um and 40um strainers. The dissociated single cells were incubated with fluorescence-conjugated primary antibodies for at least 30 mins at 4℃. The following antibodies were used: CD34-eFluor660 (1:100; eBioscience), α6-PE (1:300; BD Biosciences), Sca1-PE-Cy7 (1:100; eBioscience), and CD200-FITC (1:50; eBioscience). To isolate the suspected populations, cell purification was performed on FACS AriaIII sorters (BD Biosciences). FACS analyses were performed by LSRII FACS Analyzers and then analyzed using FlowJo program.

2.3 Mass Spectrometry work flow

2.3.1 Sample preparation for proteomic analysis

Cells were harvested in lysis buffer (12mM SDC, 12mM SLS in 100mM Tris-HCl, pH 9.0 with protease inhibitor cocktail and phosphatase inhibitors). After the incubation

doi:10.6342/NTU201800580

at 95℃ to deactivate phosphatase, cell lysate were sonicated in 4℃ water bath for 30 minutes with 30 cycles by Bioruptor Plus system (Digenode, Liege, Belgium and NJ, USA). Each cycle includes 30 seconds sonication in 1 mA amplitude and 30 sec for cooling sample. The sonicated lysate followed by centrifuge at 16000 rcf for 30 minutes. The protein concentrations of the supernatant were determined via bicinchoninic (BCA) assay. The protein was extract by chloroform-methanol precipitation and dissolved in 8M Urea,50 mM triethylammonium bicarbonate (TEABC). The protein extract was reduced with 10 mM dithiothreitol and alkylated with 55 mM iodoacetamide. Alkylated proteins were digested with Lys-C (1:100, w/w; Wako) for 3 hours followed by overnight digestion with trypsin (1:50, w/w; Promega) at 37℃. Peptides acidified to 0.5% triflouroacetic acid (TFA) and desalted by styrene-divinylbenzene copolymer (SDB-XC) solid-phase extraction cartridge (Empore, 3M). Peptides were eluted in 80% acetonitrile (ACN) and 0.1% TFA. The concentration of desalted peptide was estimated by BCA assay.

2.3.2 Tandem-Mass-Tag (TMT) label

60 μg of desalted peptide was dissolved in 100 mM TEABC and react with corresponding TMT six-plex reagent (Thermo Pierce, USA) for 1 hour at room

doi:10.6342/NTU201800580

temperature. The reaction was quenched with 5% hydroxylamine for 15 min at room temperature. The six samples were mixed, acidified, and desalted using SDB-XC cartridges. TMT-labeled peptide was eluent in 80% ACN and 0.1% TFA followed by dried using a vacuum centrifuge overnight.

2.3.3 Phosphopeptide enrichment

The inhouse-constructed IMAC tip was capped at one end with a 20 mm polypropylenefrits disk (Agilent, Wilmington, DE, USA) enclosed in a tip-end fitting. The tip was packed with 20 mg of Ni-NTA silica resin. All purification steps for buffer exchange and sample loading involved manipulation via centrifugation. Ni2+ ions were removed with 50mM EDTA in 1M NaCl. The tip was then activated with 100mM FeCl3 and equilibrated with loading buffer (6% (v/v) acetic acid at pH 3.0) prior to sample loading. Tryptic peptides were reconstituted in loading buffer and loaded onto the IMAC tip. After successive washes with 6% (v/v) acetic acid, 25% ACN and 6% (v/v) acetic acid (AA), the bound peptides were eluted with 200mM NH4H2PO4. The eluted peptides were desalted using reversed phase-Stage Tips

doi:10.6342/NTU201800580

2.3.4 LC-MS/MS Analysis

TMT-labeled peptide was analysis on thermo UltiMate 3000 HPLC system and connected to Orbitrap Fusion Tribrid platform through a nanoelectrospray ion source. Peptides were separated on a 25 cm analytical column (75 μm inner diameter) packed with 2 μm reverse-phase C18 particle size (Acclaim PepMap RSLC, Thermo Scientific) with 150 minutes gradient from 1% to 35 % ACN in 0.1% formic acid (FA) at a flow 500 nL/min. The spray voltage is 1.65 kV. The Orbitrap Fusion Tribrid platform was operated in data-dependent acquisition mode. Survey full-scan MS spectra (from m/z 300 to 1650) were detected in Orbitrap analyzer with resolution 60K at m/z 400 after accumulation to a target value of 3 e6 and a maximum injection time of 150 ms. MS/MS scans were acquired by the LTQ with a target ion setting of 1.5e6 and a max injection time of 150 ms Ions were fragmented (collision energy: 35%). The resulting fragments were detected with a resolution of 30K in the Orbitrap system.

2.3.5 Proteome Data Processing and Identification

All full-scan MS and MS/MS spectra were analyzed with the MaxQuant software suite version 1.5.6.5. Protein were identified by searching MS/MS peak list against the UniProt mouse database (release on May 2015, containing 16,733 protein sequence).

doi:10.6342/NTU201800580

Digestion enzyme specificity was set to trypsin and Lys-C, and up to two missed cleavage sites were allowed. Phospho (S,T,Y), oxidation (M), and protein N-terminal acetylation for variable modifications; carbamidomethyl was chosen for fixed modifications. The maximum false discovery rate (FDR) was set to 1% for both the peptides spectrum match (PSM) and proteins. The minimum required peptide length was set at seven amino acids.

2.4 Pharmaceutical mTORC1 inhibition

mTORC1 inhibitor, rapamycin, was purchased from Sigma-Aldridge (R8781). Rapamycin (4μg/g body weigh) was administrated 2 hours before IR treatment by intraperitoneal injection. In the following days, mice received daily rapamycin treatment until skin sampling.

2.5 Irradiation treatment

Before irradiation treatment, the dorsal skin of 3-week-old female mice was carefully shaved without injuring the skin. At about postnatal day 29 when the dorsal HFs entered anagen V, mice were anesthetized for ionizing radiation treatment by a 4Gy ^{137}Cs source (IBL-637 gamma-irradiator, 662keV photons, CIS Bio International). Mice were irradiated from the dorsal side.

doi:10.6342/NTU201800580

2.6 Histology examination

Harvested mouse skin samples after patch experiments were fixed in 4% paraformaldehyde overnight and then embedded in paraffin wax. These paraffin-embedded tissues were stained with hematoxylin and eosin for further histological examination.

2.7 Immunofluorescent staining and microscopy

The mouse skin specimens were fixed with 4% paraformaldehyde (PFA) at 4℃ overnight, dehydration, and paraffin embed. The paraffin sections The primary antibodies used were mouse anti-β-catenin (BD, 1:100), mouse anti-AE13 (abcam, 1:200), mouse anti-AE15 (abcam, 1:200), rabbit anti-cytokeratin 5 (abcam, 1:200), rat anti-BrdU (abcam, 1:200), rabbit anti-γ-H2AX (Millipore, 1:100), goat anti-p-cadherin (R&D Systems, 1:200), rabbit anti-pS6 (Cell Signaling, 1:400), rabbit anti-Lef1 (Cell Signaling, 1:200). Secondary antibodies were used as follows: Alexa Fluor Cy3-conjucated donkey anti–mouse IgG (H+L) (Jackson ImmunoResearch, 715-585-151; 1:500), Alexa Fluor Cy3-conjugated AffiniPure donkey anti–rabbit IgG (Jackson ImmunoResearch, 711-165-152; 1:500) and Alexa Fluor 488-AffiniPure $F(ab')_2$ Fragment donkey anti–goat IgG (IgG) (H+L) (Jackson ImmunoResearch,

doi:10.6342/NTU201800580

705-543-003; 1:500). To identify the apoptotic cells, the DeadEnd™ Fluorometric TUNEL System kit (Promega) was used for detecting apoptotic cells according to the instruction of the manufacturer. The fluorescence images were captured and analyzed by Zeiss LSM700 confocal microscope driven by Zen software. The histological images were acquired by Nikon, NiE microscope

2.8 Statistical analysis

The quantitative data was expressed as mean ±standard error (S.E.).The comparison between each group was performed with a two-tailed Student's *t*-test using Prism6 software (GraphPad Software, Inc). To determine significance between two groups, indicated in figures by asterisks, comparisons were made using Student's t test. Difference was considered statistically significant when $p < 0.05$.

doi:10.6342/NTU201800580

Chapter 3 Results

3.1 Isolation of pSCs and qSCs of HFs in telogen and early anagen

The activation of HFSCs for replenishing the consumption during skin homeostasis and hair cycle depends on complicated signaling networks. Thus, to gain further insight of how the signals were transmitted would help us to understand the mechanisms of stem cell activation. HFSCs provided a stable model for study stem cell biology because of the clear-cut growing and resting phase. (Fig 5A-B)

To understand the environmental cues required for initiating hair cycle, we focused on protein phosphorylation, which is the most important post-translational modification (PTM) in signal transduction. It is well-known that the transmission of morphogenic signals such as, wnt, BMP, TGF-β, and Shh, depend on protein phosphorylation to modulate the activity of downstream targets (Kretzschmar, Liu et al. 1997, Xu, Chen et al. 2000, Chen, Sasai et al. 2011). Thus, we isolated the HFSCs during postnatal Day21 to Day25 as the active pSCs and qSCs. On the other hand, we prepared the postnatal 8-week-old mice for isolating the dormant pSCs and qSCs. To separate the different populations in the skin and its appendages for analysis, Sca-1 was used to exclude interfollicullar epidermal cells, and integrin alpha6 was use to mark all the basal cells.

doi:10.6342/NTU201800580

Since CD200 was expressed in both HFSCs, the differential expression of CD34 was identical for qSCs, not for pSCs. Hence, the pSCs could be defined by Sca-1^{-}/ alpha6^{+}/ CD200^{+}/ CD34^{-}, and the qSCs should be defined as Sca-1^{-}/ alpha6^{+}/ CD200^{+}/ CD34^{+}. (Fig 6A-B) Each population were examined >96% purity.

The isolated cell populations were lysed for protein extraction and purification (Fig 7). After digested into small peptides, the TMT molecules were labeled for each population. After labeling, equal amount of peptides were mixed for subsequent MS/MS analysis.

doi:10.6342/NTU201800580

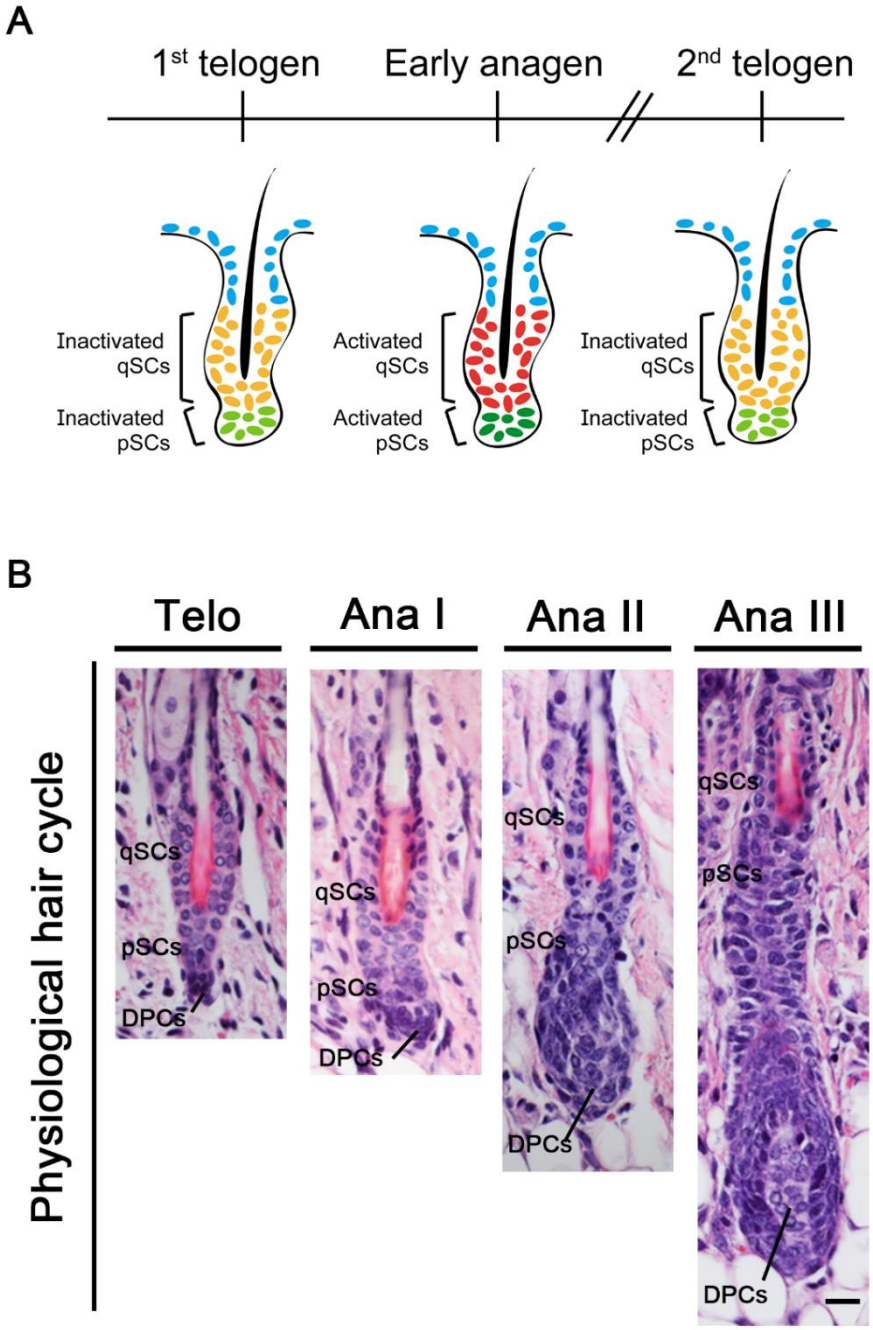

Figure 5. Schematic of hair cycle and the dynamics of HF structure.

(A) The illustration of pSCs and qSCs in telogen and early anagen

(B) The anatomy of HFs from 1st telogen to early anagen showed the histological changes. The activated pSCs and qSCs were sorted in anagen I to anagen II. The inactivated pSCs and qSCs were sorted at 2nd telogen, respectively.

doi:10.6342/NTU201800580

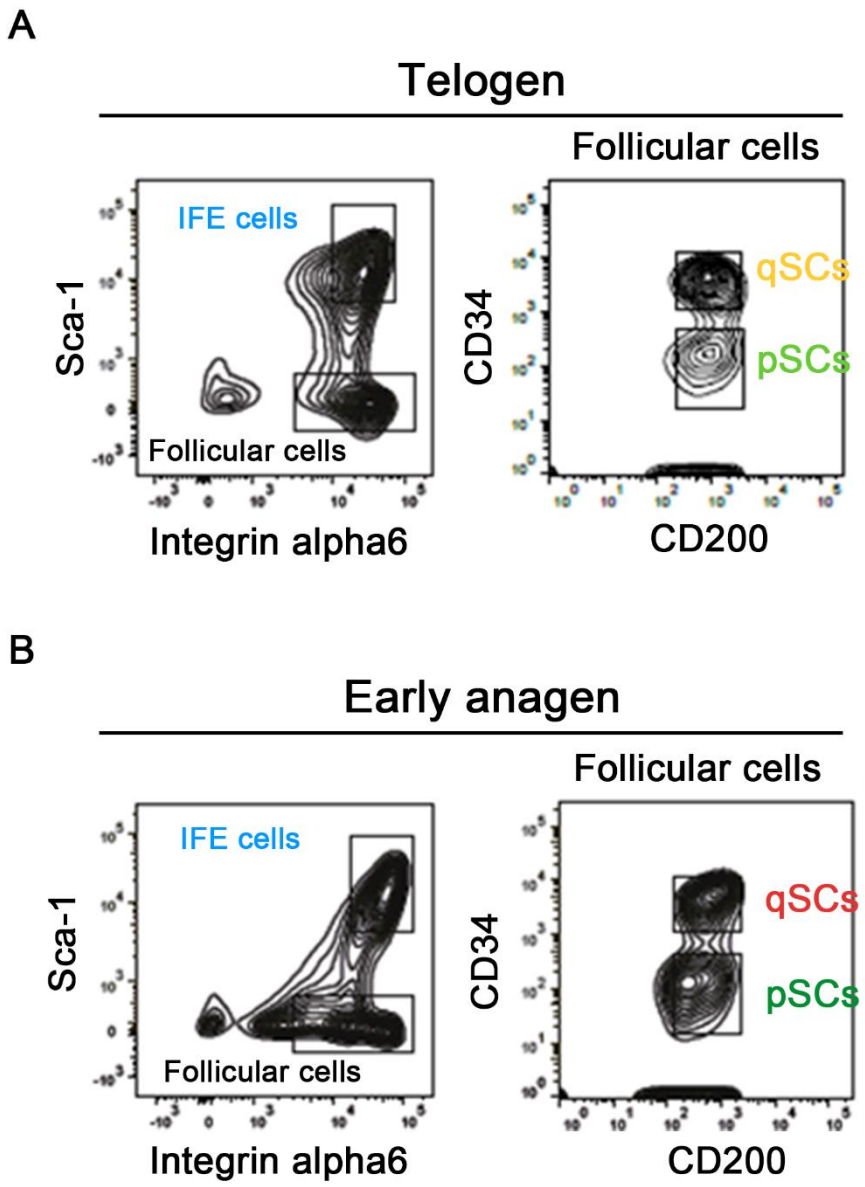

Figure 6. The strategy for isolating and purifying the qSCs and pSCs

(A) To isolate inactivated HFSCs, we first gated the Sca-1^{-}/ Itg α6^{+} population to select follicular cells. Then, we used the CD34^{+}/ CD200^{+} for isolating qSCs and the CD34^{-}/ CD200^{+} for pSCs.

(B) The isolation of HFSCs in early anagen. The condition for sorting qSCs and pSCs are similar to the telogen.

doi:10.6342/NTU201800580

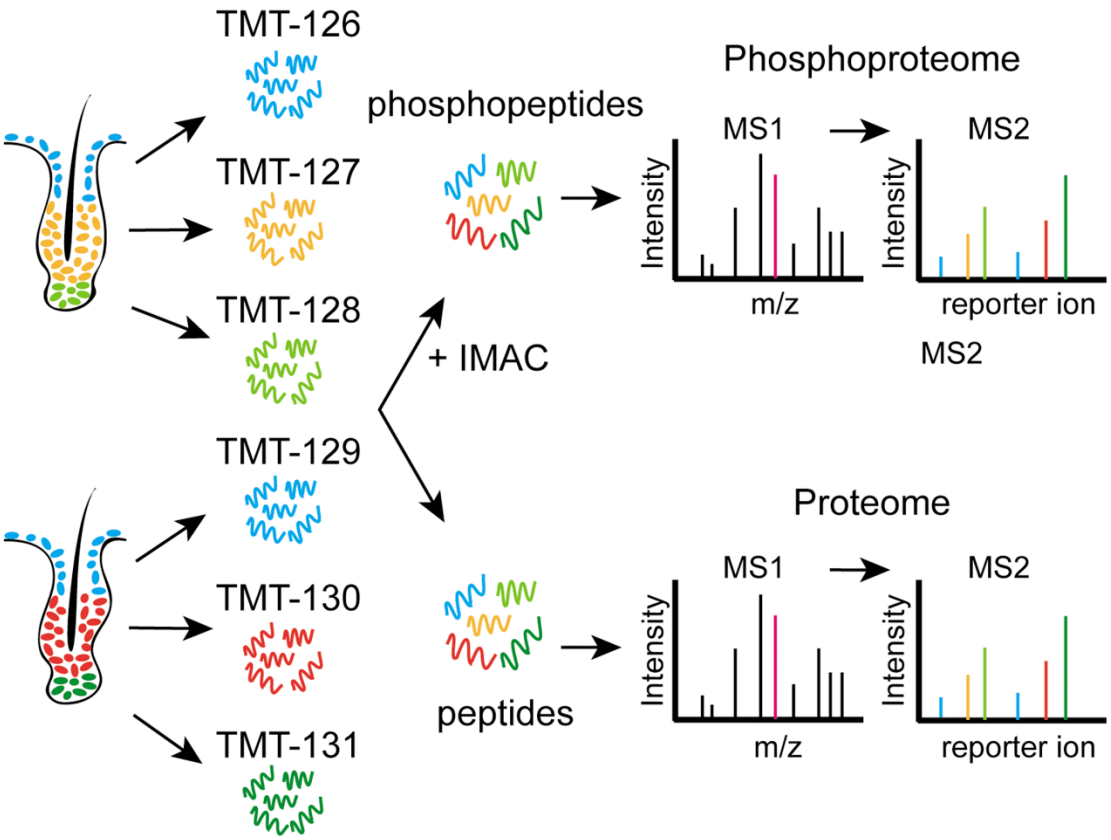

Figure 7. The experimental procedure from cell isolation to mass spectrometry

The isolated populations were lysed and digest into small peptides. These peptides were labeled with certain types of TMT molecules, which can show the relative intensity in the result. The labeled peptides were mixed and went through the following IMAC process for acquiring phosphoproteome result. By comparing with each group, we can acquire the semi-quantitative dataset, including proteome and phosphoproteome.

doi:10.6342/NTU201800580

3.2 Comparing the phosphoproteome between each population

To investigate the difference in protein expression/ modification within the two populations in HFSCs, we compared the proteome/ phosphoproteoem between pSCs and qSCs. (Fig.8A) Since we harvested two stages of pSCs and qSCs, we could investigate the difference in telogen and in early anagen, respectively. In telogen, there were 169 proteins and 217 phosphopeptides enriched in the qSCs (Fig.8B). On the contrary, the enrichment of 30 proteins and 64 phosphopeptides were found in pSCs. In early anagen, we could also found 60 proteins and 42 phosphopeptides enriched in qSCs; meanwhile, there were 159 proteins and 155 phosphopeptides enriched in pSCs. The enriched proteins/ phoshopeptides might overlap in both telogen and early anagen; therefore, the enriched IDs in telogen and in early anagen were processed by venn diagram (Fig.11A). This combination allow us to classify the enriched proteins/ phosphopeptides into 3 groups: telogen-specific, anagen-specific, and in both stages. We speculated that the certain HFSC markers might be discovered through the classification, so we first analyzed the proteins/ phsphopeptides that increased in both telogen and early anagen.

To determine if our dataset contained the well-known HFSCs markers, we

doi:10.6342/NTU201800580

examined the IDs from venn diagram, and 55 proteins were constantly enriched, no matter in telogen or in early anagen (Fig.11A). These 55 proteins included several well-known bulge stem cell markers identified in the previous reports, including Cd34, Krt15, Krt6, Krt24, Col17A1, S100A4, and S100A6 (Fig.9A) (Ito and Kizawa 2001, Ito, Kizawa et al. 2004, Tumbar, Guasch et al. 2004, Adam, Yang et al. 2015, Matsumura, Mohri et al. 2016). Except for the increased in translational level of HFSC markers, they could also be phosphorylated at multiple sites, such as Krt15 $^{S28, S33, S40, S141}$, and Krt6 $^{S35, S42, S58, S69, S531}$ (Fig.10A). Although the function of phospho-sites are not well-understood, such as Bnc2 ^{S336}, Macf1 ^{S3349}, and Pkp $^{S180, S314}$, these phospho-sites could be regarded as the putative "phosphor-marks" for qSCs (Fig.10B). In the previous study, Bnc2 was reported to regulate anagen entry (Vanhoutteghem, Delhomme et al. 2016), and Macf1 was reported to be involved in Wnt signaling, which is crucial for anagen entry (Wu, Shen et al. 2011).

On the other hand, we discovered that several keratin proteins were enriched in pSCs in both activated and inactivated state, such as Krt25, Krt27, Krt71, Krt76, and Krt79 (Fig.9A, C). It has been shown that Krt25 and Krt27 were expressed in the inner root sheath in full anagen, but their expression in telogen was unclear. Since Krt25 and Krtr27 were expressed in the differentiating transit amplifying cells, we still suspected

doi:10.6342/NTU201800580

that the other keratens might be able to be the marker of pSCs (Fig.9C). Similar to the qSCs, these enriched proteins were also phosphorylated at multiple sites, including Marcks ^{S27}, and Irf6 ^{S424} (Fig.10C). Although the function of Irf6 is still not fully understood, it was reported to be the downstream target of p63 (Richardson, Dixon et al. 2006).

Thus, by comprehensive proteomic/phosphoproteomic comparison of pSCs and qSCs in inactivated and activated states, we found distinct proteins/ phosphoproteins that were enriched in either pSCs or qSCs around hair cycle. The enriched IDs shows high similarity comparing with previous study in transcriptional level and immunostaining result. Our results not only perform the reliability and accuracy of TMT-based technique, but also indicate several putative qSCs and pSC markers in translational level.

In addition to find out the signature proteins/ phosphoproteins, we would like to understand whether there is difference in protein expression/ modification between qSCs and pSCs in each state. We would like to know if the enriched proteins/ phosphoproteins in telogen-specific contained were responsible for stem cell maintenance, so we used GO term analysis to annotate the biological process of these proteins/ phosphopeptide. Interestingly, we found that cell-redox homeostasis, ATP

doi:10.6342/NTU201800580

biosynthesis, and oxidation-reduction process were highly enriched in qSCs, specifically in telogen (Fig.11B). The amount of anti-oxidant enzyme family, including Prdx1, Prdx4, and Prdx5, were increased in qSCs in the resting state (Fig.11C). The ATP5 subunits, which regulates mitochoria activity, were also increased in qSCs. The oxidation-reduction related proteins, such as Ndufa11, Ndufb11, Cyb5r3 and Aldh4a1 were elevated in qSCs. This result showed the association between the cellular energy management and the maintenance of quiescent state. Although the correlation between energy homeostasis and hair cycle activation are remained unknown, it was reported that inhibition of electron transport chain would lead to the activation of hair cycle. The GO analysis for phosphoproteomic results indicated that the cell-cell adhesion and hemidesmosome assembly were enriched (Fig.12B). The regulatory proteins of cell-cell adhesion included Plec and Pkp3, which modulate the structure of cytoskeleton (Fig.12C). The hemidesmosome proteins, such as Itgb4 and Col17a1, were found highly phosphorylated in qSCs. These results implied that there might exist certain mechanism to maintain the survival of qSCs, and the cell-cell interaction within qSCs might be regulated via protein phosphorylation.

To investigate whether the enriched proteins/ phosphopeptides might proceed

doi:10.6342/NTU201800580

similar features, the GO analysis of enriched proteins specifically in anagen showed the significant changes in metabolic process, DNA replication, and oxidation-reduction process (Fig.11B). These three enriched GO term corresponded to the state of pSCs in the early anagen, which the pSCs might need higher metabolic activity for massive cell proliferation. The Mcm protein family, including Mcm3, Mcm4, Mcm6, and Mcm7 were increased in pSCs in early anagen (Fig.11C). The metabolic proteins, Hmgcs1 and Hmgcs2, were also increased. The comparison of phosphoproteome revealed the GO term of transcription, translation initiation, and cell cycle were highly enriched in pSCs (Fig.12B). A bunch of elongation initiation factors, Eif3b, Eif3e, Eif3k, and Eif4a1, were highly phosphorylated in pSCs, which indicated the protein translation might be more active in pSCs than in qSCs (Fig.12C). Combined with the proteome/ phosphoproteome result, the pSCs were provided with high metabolic and proliferative activity for processing robust transcription and translation in the early anagen.

doi:10.6342/NTU201800580

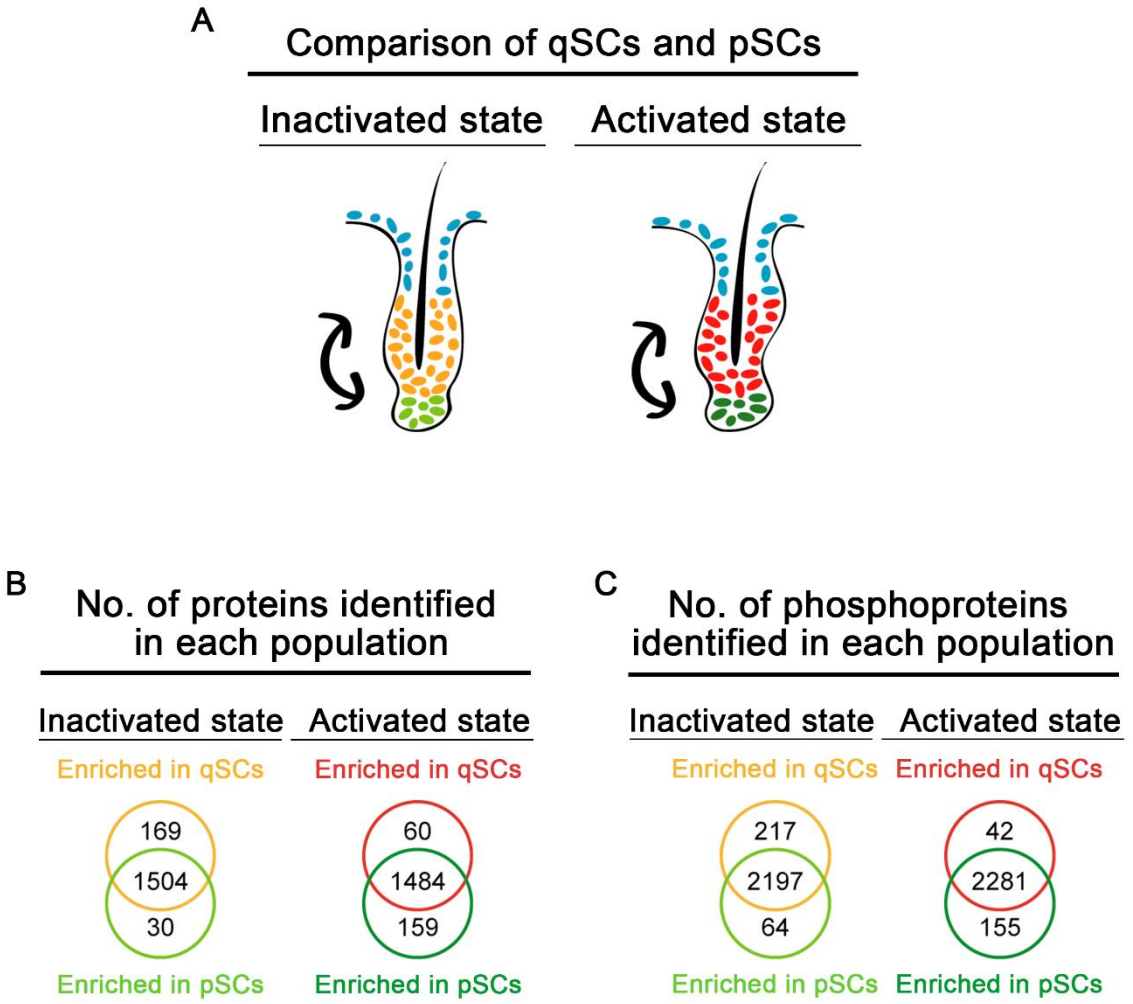

Figure 8. The numbers of identified proteins and phosphopeptides in each hair cycle stage.

(A) Schematic of the comparison of pSCs and qSCs in inactivated and activated state, seperately.

(B) Quantification of identified protein numbers in each stage.

(C) Quantification of identified phosphopeptide numbers in each stage.

doi:10.6342/NTU201800580

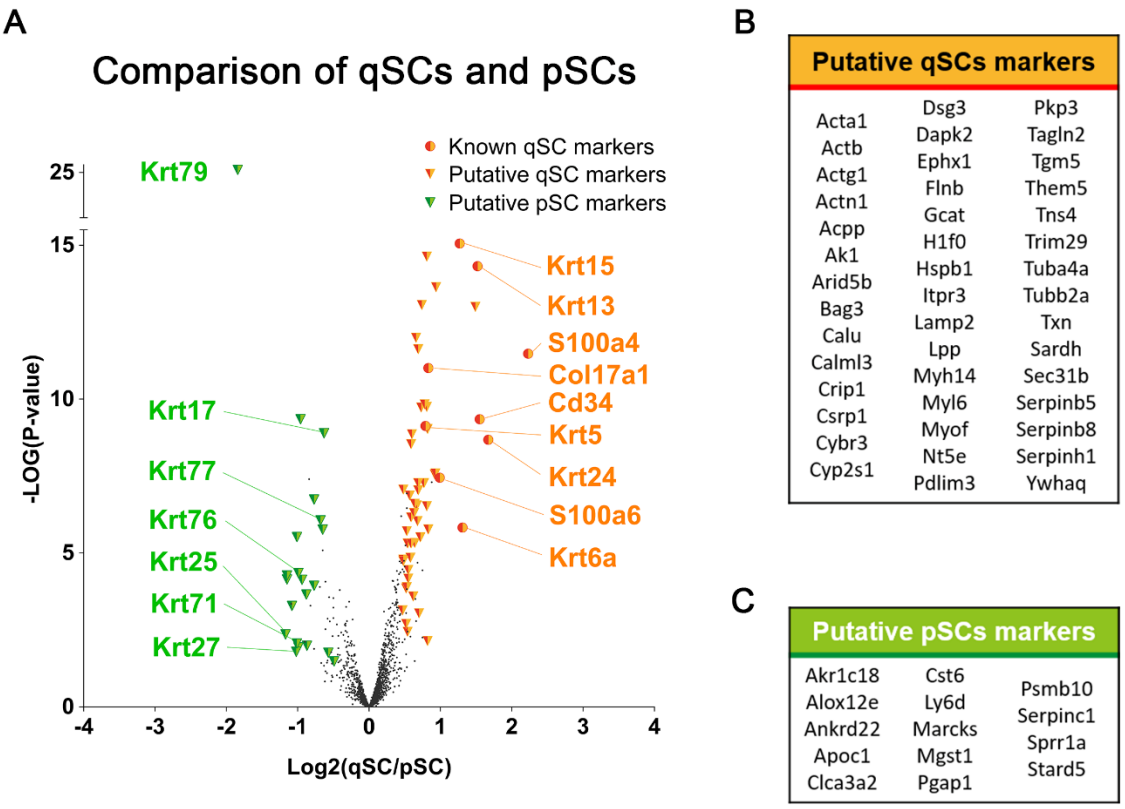

Figure 9. Identified putative qSC and pSC markers in the volcano plot

Through the comparison of pSCs and qSCs, several proteins are identified specifically in the pSCs or qSCs, including the well-known HFSC markers.

(A) The volcano plot indicates the specifically expressed proteins, including the reported HFSC markers, and the putative pSC or qSC markers.

(B) The enrichment of identified proteins in qSCs might be the putative qSC markers.

(C) The enrichment of identified non-keratin proteins in pSCs might be the putative pSC markers.

doi:10.6342/NTU201800580

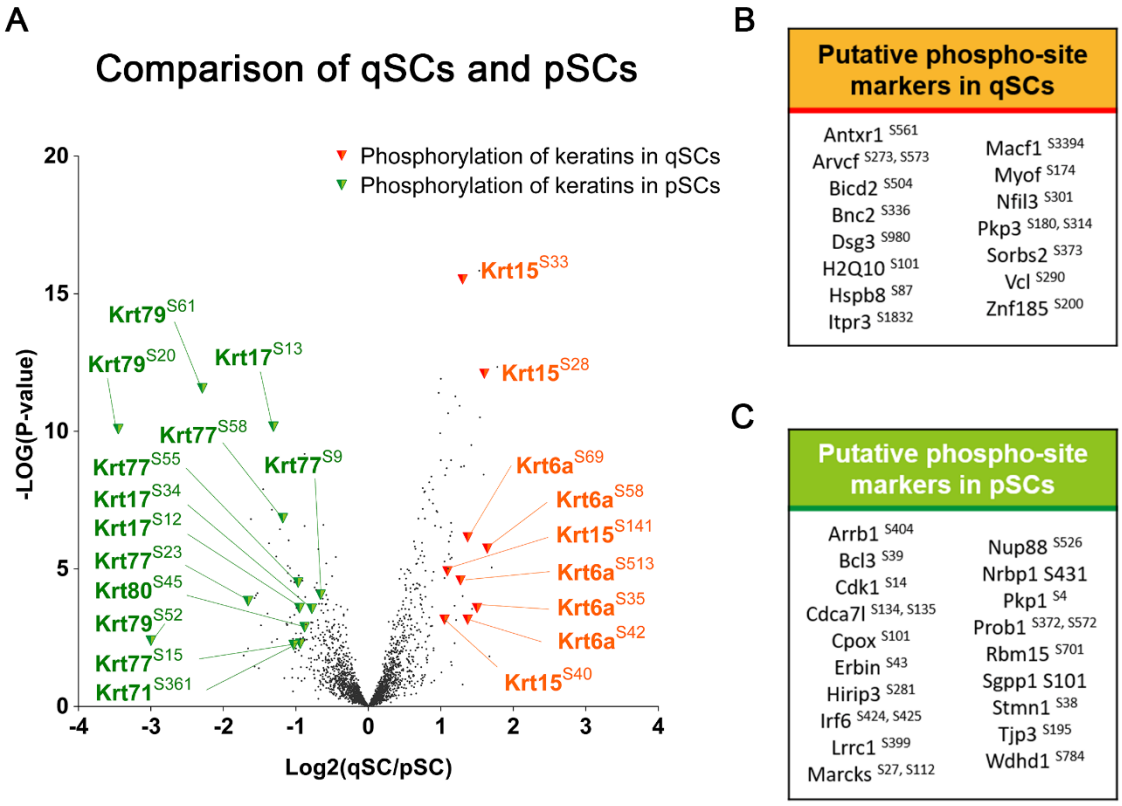

Figure 10. Through the comparison of pSCs and qSCs, ceratin phosphopeptides are identified specifically in the pSCs or qSCs.

(A) The volcano plot indicates the phospho-site of keratin proteins which are enriched in pSCs or qSCs.

(B) The enrichment of identified phosphopeptides and the phosphor-sites in qSCs might be the putative phospho-site markers.

(C) The enrichment of identified phosphopeptides and the phosphor-sites in pSCs might be the putative phospho-site markers.

doi:10.6342/NTU201800580

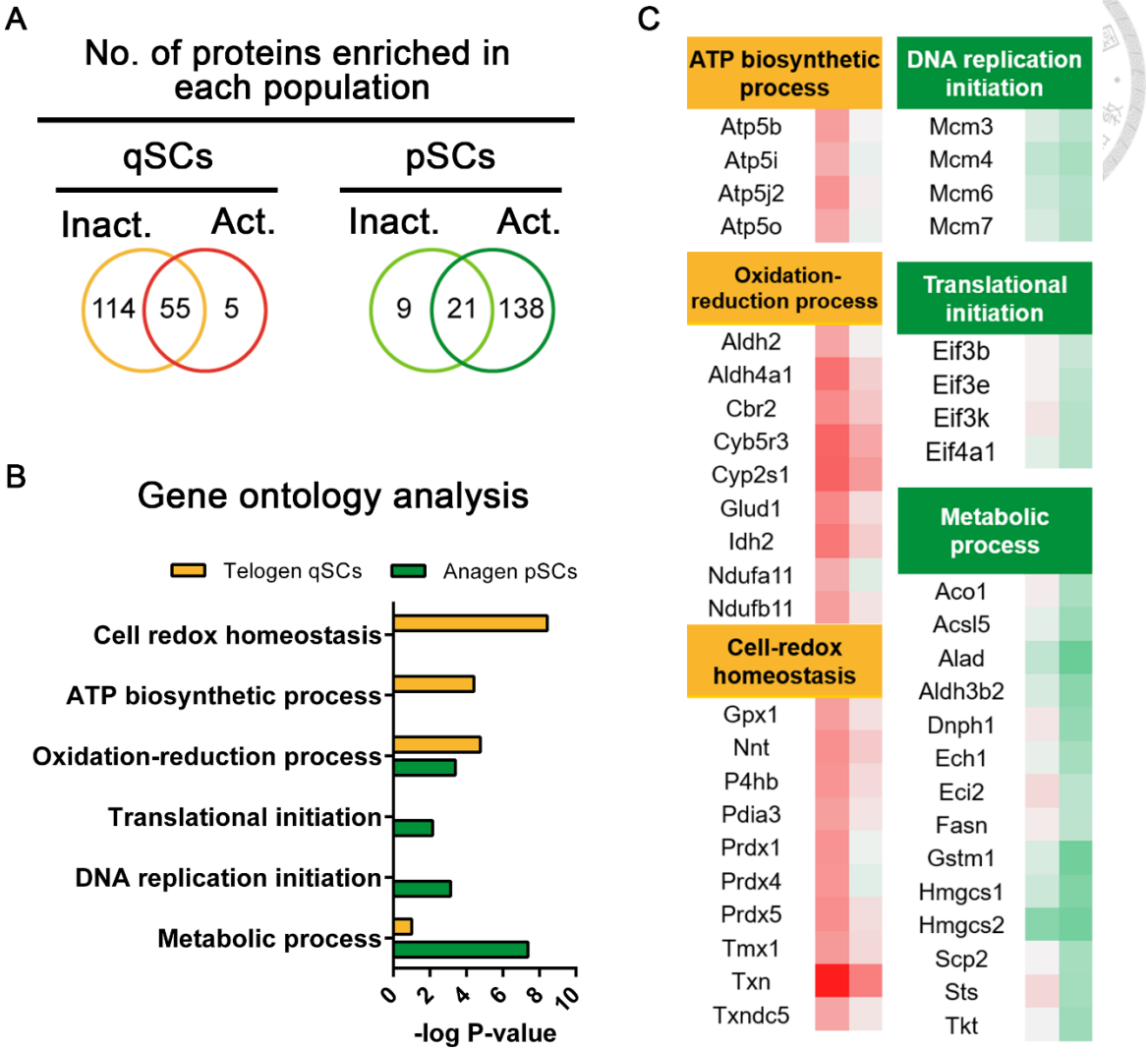

Figure 11. The GO analysis of proteome indicates the activated state in anagen pSCs and in teloge qSCs.

(A) Via Venn diagram, proteins enriched in qSCs or pSCs could be classified into 3 groups: activated, inactivated, and stage independent.

(B) GO term analysis of qSCs in inactivated state, and pSCs in activated state.

(C) Protein IDs of qSCs in inactivated state, and pSCs in activated state.

doi:10.6342/NTU201800580

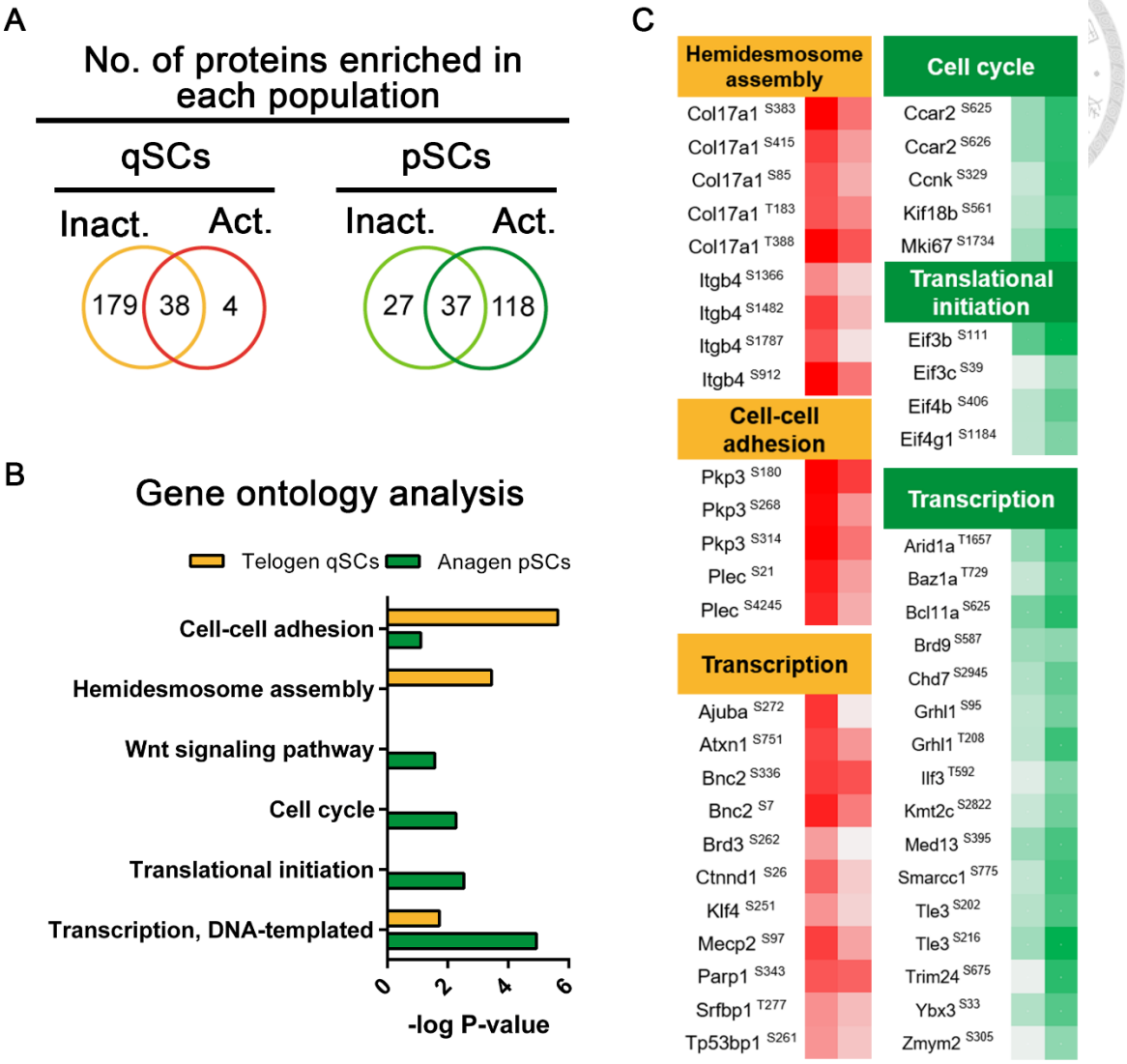

Figure 12. The GO analysis of phosphoproteome indicates the activated state in anagen pSCs. In telogen qSCs,

(A) Via Venn diagram, phosphopeptides enriched in qSCs or pSCs could be classified into 3 groups: activated, inactivated, and stage independent.

(B) GO term analysis of qSCs in inactivated state, and pSCs in activated state.

(C) Phosphopeptides of qSCs in inactivated state, and pSCs in activated state.

doi:10.6342/NTU201800580

3.3 The phosphoproteome varied dramatically during the transition from telogen to anagen

To characterize the dynamic changes of protein expression/ modification in the telogen to anagen transition, we compared the proteomes/ phosphoproteomes between inactivated and activated states (Fig.13A). In qSCs, 67 proteins and 257 phosphopeptides were enriched in telogen, and 99 proteins and 347 phosphopeptides were enriched in early anagen (Fig.13B-C). Strikingly, in pSCs, the enriched proteins and phosphopeptides were numerous in the early anagen, which 711 proteins and 936 phosphopeptides were increased. On the contrary, in telogen, there were only 62 proteins and 63 phosphopeptides increased.

To identify whether the proteins and phosphopeptides were increased specifically in certain population of HFSCs, we utilized venn diagram to sort out the proteins/ phosphopeptides in each group: qSC-specific, pSCs-specific, or both populations (Fig.16A, Fig.17A). We found there were 97 proteins and 320 phosphopeptides existed in both pSCs and qSCs, which implied these proteins were correlated to the onset of anagen, no matter which type of HFSCs. On the other hand, there were 614 proteins and 616 phosphopeptides were increased only in pSCs, which indicated the great difference between pSCs and qSCs in translation and PTM level (Fig.14, Fig.15). Since it has been

doi:10.6342/NTU201800580

widely accepted that transit amplifying cells are committed from pSCs, we would focus on the differential expression of the proteins/ phosphoproteins for further analysis.

To further investigate the abundant proteins/ phosphopeptides, GO tem analysis were applied to analyze the proteome/ phosphoproteome in pSC-specific and both, respectively (Fig.16B). Interestingly, the GO term of nucleosome assembly was significantly increased in both pSCs and qSCs, which implied the changes in chromosome structure might be similar in these two different type of SCs. To annotate the significantly changed GO terms in pSCs specifically, we found that the mRNA processing, oxidation-reduction process, and translation related GO terms were all significantly enriched in translational level (Fig.16C). In mRNA processing, the enriched proteins could be sorted into 5 groups: heterogeneous nuclear ribonucleoporteins, small nuclear ribonucleoproteins, serine/ argining-rich splicing factors, splicing factors, and RNA binding motif proteins (Fig.16C). In translational control, the enriched IDs could also be sorted into 5 groups: Ribosomal protein large subunits, ribosomal protein small subunit, eukaryotic translation initiation, eukaryotic translation elongation, and solute carrier family 25 (Fig.16C). For phosphopeptides, the GO terms for transcription regulation, mRNA processing, and chromatin remodeling were highly enriched in pSCs specifically (Fig.17B). Since it is widely accepted that

doi:10.6342/NTU201800580

pSCs can undergo massive proliferation and differentiation to give rise to different lineages of transit amplifying cells, our data seemed correlated to the real situation for the onset of HFSC activation. Thus, we kept focused on the regulation of transcription to decipher the function of each protein/ phosphoprotein.

Several important transcription regulatory proteins in our phosphoproteome results were reported to play a crucial role in HFs (Fig.15A, Fig.17C). In pSCs, Trp63, Hdac2, and Tcf3 were investigated to regulate the differentiation process in epidermal differentiation or HF morphogenesis (Mills, Zheng et al. 1999, LeBoeuf, Terrell et al. 2010). Tead3 is involved in the downstream of Hippo pathway, which controlled placode invagination into dermis when HF morphogenesis. (Zhang, Pasolli et al. 2011) Cux1 and Grhl1 were correlated to the differentiation process (Wilanowski, Caddy et al. 2008). Although the function of Cux1 and Grhl1 were still remained known, the immunostaining and NGS result showed to be highly increased in the pSCs and its progenies (Ellis, Gambardella et al. 2001, Luong, van der Meijden et al. 2002). The hairless gene, which control the hair regeneration, was also phosphorylated in pSCs while early anagen (Panteleyev, Botchkareva et al. 1999, Zhu, Xu et al. 2017). The Foxk1/2 proteins, which are reported to be the downstream target of wnt and mTORC1 pathway, were also be phosphorylated according to our profile (Wang, Li et al. 2015).

doi:10.6342/NTU201800580

Another mTORC1 downstream, Rps6ka4, was also been phosphorylated, which implied the mTORC1 might be involved in the activation of pSCs. Several phospho-sites were both enriched in pSCs and qSCs, such as Dnmt1 ^{S22}, Gata3 ^{S161}, Bnc2 ^{S336}, Irf6 $^{S424, T425}$, Trp63 ^{S365} and Tfap2c ^{S472}, ect. Of these phsohpo-proteins, the *Gata3* is important for developing IRS structure (Kaufman, Zhou et al. 2003, Kurek, Garinis et al. 2007). Loss of Gata3 would lead to the malformation of mature hair fibers. Taken together, the proteome/ phospho-proteome profile provided the useful hind that demonstrate which protein/ phosphoprotein might be involved in the activation of HFs. Via comparing with previous functional study, we found several important candidates were also in our profile, which indicated the accuracy of the TMT-based Mass technique.

doi:10.6342/NTU201800580

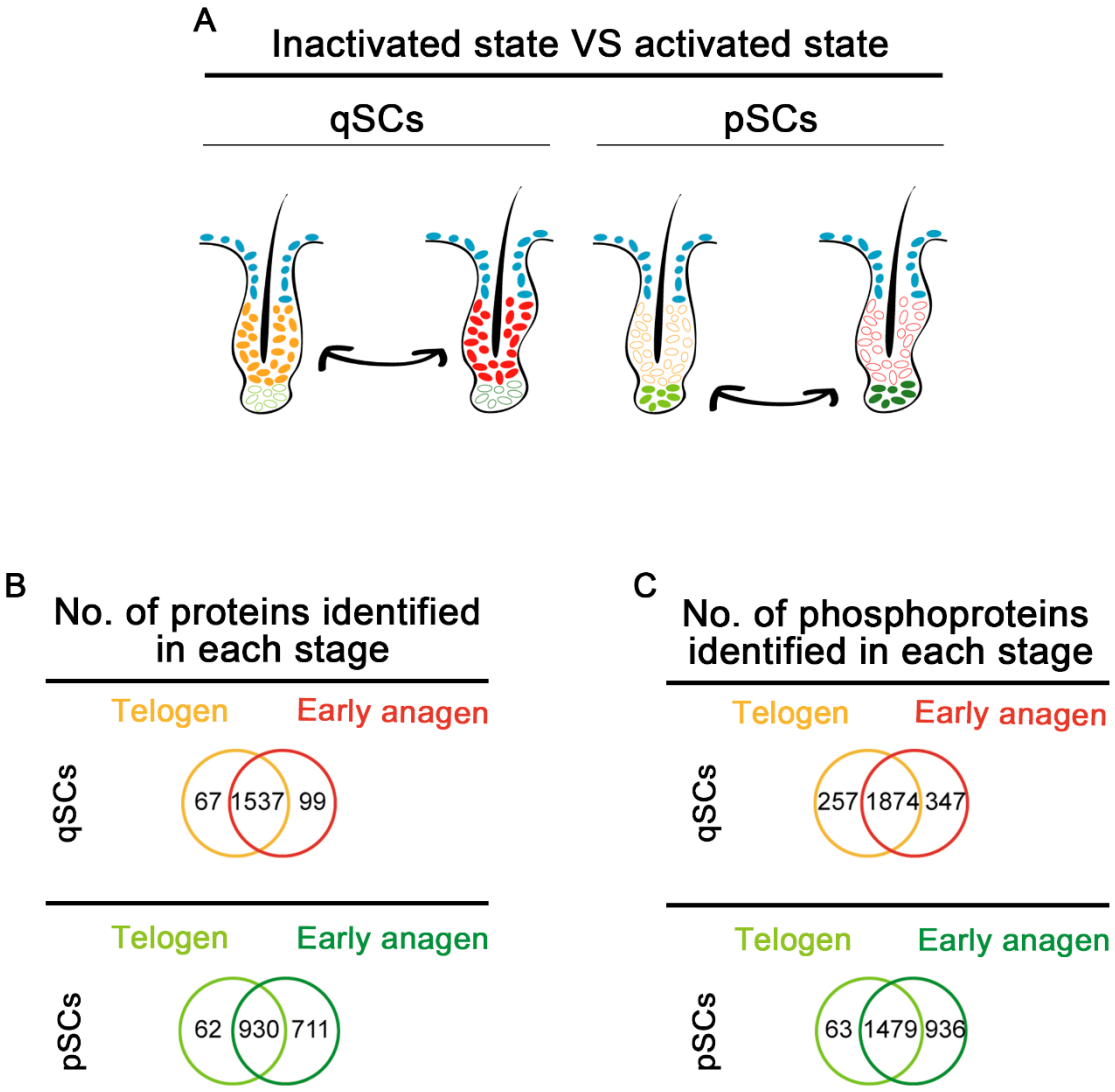

Figure 13. The numbers of identified proteins and phosphopeptides in each hair cycle stages.

(A) Schematic of the comparison of inactivated and activated state in pSCs or pSCs, respectively.

(B) Quantification of identified protein numbers in each population.

(C) Quantification of identified phosphopeptide numbers in each population.

doi:10.6342/NTU201800580

A

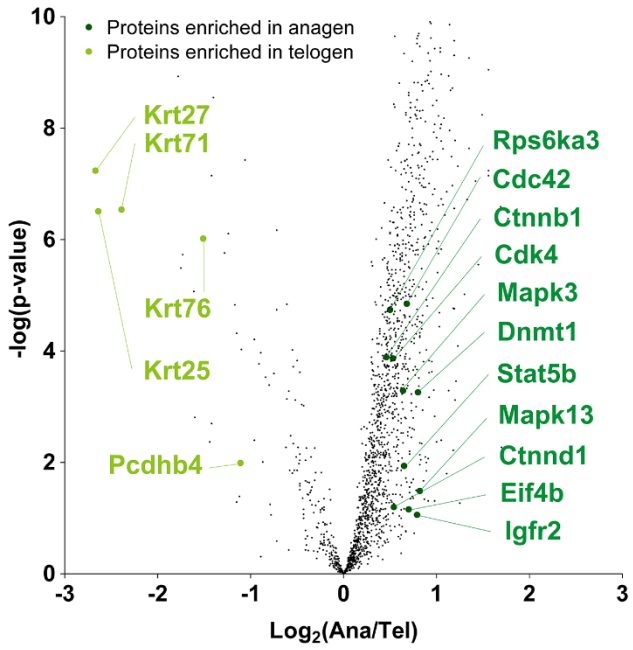

B

Kinases and its associated proteins in activated state	
Ak1	Mob4
Cdk4	Nme1
Csnk1a1	Nme2
Dapk2	Oxsr1
Mapk3	Pfkl
Mapk13	Pgk1
Mob1a	Rps6ka3

Figure 14. Identified proteins associated with signal transduction in pSCs volcano plot

Through the comparison of inactivated and activated state, several proteins are identified specifically in the activated pSCs or qSCs, including the proliferation related proteins.

(A) The volcano plot indicates the specifically expressed proteins, including the reported HFSC markers, and the putative pSC or qSC markers.

(B) The enrichment of kinases and its related proteins in proteome are identified in activated pSCs.

doi:10.6342/NTU201800580

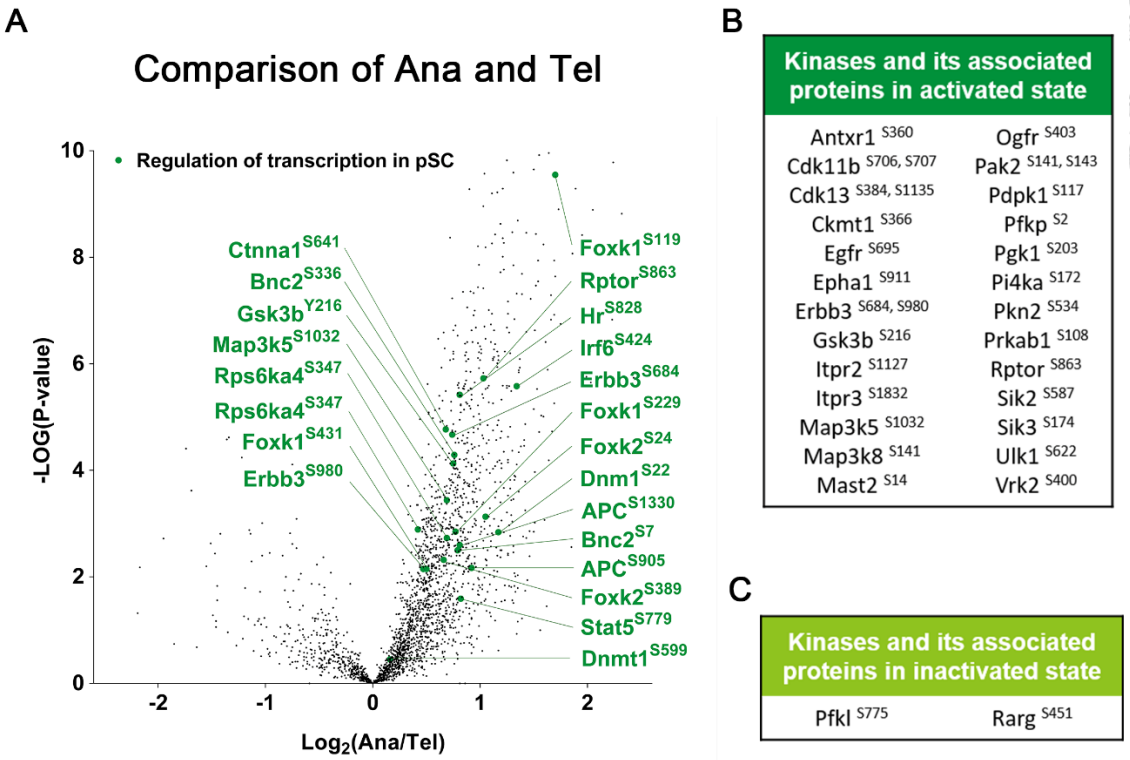

Figure 15. Through the comparison of pSCs and qSCs, ceratin phosphopeptides are identified specifically in the pSCs or qSCs.

(A) The volcano plot indicates the phospho-site of keratin proteins which are enriched in pSCs or qSCs.

(B) The enrichment of kinases and its related proteins in phosphoproteome are identified in activated pSCs.

(C) The enrichment of kinases and its related proteins in phosphoproteome are identified in inactivated pSCs.

doi:10.6342/NTU201800580

A

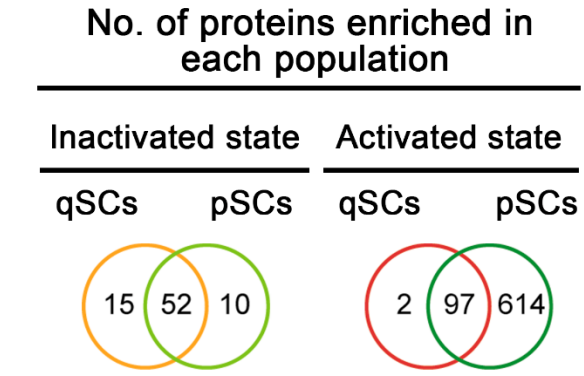

B

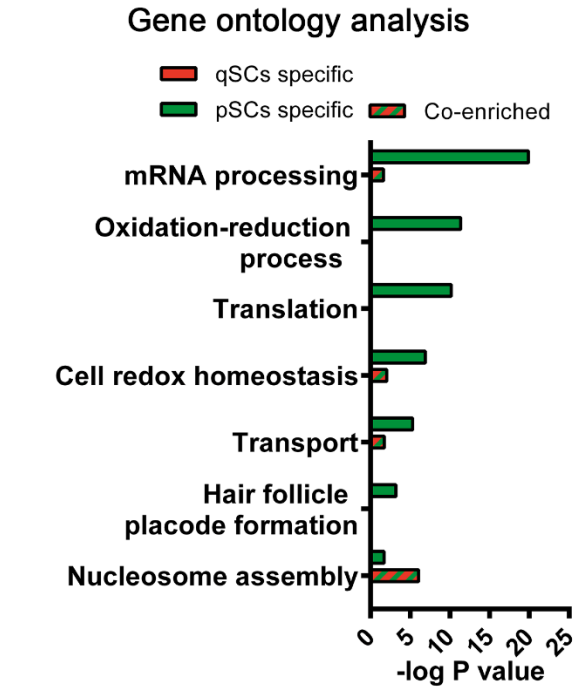

C

mRNA processing	
Heterogeneous nuclear ribonucleoprotein	Hnrnpa3, Hnrnpf, Hnrnpl, Hnrnpll, Hnrnpu
Small nuclear ribonucleoprotein	Snrnp40, Snrpb, Snrpd3, Snrpe, Snrpa
Serine/ arginine-rich splicing factor	Srsf1, Srsf2, Srsf3, Srsf6
Splicing factor	Sf3a2, Sf3a3, Sf3b4
RNA binding motif protein	Rbm25, Rbm8a
Oxidation-reduction process	
NADH dehygrogenase	Ndufa10, Ndufa11, Ndufa7, Ndufa8, Ndufa9, Ndufs4, Ndufs5, Ndufs8
Cytochrome protein	Cyp2s1, Cyb5r3, Cyb5a, Cyb5b
Ubiquinol-cytochrome c reductase protein	Uqcrb, Uqcrc1, Uqcrq
Peroxiredoxin protein	Prdx1, Prdx2, Prdx4, Prdx5
Succinate dehydrogenase complex	Sdha, Sdhb, Sdhc
Translation	
Ribosomal protein large subunit	Rpl10a, Rpl18, Rpl18a, Rpl23a, Rpl24, Rpl26, Rpl35, Rpl4, Rpl7
Ribosomal protein small subunit	Rps12, Rps13, Rps15a, Rps19, Rps2, Rps24, Rps27l, Rps27a, Rps28, Rps4x, Rps9
Eukaryotic translation initiation	Eif1ax, Eif3e, Eif3i, Eif3l, Eif4g1, Eif4b, Eif5a
Eukaryotic translation elongation	Eef1a1, Eef1b, Eef1g
Solute carrier family 25	Slc25a13, Slc25a5, Slc25a1, Slc25a3

Figure 16. The GO analysis of proteome indicates the difference between activated and inactivated stage of pSCs.

(A) Via Venn diagram, proteins enriched in qSCs or pSCs could be classified into 3 groups: pSC specific, qSC specific, and co-enriched.

(B) GO term analysis of qSCs in inactivated, activated, and co-enriched state.

(C) pSC specific protein IDs is largely consisted of mRNA processing, Oxidation reduction process and translation.

doi:10.6342/NTU201800580

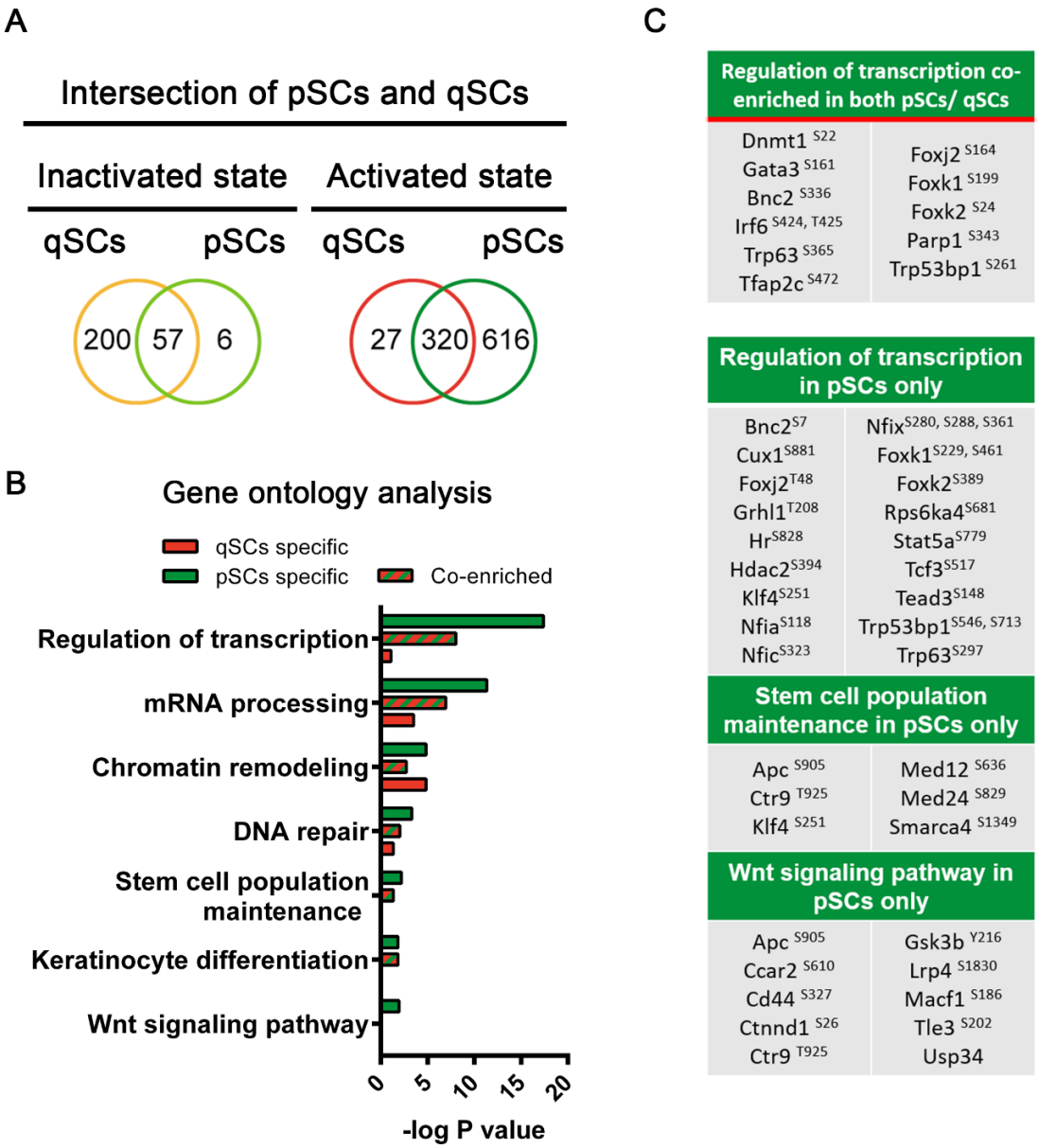

Figure 17. The GO analysis of phosphoproteome indicates the pSC specific and co-enriched groups.

(A) Via Venn diagram, phosphopeptides enriched in qSCs or pSCs could be classified into 3 groups: pSC specific, qSC specific, and co-enriched.

(B) GO term analysis of 3 groups.

(C) Several important proteins factors are found to be phosphorylated in the GO analysis of pSC specific and co-enriched groups.

doi:10.6342/NTU201800580

3.4 The kinase prediction shows the possibility to regulate activation process of hair cycle.

Since the phosphoproteome provided the phospho-site of the enriched proteins, we would like to generate the prediction of kinases that might involve in the activation of pSCs. In this prediction result, 14 motif logos was identified through motif-X analysis (Schwartz, Chou et al. 2009, Chou and Schwartz 2011). The phosphopeptides in certain motif logo were further analyzed by GPS3.0 to predict the upstream kinases (Xue, Ren et al. 2008). Therefore, we summarized the frequency of predicted kinases of certain motif logo to get the score, and the heat map showed that there existed the trend of kinases to phosphorylate certain motif.

In our predicted kinome result, we found that Akt, RSK, and SGK kinase family shared similar motif logo, such as R..S, R..SD, RR.S, and R..SP. Another group of motif logo, inducing R..SP, P.SP, TP, SP, were tend to be phosphorylated by mTOR, CDK, and MAPK kinase family. Although CK1 has the wide spectrum to phosphorylated a variety of motifs, the heat map still indicated that CK1 and CK2 have the higher score in the prediction of phosphorylating S..E, SD..E, SD.E.E, and S..EE. Additionally, the BMPR1B showed lower score in the heat map, which corresponded to previous research that BMP signaling was compromised in the activation of hair cycle. Several of the

doi:10.6342/NTU201800580

predicted kinases or its associated proteins were identified in the phosphoproteome result, such as Rps6ka4, Rptor, Cdk11b, Cdk13, GSK3β, Map3k5, and Map3k8 (Fig.15A, B). It has been reported that Rps6ka4 is the downstream target of mTORC1 to mediate cell proliferation and translation (Tsai, Chen et al. 1993, Bragado, Groblewski et al. 1998). Rptor, the adaptor proteins of mTORC1, was found that the phosphorylation of serine 863 was primed for subsequent phospho-sites to reach the best kinase activity (Foster, Acosta-Jaquez et al. 2010). Thus, we got a hint from both the phosphoproteome and the kinome result that mTORC1 might play a key role in regulating hair cycle entry. Based on previous study, the high scored kinases were also associated with mTORC1, such as Akt, S6K, and JNK in our predicted kinome. It has also been suggested that Akt-mTOR-S6K axis plays a key role in transducing morphgenic signals, which corresponds to the state of pSCs in early anagen to undergo massive proliferation and differentiation. In brief, this predicted kinome result provided the hint that mTORC1 signaling pathway might play a centrol role in the activation of pSCs in the early anagen.

doi:10.6342/NTU201800580

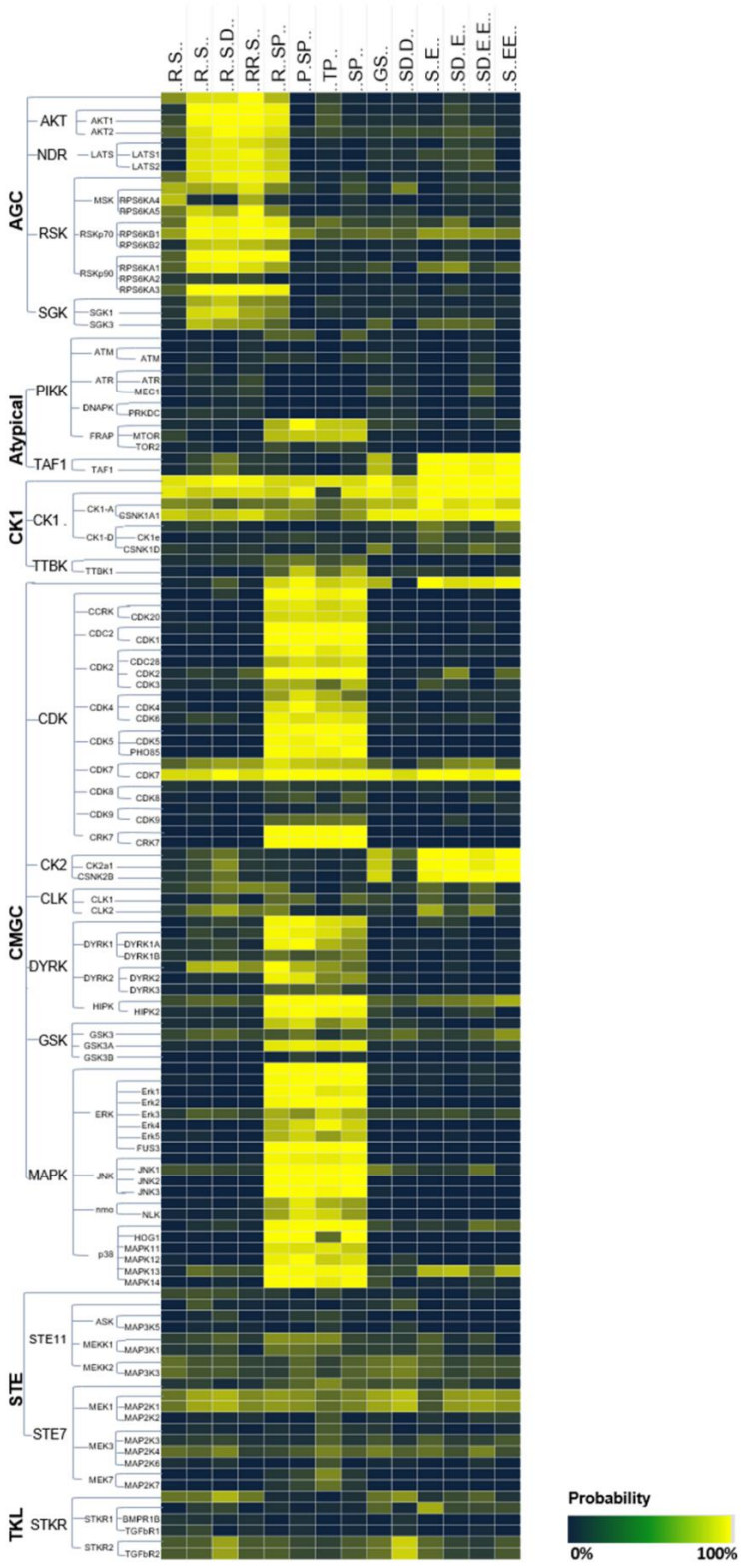

Figure 18. The kinase prediction of phosphoproteome in early anagen of pSCs indicates that mTOR, CDKs, and MAPKs are correlated to anagen entry.

doi:10.6342/NTU201800580

3.5 Reactome reveals more confidential result for mTORC1 signaling in the early anagen.

To reveal the kinase prediction result, we generate the reactome to search for the correlation between the predicted kinases and the substrates in phosphoproteome (Fig.19). To achieve the mapping of reactome, we selected the predicted kinase, such as Akt, mTOR, Rps6ka4, and JNK, to establish the physical interaction by STRING (Szklarczyk, Morris et al. 2017). The phosphopeptides were categorized by its motif logo as previous result (Fig.18), and the subsequent reactome was established followed by this classification. Therefore, we would get the physical interaction between the predicted kinases and the classified phosphopeptides.

Based on the reactome data, we found that mTOR would interact with several well-known proteins, such as APC, Trp63, Stat5, and Rps6ka4 under the SP motif. The adaptor protein, Rptor, and the other kinases like Map3k5 and Tp53bp1 were identified in the P.SP motif. Except for mTOR signaling, the interaction also exists between Rptor and JNK, and this result increases the complexity of reactome. Therefore, the reactome data provided more confidential clues of mTORC1 signaling to regulate the onset of hair cycle.

doi:10.6342/NTU201800580

In addition to Rptor protein, Map3k5 in our phosphoproteome result , was also been found to interact with mTOR and JNK. Although the function of Map3k5 is not fully understood, it might still play a role in the activation of pSCs in the early anagen. The other substrates, such as Foxk1 and Foxk2, is known to be phosphporylated by mTORC1 to regulate autophage and HDAC (Bowman, Ayer et al. 2014, Nakatsumi, Matsumoto et al. 2017). The Trp63 protein, which controls the development of epidermis and its appendages, are also correlated to mTORC1 activity through Notch signaling (Li, Lee et al. 2014). The Trp53bp1, which stabilized the p53 in the nucleus, is also been mediated by mTORC1, especially under the DNA damage response (Bandhakavi, Kim et al. 2010).

doi:10.6342/NTU201800580

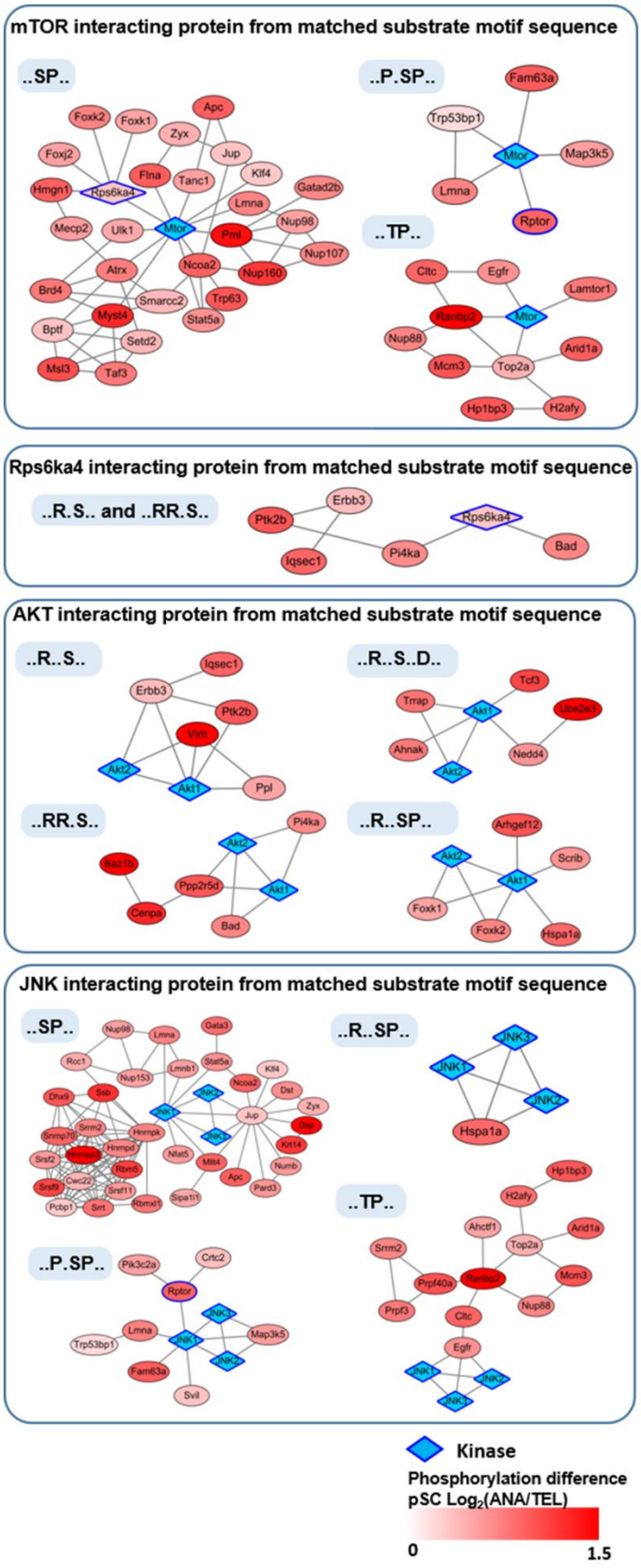

doi:10.6342/NTU201800580

Figure 19. Reactome analysis of early anagen in pSCs indicates that the predicted kinase might exist physical interactions.

doi:10.6342/NTU201800580

3.6 Validation of the mTORC1 signaling of pSCs in the onset of early anagen

To identify the mTORC1 signals in the transition of hair cycle, we utilized immunostaining to prove the increased phosphorylation of its downstream targets, such as S6K and S6 (Fig.20A-C). In order to investigate if the activation of mTORC1 also followed the roles of two-step activation, we double stained with qSCs marker Cd34 and gave short-pulse BrdU labeling to mark the proliferating cells (Fig.20A-C). Interestingly, the p-mTOR, p-S6K and p-S6 were dramatically increased first in the proliferating 2^{nd} HG in anagen I (Fig.20A-C). In the following anagen II, the phosphorylation of mTOR, S6K and S6 were shown to be increased in the invaginating 2^{nd} HG and the lower bulge. Besides, those 2^{nd} HG cells was undergoing massive proliferation and differentiation in early anagen. This result demonstrated that mTORC1 signaling presented high similarity with two-step activation model, which the pSCs were activated prior to qSCs. Therefore, our immunostaining proved the hypothesis from the enriched phospho-sites of Rptor ^{S836}in the phosphoproteome, mTOR kinase in the predicted kinome, and the S6K in the reactome. Next, we would like to examine the functional assay to perturb mTORC1 signaling in pSCs in the onset of early anagen.

doi:10.6342/NTU201800580

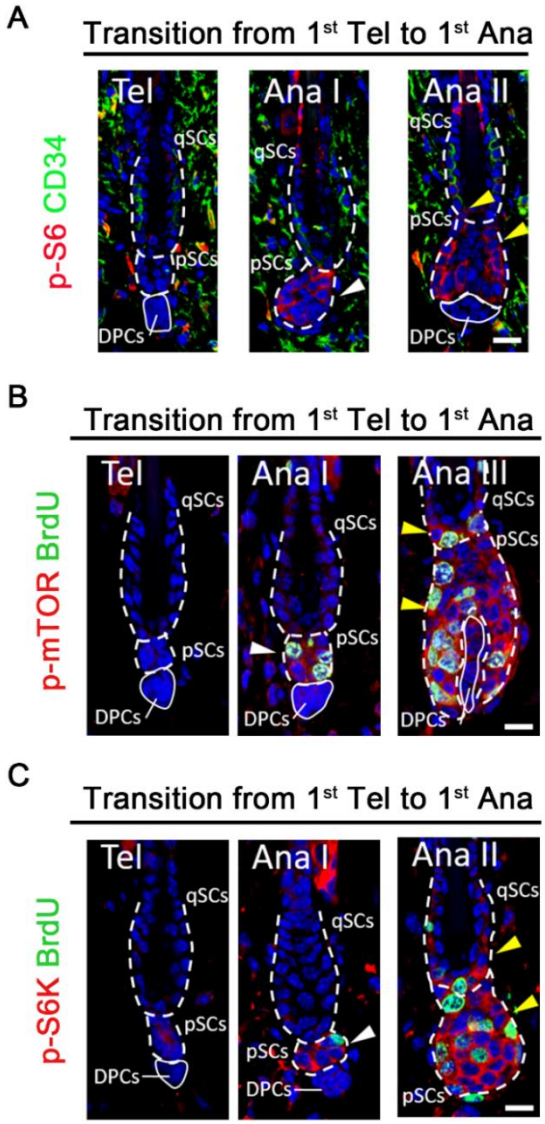

Figure 20. Immunostaing of mTORC1 related proteins in early anagen

The phosphorylation of mTORC1 signaling, which is highly increased in pSCs prior to qSCs, and the phosphorylation of mTORC1 is correlated to the two-step activation model.

(A) The S6 phosphoylation indicates the activation of mTORC1 is activated in the pSCs prior to qSCs.

(B, C) The phosphorylation of S6 and mTOR denote that mTORC1 activity is highly increased in the proliferating pSCs rather than qSCs. The white dash line marks the region of pSCs and qSCs. The white solid line denotes the DPCs. The white arrow head and yellow arrow head indicate the positive signaling in anagen I and anagen II, respectively. Scale bar = 20 μm.

doi:10.6342/NTU201800580

3.7 *Rptor* is required for pSC activation in the early anagen

To determine if the mTORC1 regulates the hair cycle entry in pSCs, *Lgr5creER; Rptor*$^{flox/flox}$ mice were crossed for conditional ablation of mTORC1 signaling. Tamoxifen was given every second day for 3 times by intraperitoneal injection to 18-day-old mice (Fig.21A). In the control littermate with TAM injection, the hair cycle progression followed as the previous report (Muller-Rover, Handjiski et al. 2001). However, the hair regeneration in the *rptor* deficient HFs was significantly postponed (Fig.21B). The histology analysis revealed the HF structure in control littermates had entered into anagen II, but the HF structure of cKO mice were stayed and remained in telogen (Fig.21C). The expression of Rptor protein was strong in the control 2nd HG, but was attenuated in the cKO 2nd HG (Fig.21D). Although *rptor* deficiency would cause lethality while embryonic development (Murakami, Ichisaka et al. 2004, Guertin, Stevens et al. 2006), the ablation of *rptor* in pSCs did not cause dystrophic changes in telogen HFs (Fig.21C). To verify if the delayed hair cycle entry was caused by decreased proliferation, the pulse-chase BrdU labeling assay demonstrated the proliferation was ceased in both pSCs and qSCs (Fig.22B). To check if the mTORC1 was activated in HFSCs, we justified the mTORC1 activity by p-S6 (Ser265/267) antibody (Fig.22B). Our result showed the mTORC1 signaling was significantly

doi:10.6342/NTU201800580

increase in the lower bulge and the ORS of control HFs, but the p-S6 staining of cKO HFs showed extremely low in the pSCs or qSCs. These results indicated that mTORC1 activity was required for the activation of hair cycle, and the loss of mTORC1 activity would postpone the activation of HFSCs. In addition to mTORC1 downstream targets, we also found the Wnt signaling was also be attenuated in the 2nd HG (Fig.22A-B). In the control HFs, the translocation of β-catenin was obvious in the 2nd HG surrounding the DPCs (Fig.22A), but the expression of β-catenin remained low in the cKO HFs. The downstream effector, Lef1, could not accumulated in the nucleus of 2nd HG of cKO HFs (Fig.22A). To summarized the functional study of Rptor in pSCs, we proved that the phosphoprotome and kinome data provided useful hints to investigate the instructive cues in the pSCs, and one of the instructive cues, Rptor, can functionally control the activation of mTORC1 signaling to wake up the inactivated pSCs in the late telogen.

doi:10.6342/NTU201800580

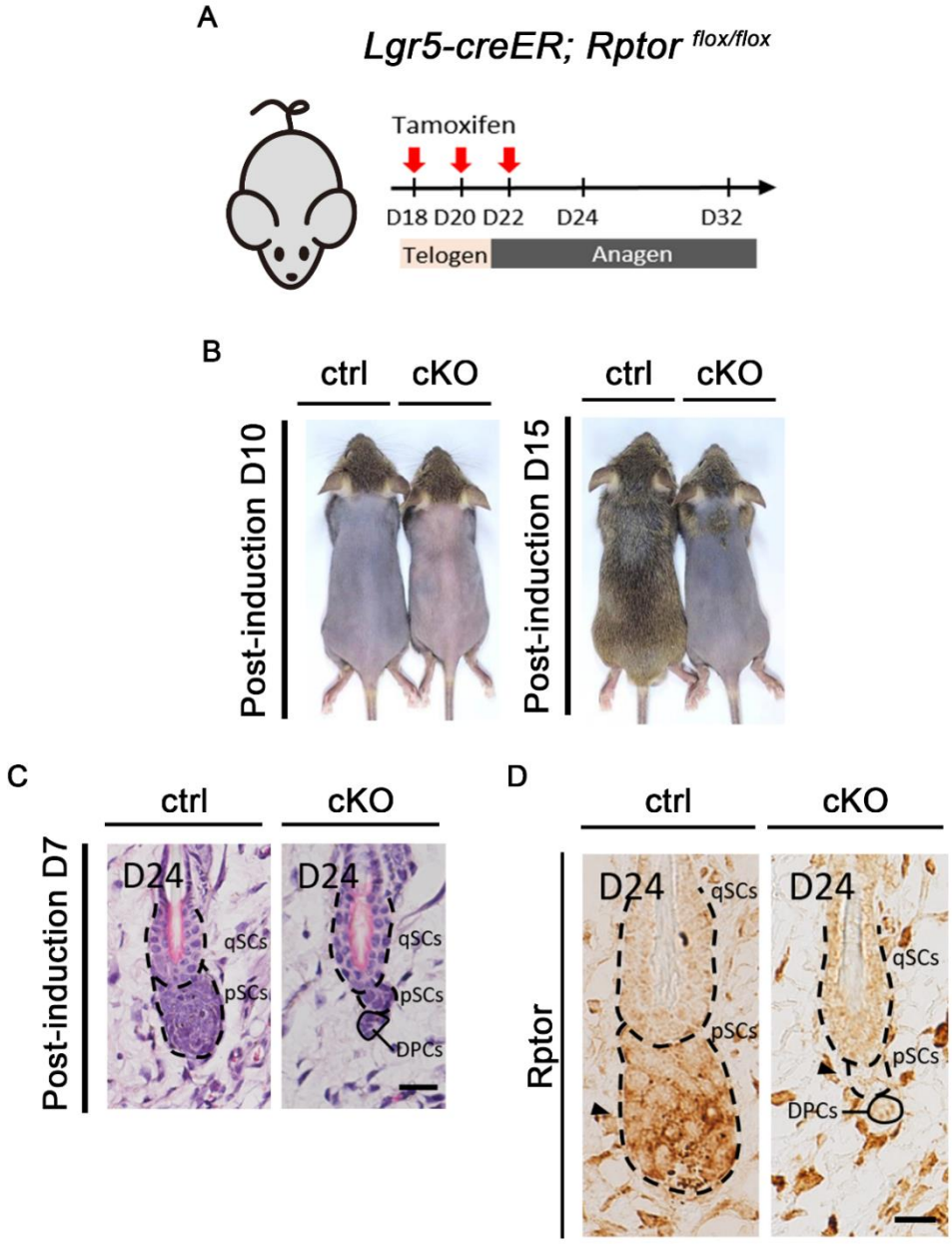

Figure 21. Genetic ablation of *Rptor* gene would postpone the HFSCs activation and delayed the anagen entry

(A) Experimental design of transgenic mice model to ablate *Rptor* in $Lgr5^{+}$ cells.

(B) The hair cycle progression is postponed by ablation of pSCs

(C) The anatomy of HFs shows the delayed anagen entry at postnatal Day24.

(D) *Rptor* is expressed higher in the control littermate, but diminished in the pSCs in cKO mice. The black dashed line marks the region of pSCs and qSCs, and the black solid line indicates the DPCs. The black arrow head points to the positive staining of Rptor. Scale bar = 20 μm.

doi:10.6342/NTU201800580

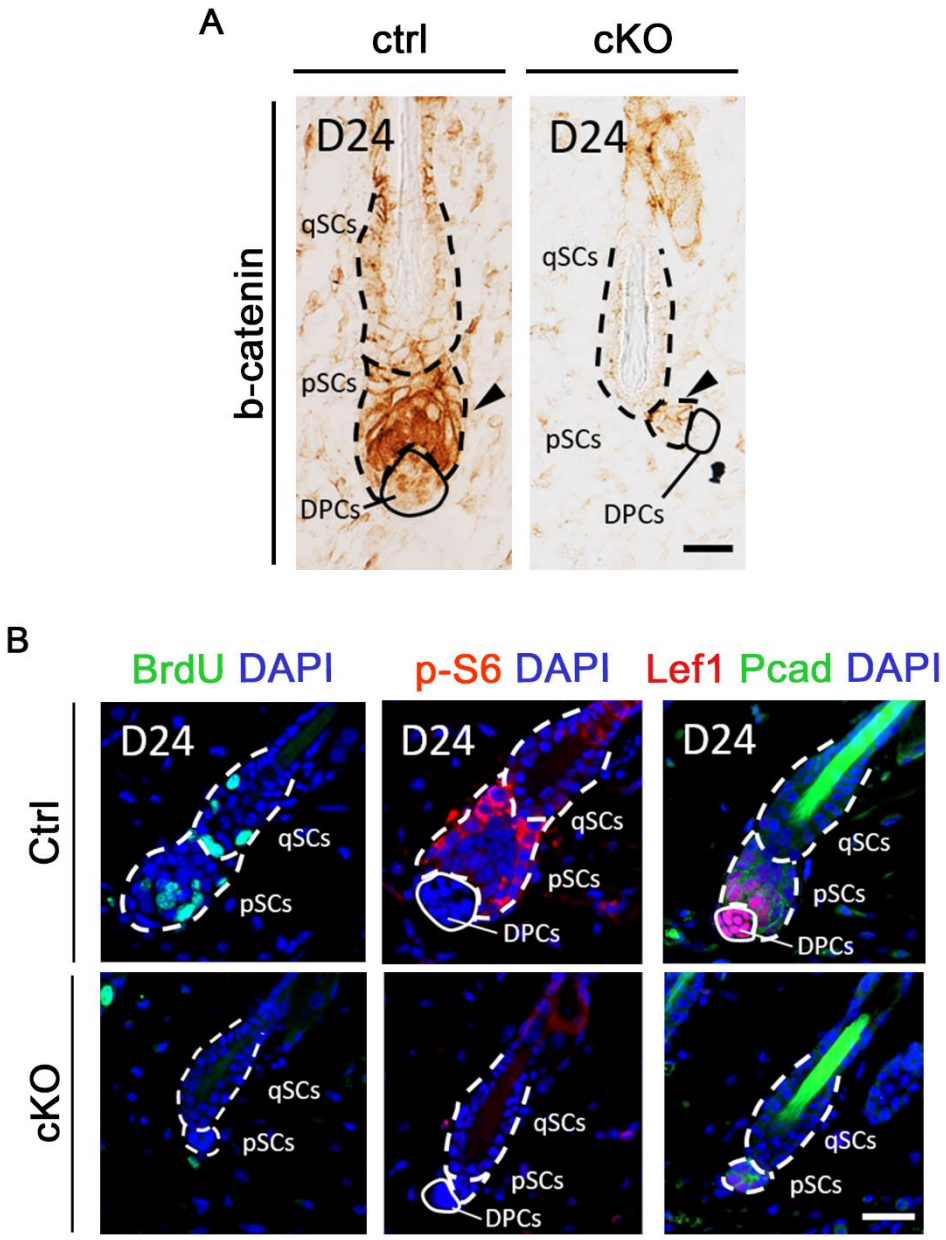

Figure 22. Genetic ablation of *Rptor* gene diminished mTORC1 and Wnt signaling

(A) The translocation into nucleus of b-catenin indicates the activation of Wnt signaling in ctrl pSCs, but Wnt signaling is attenuated in cKO pSCs.

(B) Immunostaining of BrdU, p-S6 and Lef1 indicates that *Rptor* is required for activation of hair cycle, and the deficiency of *Rptor* might lead to inactivation of mTORC1 signaling and Wnt signaling. The white solid line denotes the DPCs. Scale bar = 20 μm.

doi:10.6342/NTU201800580

3.8 IR induces dystrophic change of hair bulb whose regeneration is associated with activation of mTORC1 activity

To investigate the response of anagen HFs to IR injury, 29-day-old mice were irradiated at 4Gy when dorsal HFs were in anagen and skin specimens were collected after IR injury. In the following 9 days after IR, there was no significant hair loss, and the growth of hair coat seemed unaffected when compared with the un-irradiated control mice (Fig3.19). The degree of IR injury to HF structures was also analyzed histologically (Fig 3.20A-D). It showed that 4Gy IR induced progressive hair bulb dystrophy for up to 48 hours after IR and the injured hair bulb was gradually repaired from 48 hours to 96 hours after IR (Fig 3.20C). The results showed that cells in hair bulbs were highly sensitive to IR injury, leading to IR-induced dystrophic changes of HF. Despite the severe dystrophic change after IR, HFs were able to mount regenerative attempts to resume hair growth.

Since mTORC1 signaling was required for HFSC activation during physiological HF regeneration from telogen, we explored whether mTORC1 was also activated following IR injury. To detect the activation of mTORC1 signaling, we stained for phospho-S6 (pS6) protein, the downstream target of activated mTORC1 signaling

doi:10.6342/NTU201800580

(Fig.25). In normal anagen HFs, while the cells in outer root sheath showed intense pS6 staining (Fig.25), the TACs in the hair bulb showed little, if not any, presence of pS6. Soon after IR treatment, the signals of pS6 emerged in hair bulb, with extension to the outer root sheath, inner root sheath, and pre-cortex (Fig.25). The signals in the hair matrix progressively increased from 3 hour to 24 hours and gradually vanished in the hair bulb region from 48 hours to 96 hours. At 96 hours, the hair bulb structure was almost restored from the dystrophic change (Fig.24A-D). The temporospatial dynamics of mTORC1 activity which correlated with the regeneration process of the hair bulb suggests that activation of mTORC1 might contribute to the regenerative process in IR-induced injury, especially in the TAC compartment.

doi:10.6342/NTU201800580

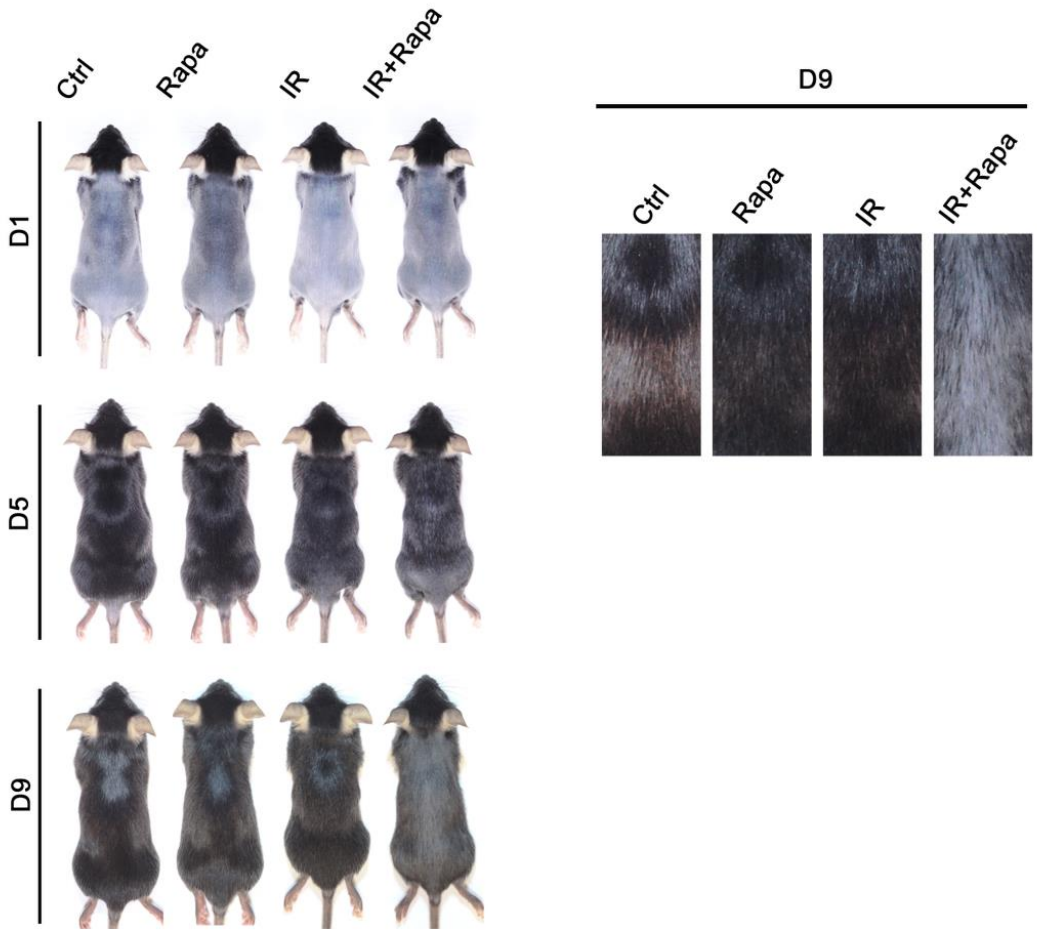

Figure 23. Inhibition of mTORC1 signaling did not perturb physiological cycling of hair growth but led to alopecia from IR injury.

(a) Mice were shaved before IR treatment. 4Gy IR or rapamycin alone did not induce significant hair loss and hair continued to emerge from the skin surface. Combination of 4Gy IR and rapamycin induced hair loss that began form post-IR day 5 and became more severe on post-IR day 9. (N=3~5 mice in each group) Rapa: rapamycin.

(b) Magnified pictures of mouse pelage hair from panel (a).

doi:10.6342/NTU201800580

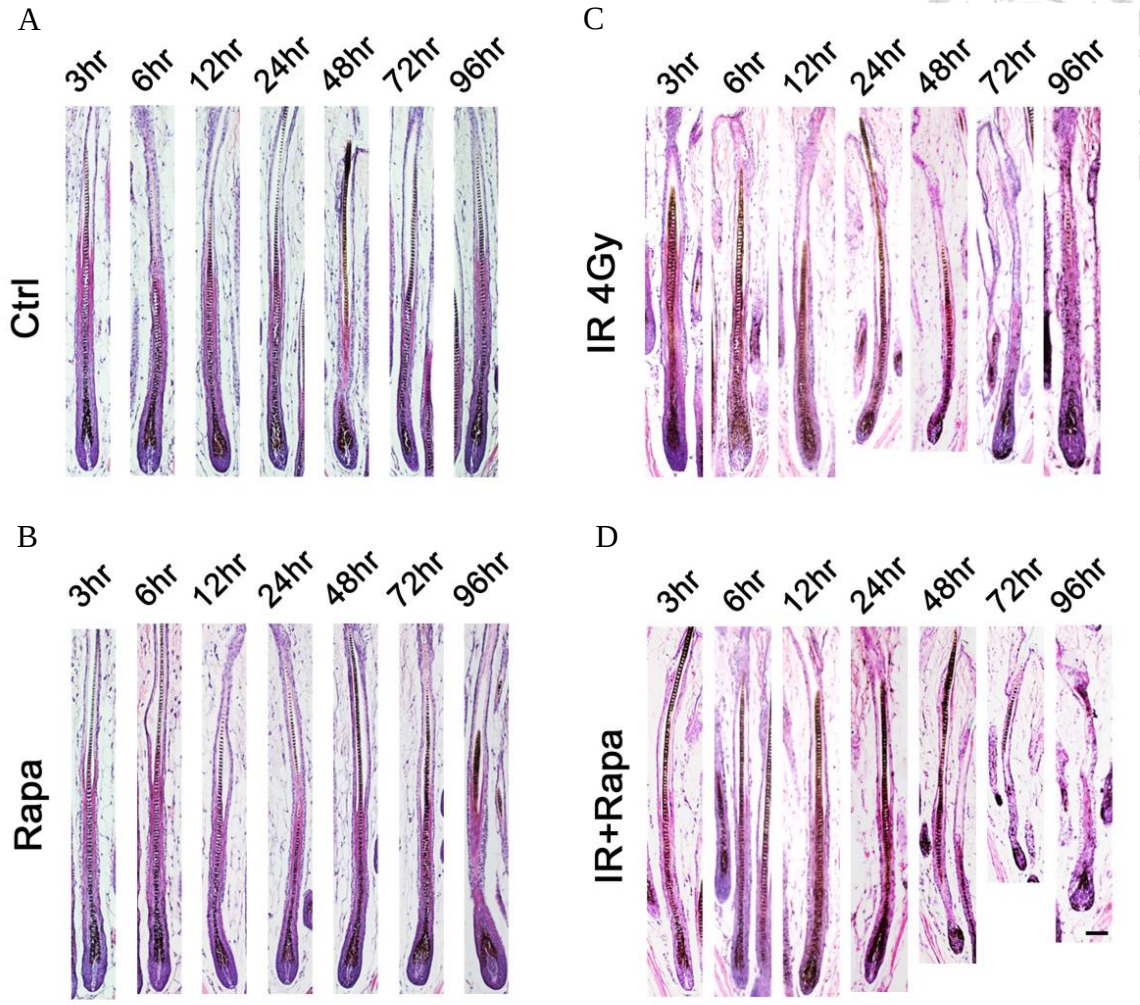

Figure 24. The histology of HFs after different treatment.

(A) The control mice without any treatment.

(B) Rapamycin alone did not induce structural changes of HFs.

(C) 4Gy IR induced dystrophy with shrinkage of hair bulbs within 24 hours and the atrophic hair bulbs quickly grew back to its normal size at 96 hours.

(D) Combination of 4Gy IR and rapamycin induced more severe and prolonged HF dystrophy. Normal hair bulbs were not fully recovered at 96 hours post IR.

doi:10.6342/NTU201800580

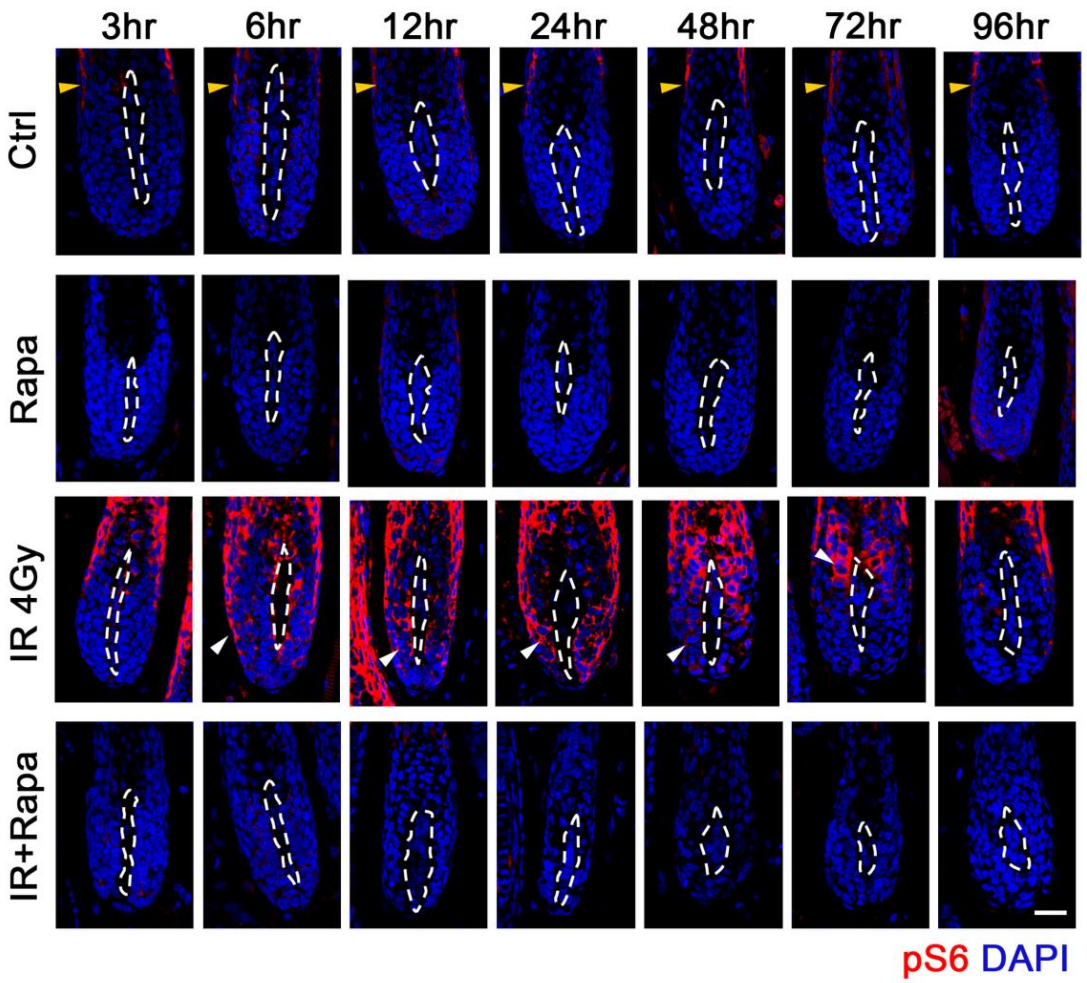

Figure 25. Immunostaining of mTORC1 downstream target pS6.
In the control mice, the pS6 signals were only present in the outer root sheath cells above the hair matrix (yellow arrowheads). Rapamycin alone abolished the pS6 signals in HFs. After 4Gy IR treatment, the pS6 staining was highly strengthened in the hair matrix (white arrowheads). The administration of rapamycin suppressed the IR-induced pS6 signals in the hair matrix. Dashed lines indicate dermal papilla. Scale bar = 20μm

doi:10.6342/NTU201800580

3.9 mTORC1 inhibition does not affect normal anagen progression but inhibits regeneration after IR injury

Because IR induced hair loss in rapamycin-treated mice, we examined whether the production of mature hair shafts was affected. Hair cortex and IRS were recognized by specific antibodies, AE13 and AE15, respectively. Compared with control mice, mice treated with rapamycin still preserved differentiation toward IRS and hair cortex (Fig.24). Without rapamycin treatment, IR only induced mild disruption of hair cortex and IRS, and both became fragmented in the region right above the hair bulb on day 2 (Fig.26B, 26E) and their expression was quickly restored on day 3 (Fig.26C, 26F). Under rapamycin treatment, IR induced severe disruption of hair cortex and IRS (Fig.26B-E). Their expression was progressively reduced from day 1 to day 3 following IR and the expression was almost absent on day 3 after IR injury. Since the concentric layers from IRS to the hair shaft were derived from the hair matrix, the transient disruption of IRS and hair cortex right above the hair bulb after IR suggested that cell output from hair matrix and their subsequent differentiation were suppressed by IR on day 2. HFs were endowed to quickly repair the structural defects to prevent further dystrophy and hair loss. However, rapamycin treatment suppressed the regenerative attempts, leading the halted hair shaft production with subsequently hair loss.

doi:10.6342/NTU201800580

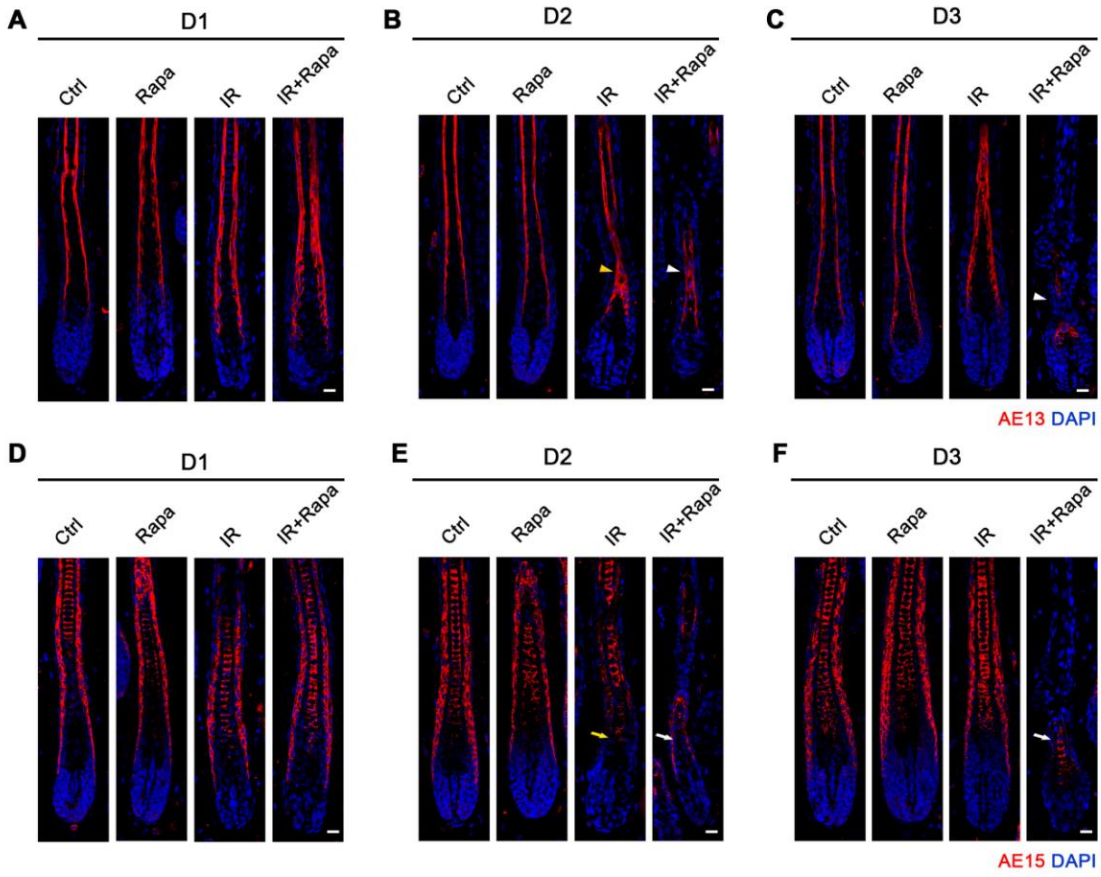

Figure 26. Inhibition of mTORC1 signaling disrupted HS and IRS production after IR injury.

Hair cortex and IRS were detected by antibodies, AE13 and AE15, respectively. (A-C) AE13 staining. Rapamycin treatment only did not affect hair cortex production. 4Gy IR transiently disrupted hair cortex on day 2 (yellow arrowhead) and hair cortex structure was recovered on day 3. Rapamycin treatment leads to severe disruption of hair cortex on both day 2 and day 3 (white arrowheads). (D-F) AE15 staining. Rapamycin treatment only did not affect the structure of IRS. IRS was transiently disrupted by 4Gy IR on day 2 (yellow arrow) and the IRS structure was repaired on day 3. Rapamycin treatment severely disrupted IRS on day 2 (white arrow, day 2) and the structure of IRS was almost absent on day 3 (white arrow, day 3). Scale bar: 20μm.

doi:10.6342/NTU201800580

3.10 Inhibition of mTORC1 signaling increases cell apoptosis and suppresses regenerative proliferation after IR-induced injury

To explore whether mTORC1 signaling affects cell survival after IR injury, we quantified cell apoptosis by TUNEL (terminal deoxynucleotidyl transferase dUTP nick end labeling) staining. In control mice and rapamycin-treated mice, we did not detect cell apoptosis in the hair bulbs (Fig.27A-B). IR induced cell apoptosis that progressively increased from 6 hours to 12 hours following IR and then gradually decreased, becoming absent at 72 hours. With rapamycin treatment, IR-induced apoptosis was more extensive and persistent. This result showed that mTORC1 inhibition sensitized the TACs in the hair bulb to IR-induced genotoxic stress, contributing to a greater loss of TACs in the hair bulb. To explore how inhibition of mTORC1 signaling leads to severe dystrophy of HFs after IR injury, we next evaluated cell proliferation by BrdU labeling. In mice with rapamycin treatment only, cell proliferation was similar to the level of control mice (Fig.28A-B). In mice without rapamycin treatment, BrdU+ cells in hair matrix first decreased the first 12 hours after IR treatment and then increased from 24 hour to 72 hours. Under rapamycin treatment, the number of BrdU+ cells was more severely decreased after IR. This result showed

doi:10.6342/NTU201800580

that inhibition of mTORC1 signaling in normal anagen HFs does not suppress the proliferation of hair matrix cells. However, inhibition of mTORC1 impaired the regenerative cell proliferation in hair matrix following IR injury and the decreased proliferation TACs contributed to the delayed repair of the dystrophic hair bulb.

doi:10.6342/NTU201800580

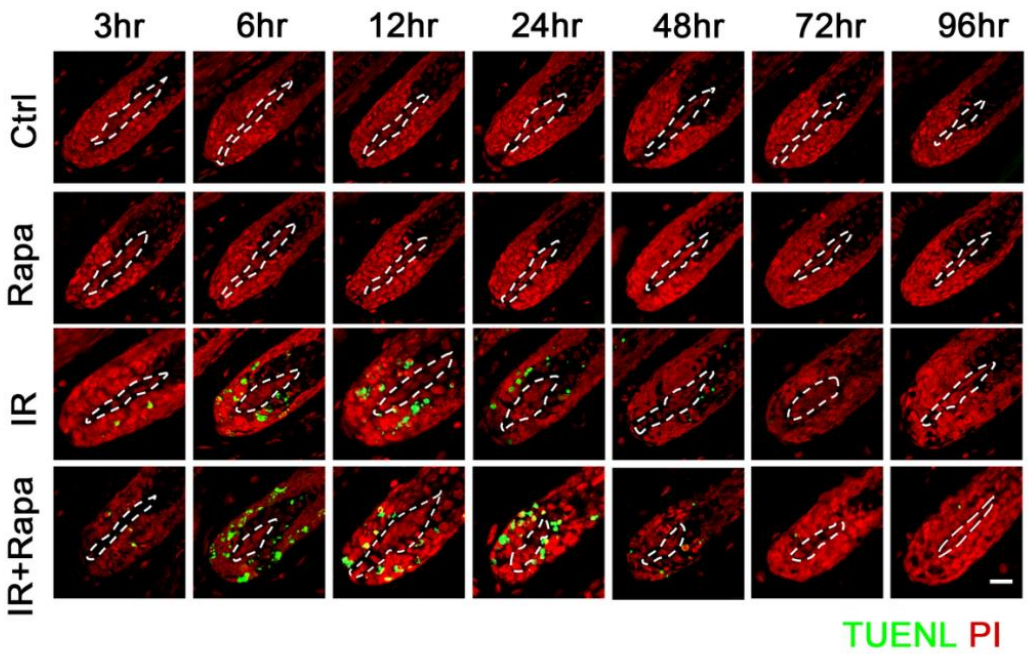

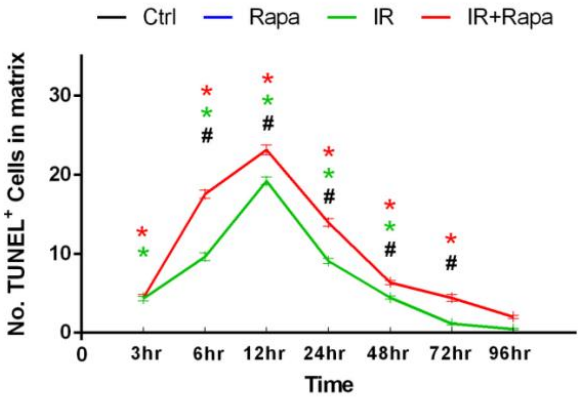

Figure 27. Inhibition of mTORC1 signaling increased apoptosis in the hair matrix after IR injury.

Rapamycin alone did not induce cell apoptosis. 4Gy IR induced cell apoptosis that reached the maximum at 12 hours post IR and the number of apoptotic cells then gradually decreased. Compared with 4Gy IR alone, rapamycin treatment induced higher apoptosis in the hair matrix following 4Gy IR treatment.

Quantification of TUNEL positive cells in the hair matrix. *Green star* * $p<0.05$, IR vs Ctrl; *red star* * $p<0.05$, IR+Rapa vs Ctrl; # $p<0.05$, IR vs IR+Rapa.

Dashed lines indicate dermal papilla. Dotted lines denote the DP cells. Rapa: rapamycin; Ctrl: control.

doi:10.6342/NTU201800580

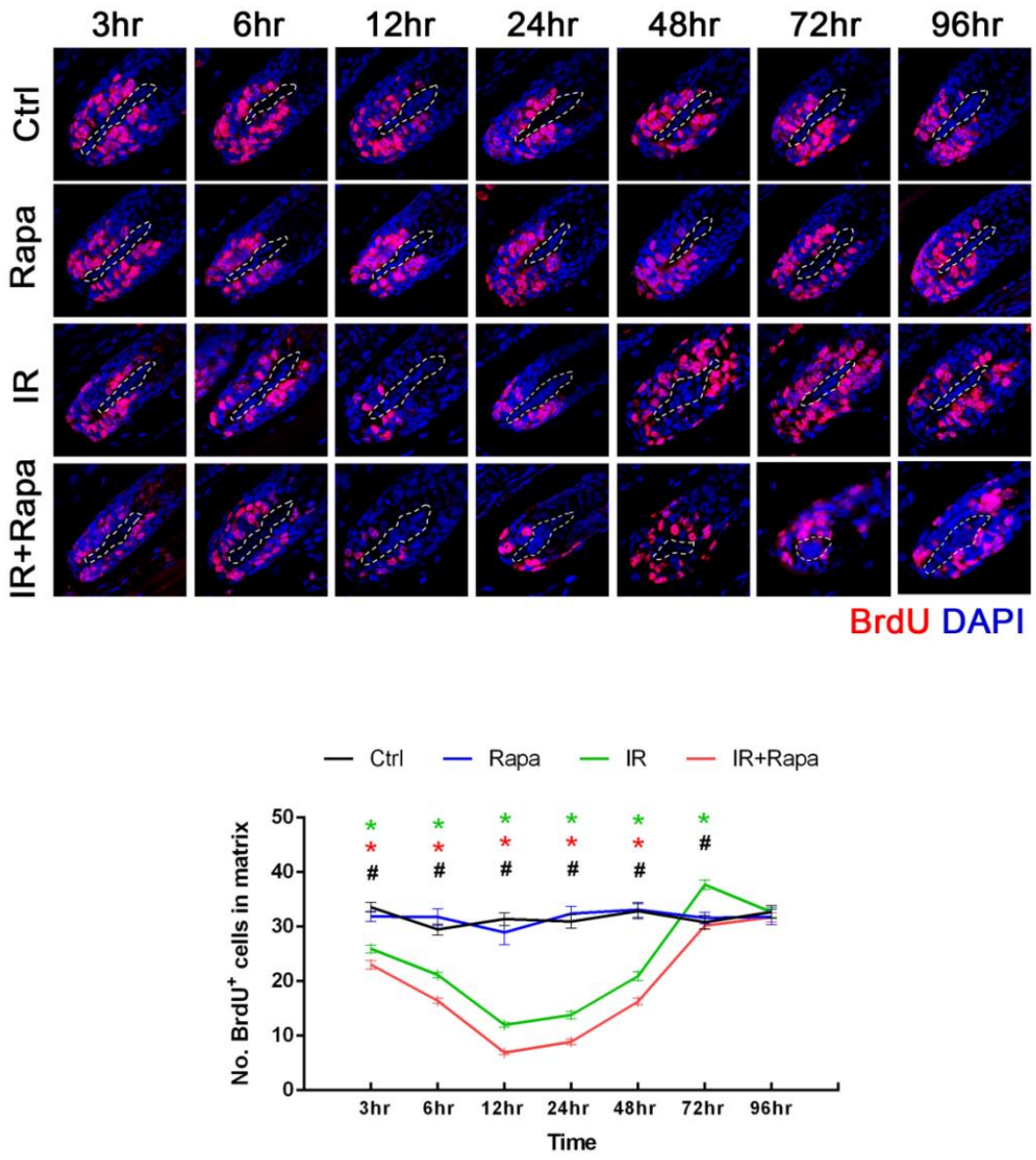

Figure 28. Pulse BrdU labeling and quantification of BrdU in hair matrix.

Rapamycin alone did not significantly reduce cell proliferation in the hair matrix. 4Gy IR reduced cell proliferation in the hair matrix that was most severe at at 12 hours post IR and cell proliferation then gradually increased. Compared with 4Gy IR alone, rapamycin treatment further reduced cell proliferation in the hair matrix following 4Gy IR treatment. *Green star * $p<0.05$*, IR vs Ctrl; *red star * $p<0.05$*, IR+Rapa vs Ctrl; *# $p<0.05$*, IR vs IR+Rapa.

Dashed lines indicate dermal papilla. Dotted lines denote the DP cells. Rapa: rapamycin; Ctrl: control.

doi:10.6342/NTU201800580

3.11 mTORC1 inhibition delayed the recovery of Wnt/β-catenin signaling in hair matrix after IR injury

Wnt/β-catenin signaling pathway plays a crucial role in the activation of HFSCs during telogen to anagen transition. It is also activated in hair matrix during anagen and the maintenance of Wnt/β-catenin signaling is required for anagen progression. We then analyzed Wnt/β-catenin signaling. We found that in both the control mice and un-irradiated rapamycin-treated mice, Lef1, the downstream target of β-catenin, were highly enriched in the hair bulb and IRS (Fig.29). After IR injury, Lef1 expression was reduced from 12 hours to 24 hours and its expression was restored from 48 hours to 72 hours (Fig.29). In contrast, when mTORC1 activity was suppressed by rapamycin, suppression of Lef1 expression was more severe and prolonged after IR and its expression was not completely restored at 96 hours. The results suggested that IR-injured HFs could spontaneously restore proper Wnt/β-catenin signaling to resume hair growth in the TAC compartment. Inhibition of mTORC1 signaling delayed the recovery of Wnt/β-catenin signaling after IR injury.

doi:10.6342/NTU201800580

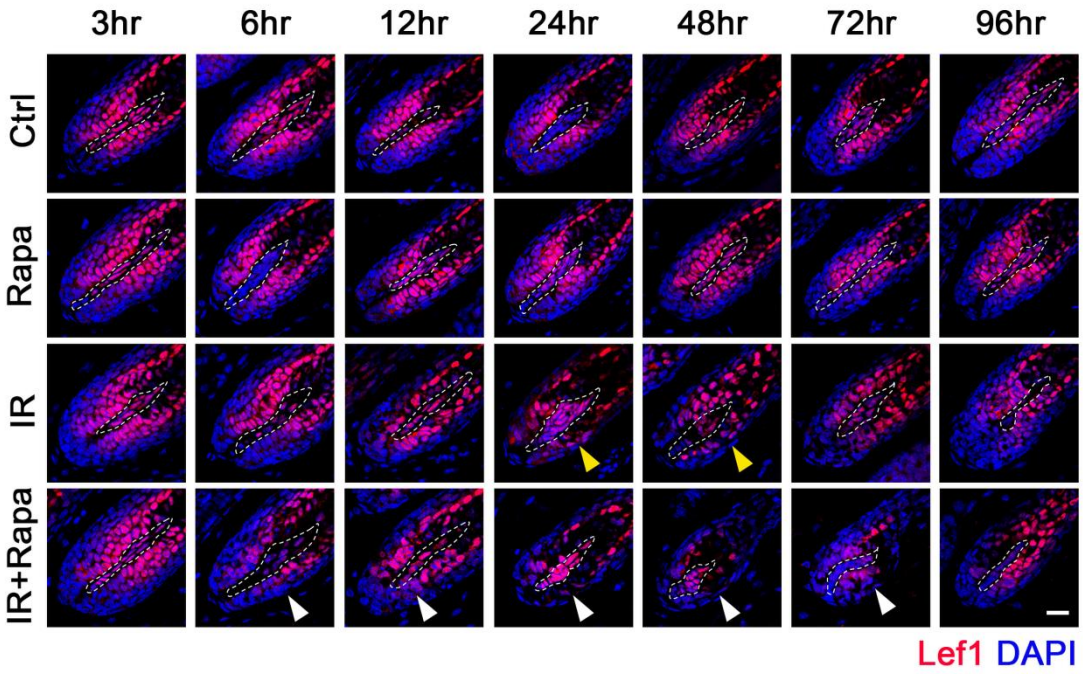

Figure 29. Inhibition of mTORC1 signaling prolonged the time for the recovery of Wnt/ β -catenin signaling in hair matrix after IR injury.

Immunostaining of Lef1, the downstream effector of β-catenin. Rapamycin alone did not suppress Lef1 expression in the hair matrix. Expression of Left1 in the hair matrix was mildly attenuated at 24 hours and 48 hours after 4Gy IR (yellow arrowheads). Expression of Lef1 in hair matrix after 4Gy IR was severely suppressed for a more prolonged period by rapamycin treatment (white arrowheads). Scale bar: 20μm.

doi:10.6342/NTU201800580

Chapter 4 Discussion

So far, the two distinct populations of ASCs have been widely investigated by transcriptomic analysis, and the comparison between pSCs and qSCs would provide useful clues to explain their function in physiological or regenerative status. To investigate how the ASCs are regulated, the environmental clues are responsible to affect ASCs by ligand-receptor interaction. Thus, to assay the post-translation modification, such as phosphorylation, would further improve our knowledge about how the ASCs react toward the outer stimuli.

The Mass-based phosphoproteomic technique could provide more details to characterize the SCs at varied cell status according to the outer stimuli or cross-talk from intrinsic protein network. To investigate the differentiation process in cultured human embryonic stem cells (hESCs) with SILAC technology (Ong, Blagoev et al. 2002), it was found the SOX2 protein would be phosphorylated under the stimulation of bone morphogenic protein (BMP), and the consecutive phosphorylation of serine residue would lead to subsequent SUMOylation (Van Hoof, Munoz et al. 2009). To maintained the hESCs in an undifferentiated state, it was indicated that numerous of receptor tyrosine kinase (RTK) were phosphorylated, and the PDGF-AA with subthreshold bFGF could maintain the undifferentiated state (Brill, Xiong et al. 2009).

doi:10.6342/NTU201800580

Another case for studying ESCs also revealed that with isobaric-tag labeling technique, iTRAQ (O'Brien, Shen et al. 2010). In our work, we isolated and purified distinct populations within HFSCs for *in vivo* profiling their phosphorylation properties between the activated and quiescent state. Because of the freshly isolated HFSCs without any passage or treatment, we provided the unperturbed results to establish a phosphoproteomic resource for functional investigation. In the previous HFSCs research, several systemic profiling has been investigated for discovering the differentiation and activation process, such as transcriptomic analysis, histone mark analysis, DNA methylation profiling, and super-enhancer analysis (Morris, Liu et al. 2004, Lien, Guo et al. 2011, Adam, Yang et al. 2015). In our study, we provided the first phosphoproteomic profile in HFSCs to depict the process during the activation of HFSCs.

Our phosphoproteome dataset revealed the enrichment in early anagen followed by temporal manner. By comparison of qSCs and pSCs, we identified several HFSCs markers enriched in phosphorylation level in qSCs, such as CD34, integrin b4, and Col17A1, which implied these phophoprotein could also be regarded as the specific markers for HFSCs. Although the biological meaning of these phospho-sites is not fully understood, these proteins still play important roles in HFSCs. The loss of Col17a1

doi:10.6342/NTU201800580

would cause severe HFs aging through transepidermal elimination of HFSCs which committed into epidermal fate (Matsumura, Mohri et al. 2016). The integrin b4 is known to involve in the hemidesmosome structure for protection, and the loss of function would lead to epidermolysis bullosa that perturbed the epidermal structure (van der Neut, Cachaco et al. 1999). CD34 is the most important markers to indicate the existence of HFSCs. These researches demonstrated the functional importance of these proteins.

On the other hand, we also identified several phosphproteins in pSCs, such as Krt25 and Krt28, which are expressed in the differentiating lineages. It has also been reported that the mutation of Krt25 and Krt28 would not induce hair loss, but lead to wooly hair and abnormal HF structure (Langbein, Rogers et al. 2006, Ansar, Raza et al. 2015). The adhesion junction protein ZO-2 and ZO-3 also be constantly phosphorylated in the pSCs. It has been reported that the occludin protein family are correlated the hemidesmosome. Taken together, the phosphoproteome data provides the useful information which not only corresponds to the previous research, but also implies the new candidates.

According to two-step activation hypothesis, in the early anagen, the pSCs start to proliferate prior than the qSCs. To compare the colony-forming capacity, the qSCs can

doi:10.6342/NTU201800580

be long-term passage by the support of feeder layer, but the clonogenecity is limited in the pSCs (Greco, Chen et al. 2009). Similar result could be reveal by chamber assay that qSCs are provided with better regenerative capacity than pSCs (Greco, Chen et al. 2009). In our phosphoproteome result, the number of enriched phosphoproteins in PSCs was increased dramatically in early anagen, which was the same as the trend in transcriptome result (Greco, Chen et al. 2009). There were several important proteins that mediating the delivery of morphogenic signals, which had been reported in the previous research. The downstream of canonical wnt/b-catenin signaling, APC and GSk3b, was found highly enriched in pSCs in the phosphoproteome data. It has also been reported that the loss of APC would cause the aberrant growth in skin and hair follicles (Kuraguchi, Wang et al. 2006). The inhibition of GSK3b has been proved to stabilized b-catenin, and the inhibition of GSK3b in HF organ culture could also enhance IGF signaling to maintain the hair growth in *ex vivo* environment (Yamauchi and Kurosaka 2009). It has also been reported that mTORC1 signaling could be activated by wnt ligand by the physical interaction between GSK3b and TSC1/2 (Inoki, Ouyang et al. 2006). In our phosphoproteome data, the adaptor protein of mTORC1, *raptor*, was found phosphorylated at Serine 863, which was primed for subsequent phosphorylation site to reach the best kinase activity (Foster, Acosta-Jaquez et al. 2010).

doi:10.6342/NTU201800580

In the previous study, mTORC1 was also investigated to affect hair cycle entry by pharmaceutical inhibition and conditional knockout of mTOR core protein (Kellenberger and Tauchi 2013, Deng, Lei et al. 2015).

mTORC1 signaling is known to regulate cell survival, proliferation, metabolic activity, and protein synthesis (Sabatini 2006, Dibble and Manning 2013). In telogen, the mTORC1 activity remained low in both pSCs and qSCs, but in the early anagen, the mTORC1 activity would be activated following the two-step activation. By pharmaceutical inhibition, HFs can be kept in the resting state. This result implies the importance of mTORC1 in provoking HFSCs activity. In adult tissues, it is suggested that the pSCs are responsible for immediate regeneration, and qSCs take part in long term maintenance. In a seldom activated adult tissue, such as skeleton muscle, MSCs could be awakened for traumatic regeneration (Bodine, Stitt et al. 2001, Bentzinger, Lin et al. 2013). Moreover, a small group of Pax7 MSC presents similar behavior as PSCs that could even sense the damage in the counterpart of body for preparing tissue regeneration (Rodgers, King et al. 2014). The loss of *mTOR* and *raptor* would lead to embryonic lethality (Murakami, Ichisaka et al. 2004); however, the loss of *raptor* does not cause the cell death in qSCs or pSCs. Similar to the loss of TGF-b signaling, *raptor* knockout in HFSCs severely postponed the anagen entrance (Oshimori and Fuchs 2012).

doi:10.6342/NTU201800580

Our finding implies the dependency of mTORC1 is more important in the pSCs, which may further differentiate into TACs. The qSCs can still survive and maintain even in the loss of mTORC1 activity, which implies the existence of a compensatory mechanism, or lower dependency toward mTORC1.

Our result not only reveals the difference between pSCs and qSCs, but also shows the changes between activating and resting stages. In physiological homeostasis, the outside-in signals trigger multiple protein phosphorylation, including mTORC1, to modulate the downstream targets. During the activation of hair cycle, mTORC1 plays an important role to provoke SC activity.

mTORC1-S6K-S6 axis is further activated in the TAC compartment of anagen HFs following IR and its activation is required for timely regeneration to avoid hair loss. Specifically, we demonstrate that activation of mTORC1 signaling is critical for restoration of the TAC pool in the hair bulb to resume the ongoing anagen. It also suggests a therapeutic strategy to reduce IR-induced hair loss by targeting the specific signaling in the TAC compartment.

Compared with the responses of HFs to IR injury, chemotherapy injury makes HFs to undergo distinct pathways: the dystrophic anagen pathway and the dystrophic catagen

doi:10.6342/NTU201800580

pathway. For dystrophic catagen pathway which is induced by higher doses of cyclophosphamide, HFs prematurely terminate the ongoing anagen due to massive apoptosis of TACs and transit through catagen to telogen. In dystrophic anagen, which is induced by lower doses of cyclophosphamide, HFs show a milder dystrophic change that is repaired soon after damage and resume the ongoing anagen. Since HFs in this study were able to repair themselves to resume the ongoing anagen, the dystrophic change induced by 4Gy of IR is analogous to the dystrophic anagen pathway induced by chemotherapeutic agent.

In anagen HFs, apoptosis of irradiated TACs not only lead to shrinkage of hair bulbs, but also transiently disrupted the continuity of HS and IRS formation. Restoration of the lost TAC population is critical to resume anagen growth after IR injury. The TAC pool in the hair bulb is balanced by cell proliferation, cell death and cell differentiation with subsequent upward cell extrusion. After IR injury in anagen, the increased cell death from genotoxic injury tilts the balance toward the loss of TACs, leading to hair bulb atrophy. The subsequently quick restoration of the normal hair bulb indicates that HFs are able to replenish the lost TACs, likely through compensatory proliferation, to maintain an adequate number of TACs.

We show that suppression of mTORC1 signaling significantly decreases the TAC

doi:10.6342/NTU201800580

population after IR injury. The enhanced apoptosis and reduced proliferation prolong the time needed to repair the damaged hair bulbs and to restore Wnt/β-catenin signaling, thereby delaying the upward output of cells from the hair bulb to support the growth and elongation of hair shafts. This leads to fragmentation of the HS and severe hair loss. Since inhibition of mTORC1 signaling in normal anagen, HFs did not induce dystrophy of the hair bulb, it highlights the specific role of mTORC1 signaling in quick restoration of the TAC population following IR injury. Our results indicate that activation of mTORC1 signaling is critical to help TACs to deal with the genotoxic stress induced by IR.

In oral mucosa, inhibition of mTORC1 signaling can attenuate IR-induced damage to filiform papillae and also prevents mucositis from IR injury. This contrasts the protective effect of mTORC1 signaling in HFs. Hence, the protective effect of mTORC1 signaling on IR injury can be context dependent and not universal in all tissues. In HFs, since HFs exhibit a similar dystrophic anagen response to both IR and genotoxic chemotherapeutic agents, the signaling pathway revealed in the follicular response to IR injury here might also be shared by HFs under chemotherapeutic injury. Targeting mTORC1 signaling pathway in TACs might be a potential strategy to prevent hair loss from genotoxic injury from IR and chemotherapy.

doi:10.6342/NTU201800580

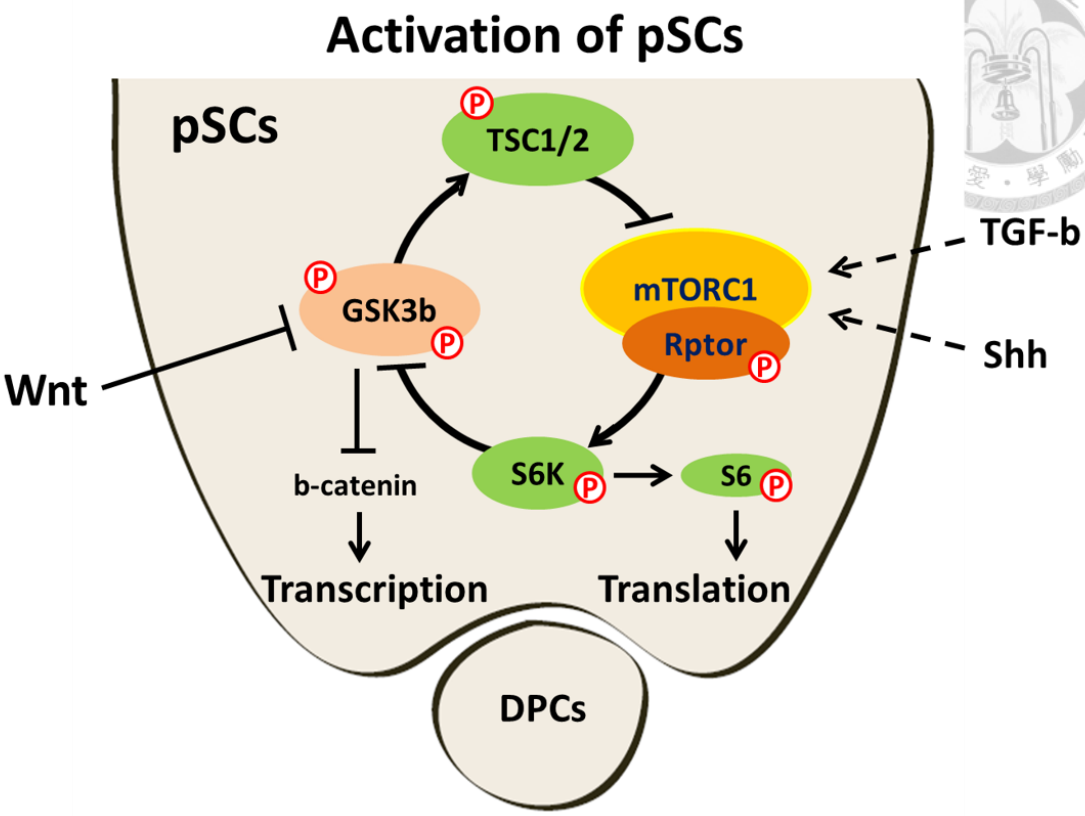

Figure 30. Model of mTORC1 in regulating the activation of qSCs in the early anagen.

mTORC1 can phosphorylate the downstream S6K and S6 for improving translation. S6K might also phosphorylation GSK3β to stabilized β-catenin. Wnt signaling could also transduce the morphogenic signals throught GSK3β. The phosphorylated inhibition of GSK3β would further enhance mTORC1 activity by attenuate TSC1/2 comples. Thus, the mTOR1 might correspond to two-step activation closely to activate the onset of hair cycle in pSCs.

doi:10.6342/NTU201800580

Chapter 5 Conclusions

Taken together, the phosphoproteome of HFSCs provides us the useful information that participates in the regulation of HFSCs. Although the coverage of phosphoproteome is not system-wide, we still identified several proteins that is possible to involve in the activation of hair cycle. By the bioinformatics tools, we hypothesize that the activation of HFSCs requires the morphogenic signals and the mTORC1 activity. The inhibition of mTORC1 can postpone the hair cycle entry in physiological cycling. The conditional ablation of mTORC1 can also achieve similar results. The inhibition of mTORC1 in anagen does not perturb the anagen progression, but the mTORC1 activity is required for HF regeneration after IR injury. Thus, mTORC1 plays multiple roles in regulating the physiological function of HFs.

doi:10.6342/NTU201800580

Chapter 6 REFERENCE

Adam, R. C., H. Yang, S. Rockowitz, S. B. Larsen, M. Nikolova, D. S. Oristian, L. Polak, M. Kadaja, A. Asare, D. Zheng and E. Fuchs (2015). "Pioneer factors govern super-enhancer dynamics in stem cell plasticity and lineage choice." Nature **521**(7552): 366-370.

Affara, N. I., C. S. Trempus, B. L. Schanbacher, P. Pei, S. R. Mallery, J. A. Bauer and F. M. Robertson (2006). "Activation of Akt and mTOR in CD34+/K15+ keratinocyte stem cells and skin tumors during multi-stage mouse skin carcinogenesis." Anticancer Res **26**(4B): 2805-2820.

Alexander, A., S. L. Cai, J. Kim, A. Nanez, M. Sahin, K. H. MacLean, K. Inoki, K. L. Guan, J. Shen, M. D. Person, D. Kusewitt, G. B. Mills, M. B. Kastan and C. L. Walker (2010). "ATM signals to TSC2 in the cytoplasm to regulate mTORC1 in response to ROS." Proc Natl Acad Sci U S A **107**(9): 4153-4158.

Alonso, L. and E. Fuchs (2006). "The hair cycle." J Cell Sci **119**(Pt 3): 391-393.

Avci, P., G. K. Gupta, J. Clark, N. Wikonkal and M. R. Hamblin (2014). "Low-level laser (light) therapy (LLLT) for treatment of hair loss." Lasers Surg Med **46**(2): 144-151.

Balcazar, N., A. Sathyamurthy, L. Elghazi, A. Gould, A. Weiss, I. Shiojima, K. Walsh

doi:10.6342/NTU201800580

and E. Bernal-Mizrachi (2009). "mTORC1 activation regulates beta-cell mass and proliferation by modulation of cyclin D2 synthesis and stability." J Biol Chem **284**(12): 7832-7842.

Bandhakavi, S., Y. M. Kim, S. H. Ro, H. Xie, G. Onsongo, C. B. Jun, D. H. Kim and T. J. Griffin (2010). "Quantitative nuclear proteomics identifies mTOR regulation of DNA damage response." Mol Cell Proteomics **9**(2): 403-414.

Bentzen, S. M. (2006). "Preventing or reducing late side effects of radiation therapy: radiobiology meets molecular pathology." Nat Rev Cancer **6**(9): 702-713.

Bentzinger, C. F., K. Romanino, D. Cloetta, S. Lin, J. B. Mascarenhas, F. Oliveri, J. Xia, E. Casanova, C. F. Costa, M. Brink, F. Zorzato, M. N. Hall and M. A. Ruegg (2008). "Skeletal muscle-specific ablation of raptor, but not of rictor, causes metabolic changes and results in muscle dystrophy." Cell Metab **8**(5): 411-424.

Blanpain, C. and E. Fuchs (2014). "Stem cell plasticity. Plasticity of epithelial stem cells in tissue regeneration." Science **344**(6189): 1242281.

Botchkarev, V. A., E. A. Komarova, F. Siebenhaar, N. V. Botchkareva, P. G. Komarov, M. Maurer, B. A. Gilchrest and A. V. Gudkov (2000). "p53 is essential for chemotherapy-induced hair loss." Cancer Res **60**(18): 5002-5006.

Bowman, C. J., D. E. Ayer and B. D. Dynlacht (2014). "Foxk proteins repress the

doi:10.6342/NTU201800580

initiation of starvation-induced atrophy and autophagy programs." Nat Cell Biol **16**(12): 1202-1214.

Bragado, M. J., G. E. Groblewski and J. A. Williams (1998). "Regulation of protein synthesis by cholecystokinin in rat pancreatic acini involves PHAS-I and the p70 S6 kinase pathway." Gastroenterology **115**(3): 733-742.

Brewis, I. A. and P. Brennan (2010). "Proteomics technologies for the global identification and quantification of proteins." Adv Protein Chem Struct Biol **80**: 1-44.

Brill, L. M., W. Xiong, K. B. Lee, S. B. Ficarro, A. Crain, Y. Xu, A. Terskikh, E. Y. Snyder and S. Ding (2009). "Phosphoproteomic analysis of human embryonic stem cells." Cell Stem Cell **5**(2): 204-213.

Calne, R. Y., D. S. Collier, S. Lim, S. G. Pollard, A. Samaan, D. J. White and S. Thiru (1989). "Rapamycin for immunosuppression in organ allografting." Lancet **2**(8656): 227.

Castilho, R. M., C. H. Squarize, L. A. Chodosh, B. O. Williams and J. S. Gutkind (2009). "mTOR mediates Wnt-induced epidermal stem cell exhaustion and aging." Cell Stem Cell **5**(3): 279-289.

Chang, C. Y., H. A. Pasolli, E. G. Giannopoulou, G. Guasch, R. M. Gronostajski, O. Elemento and E. Fuchs (2013). "NFIB is a governor of epithelial-melanocyte stem cell

doi:10.6342/NTU201800580

behaviour in a shared niche." Nature **495**(7439): 98-102.

Chang, J., Y. Kim and H. J. Kwon (2016). "Advances in identification and validation of protein targets of natural products without chemical modification." Nat Prod Rep **33**(5): 719-730.

Chang, J. Y. and S. N. Sehgal (1991). "Pharmacology of rapamycin: a new immunosuppressive agent." Br J Rheumatol **30 Suppl 2**: 62-65.

Chase, H. B. (1954). "Growth of the hair." Physiol Rev **34**(1): 113-126.

Chase, H. B., W. Montagna and J. D. Malone (1953). "Changes in the skin in relation to the hair growth cycle." Anat Rec **116**(1): 75-81.

Chen, C. C., L. Wang, M. V. Plikus, T. X. Jiang, P. J. Murray, R. Ramos, C. F. Guerrero-Juarez, M. W. Hughes, O. K. Lee, S. Shi, R. B. Widelitz, A. D. Lander and C. M. Chuong (2015). "Organ-level quorum sensing directs regeneration in hair stem cell populations." Cell **161**(2): 277-290.

Chen, X., L. J. Ko, L. Jayaraman and C. Prives (1996). "p53 levels, functional domains, and DNA damage determine the extent of the apoptotic response of tumor cells." Genes Dev **10**(19): 2438-2451.

Chen, X., S. Wei, Y. Ji, X. Guo and F. Yang (2015). "Quantitative proteomics using SILAC: Principles, applications, and developments." Proteomics **15**(18): 3175-3192.

doi:10.6342/NTU201800580

Chen, Y., N. Sasai, G. Ma, T. Yue, J. Jia, J. Briscoe and J. Jiang (2011). "Sonic Hedgehog dependent phosphorylation by CK1alpha and GRK2 is required for ciliary accumulation and activation of smoothened." PLoS Biol **9**(6): e1001083.

Chou, M. F. and D. Schwartz (2011). "Using the scan-x Web site to predict protein post-translational modifications." Curr Protoc Bioinformatics **Chapter 13**: Unit 13 16.

Claudinot, S., M. Nicolas, H. Oshima, A. Rochat and Y. Barrandon (2005). "Long-term renewal of hair follicles from clonogenic multipotent stem cells." Proc Natl Acad Sci U S A **102**(41): 14677-14682.

Coschi, C. H. and F. A. Dick (2012). "Chromosome instability and deregulated proliferation: an unavoidable duo." Cell Mol Life Sci **69**(12): 2009-2024.

Cotsarelis, G., T. T. Sun and R. M. Lavker (1990). "Label-retaining cells reside in the bulge area of pilosebaceous unit: implications for follicular stem cells, hair cycle, and skin carcinogenesis." Cell **61**(7): 1329-1337.

Delaney, G., S. Jacob, C. Featherstone and M. Barton (2005). "The role of radiotherapy in cancer treatment: estimating optimal utilization from a review of evidence-based clinical guidelines." Cancer **104**(6): 1129-1137.

Deng, Z., X. Lei, X. Zhang, H. Zhang, S. Liu, Q. Chen, H. Hu, X. Wang, L. Ning, Y. Cao, T. Zhao, J. Zhou, T. Chen and E. Duan (2015). "mTOR signaling promotes stem

doi:10.6342/NTU201800580

cell activation via counterbalancing BMP-mediated suppression during hair regeneration." J Mol Cell Biol **7**(1): 62-72.

Dennis, M. D., N. K. McGhee, L. S. Jefferson and S. R. Kimball (2013). "Regulated in DNA damage and development 1 (REDD1) promotes cell survival during serum deprivation by sustaining repression of signaling through the mechanistic target of rapamycin in complex 1 (mTORC1)." Cell Signal **25**(12): 2709-2716.

Ding, X., W. Bloch, S. Iden, M. A. Ruegg, M. N. Hall, M. Leptin, L. Partridge and S. A. Eming (2016). "mTORC1 and mTORC2 regulate skin morphogenesis and epidermal barrier formation." Nat Commun **7**: 13226.

Dowling, R. J., I. Topisirovic, T. Alain, M. Bidinosti, B. D. Fonseca, E. Petroulakis, X. Wang, O. Larsson, A. Selvaraj, Y. Liu, S. C. Kozma, G. Thomas and N. Sonenberg (2010). "mTORC1-mediated cell proliferation, but not cell growth, controlled by the 4E-BPs." Science **328**(5982): 1172-1176.

Ellis, T., L. Gambardella, M. Horcher, S. Tschanz, J. Capol, P. Bertram, W. Jochum, Y. Barrandon and M. Busslinger (2001). "The transcriptional repressor CDP (Cutl1) is essential for epithelial cell differentiation of the lung and the hair follicle." Genes Dev **15**(17): 2307-2319.

Foster, K. G., H. A. Acosta-Jaquez, Y. Romeo, B. Ekim, G. A. Soliman, A. Carriere, P. P.

doi:10.6342/NTU201800580

Roux, B. A. Ballif and D. C. Fingar (2010). "Regulation of mTOR complex 1 (mTORC1) by raptor Ser863 and multisite phosphorylation." J Biol Chem **285**(1): 80-94.

Fujiwara, H., M. Ferreira, G. Donati, D. K. Marciano, J. M. Linton, Y. Sato, A. Hartner, K. Sekiguchi, L. F. Reichardt and F. M. Watt (2011). "The basement membrane of hair follicle stem cells is a muscle cell niche." Cell **144**(4): 577-589.

Gafter-Gvili, A., B. Sredni, R. Gal, U. Gafter and Y. Kalechman (2003). "Cyclosporin A-induced hair growth in mice is associated with inhibition of calcineurin-dependent activation of NFAT in follicular keratinocytes." Am J Physiol Cell Physiol **284**(6): C1593-1603.

Gan, B. and R. A. DePinho (2009). "mTORC1 signaling governs hematopoietic stem cell quiescence." Cell Cycle **8**(7): 1003-1006.

Gangloff, Y. G., M. Mueller, S. G. Dann, P. Svoboda, M. Sticker, J. F. Spetz, S. H. Um, E. J. Brown, S. Cereghini, G. Thomas and S. C. Kozma (2004). "Disruption of the mouse mTOR gene leads to early postimplantation lethality and prohibits embryonic stem cell development." Mol Cell Biol **24**(21): 9508-9516.

Genander, M., P. J. Cook, D. Ramskold, B. E. Keyes, A. F. Mertz, R. Sandberg and E. Fuchs (2014). "BMP signaling and its pSMAD1/5 target genes differentially regulate

doi:10.6342/NTU201800580

hair follicle stem cell lineages." Cell Stem Cell **15**(5): 619-633.

Greco, V., T. Chen, M. Rendl, M. Schober, H. A. Pasolli, N. Stokes, J. Dela Cruz-Racelis and E. Fuchs (2009). "A two-step mechanism for stem cell activation during hair regeneration." Cell Stem Cell **4**(2): 155-169.

Guertin, D. A., D. M. Stevens, C. C. Thoreen, A. A. Burds, N. Y. Kalaany, J. Moffat, M. Brown, K. J. Fitzgerald and D. M. Sabatini (2006). "Ablation in mice of the mTORC components raptor, rictor, or mLST8 reveals that mTORC2 is required for signaling to Akt-FOXO and PKCalpha, but not S6K1." Dev Cell **11**(6): 859-871.

Hara, K., Y. Maruki, X. Long, K. Yoshino, N. Oshiro, S. Hidayat, C. Tokunaga, J. Avruch and K. Yonezawa (2002). "Raptor, a binding partner of target of rapamycin (TOR), mediates TOR action." Cell **110**(2): 177-189.

Hoeck, J. D., B. Biehs, A. V. Kurtova, N. M. Kljavin, E. M. F. de Sousa, B. Alicke, H. Koeppen, Z. Modrusan, R. Piskol and F. J. de Sauvage (2017). "Stem cell plasticity enables hair regeneration following Lgr5(+) cell loss." Nat Cell Biol **19**(6): 666-676.

Holz, M. K., B. A. Ballif, S. P. Gygi and J. Blenis (2005). "mTOR and S6K1 mediate assembly of the translation preinitiation complex through dynamic protein interchange and ordered phosphorylation events." Cell **123**(4): 569-580.

Hsu, Y. C., L. Li and E. Fuchs (2014). "Transit-amplifying cells orchestrate stem cell

doi:10.6342/NTU201800580

activity and tissue regeneration." Cell **157**(4): 935-949.

Hsu, Y. C., H. A. Pasolli and E. Fuchs (2011). "Dynamics between stem cells, niche, and progeny in the hair follicle." Cell **144**(1): 92-105.

Hutchins, A. P. and P. Robson (2009). "Unraveling the human embryonic stem cell phosphoproteome." Cell Stem Cell **5**(2): 126-128.

Inoki, K., H. Ouyang, T. Zhu, C. Lindvall, Y. Wang, X. Zhang, Q. Yang, C. Bennett, Y. Harada, K. Stankunas, C. Y. Wang, X. He, O. A. MacDougald, M. You, B. O. Williams and K. L. Guan (2006). "TSC2 integrates Wnt and energy signals via a coordinated phosphorylation by AMPK and GSK3 to regulate cell growth." Cell **126**(5): 955-968.

Ito, M. and K. Kizawa (2001). "Expression of calcium-binding S100 proteins A4 and A6 in regions of the epithelial sac associated with the onset of hair follicle regeneration." J Invest Dermatol **116**(6): 956-963.

Ito, M., K. Kizawa, K. Hamada and G. Cotsarelis (2004). "Hair follicle stem cells in the lower bulge form the secondary germ, a biochemically distinct but functionally equivalent progenitor cell population, at the termination of catagen." Differentiation **72**(9-10): 548-557.

Ito, M., K. Kizawa, M. Toyoda and M. Morohashi (2002). "Label-retaining cells in the bulge region are directed to cell death after plucking, followed by healing from the

doi:10.6342/NTU201800580

surviving hair germ." J Invest Dermatol **119**(6): 1310-1316.

Jahoda, C. A., K. A. Horne and R. F. Oliver (1984). "Induction of hair growth by implantation of cultured dermal papilla cells." Nature **311**(5986): 560-562.

Jensen, U. B., X. Yan, C. Triel, S. H. Woo, R. Christensen and D. M. Owens (2008). "A distinct population of clonogenic and multipotent murine follicular keratinocytes residing in the upper isthmus." J Cell Sci **121**(Pt 5): 609-617.

Kastan, M. B., O. Onyekwere, D. Sidransky, B. Vogelstein and R. W. Craig (1991). "Participation of p53 protein in the cellular response to DNA damage." Cancer Res **51**(23 Pt 1): 6304-6311.

Kastan, M. B., Q. Zhan, W. S. el-Deiry, F. Carrier, T. Jacks, W. V. Walsh, B. S. Plunkett, B. Vogelstein and A. J. Fornace, Jr. (1992). "A mammalian cell cycle checkpoint pathway utilizing p53 and GADD45 is defective in ataxia-telangiectasia." Cell **71**(4): 587-597.

Kaufman, C. K., P. Zhou, H. A. Pasolli, M. Rendl, D. Bolotin, K. C. Lim, X. Dai, M. L. Alegre and E. Fuchs (2003). "GATA-3: an unexpected regulator of cell lineage determination in skin." Genes Dev **17**(17): 2108-2122.

Kellenberger, A. J. and M. Tauchi (2013). "Mammalian target of rapamycin complex 1 (mTORC1) may modulate the timing of anagen entry in mouse hair follicles." Exp

doi:10.6342/NTU201800580

Dermatol **22**(1): 77-80.

Kim, D. H., D. D. Sarbassov, S. M. Ali, J. E. King, R. R. Latek, H. Erdjument-Bromage, P. Tempst and D. M. Sabatini (2002). "mTOR interacts with raptor to form a nutrient-sensitive complex that signals to the cell growth machinery." Cell **110**(2): 163-175.

Krause, K. and K. Foitzik (2006). "Biology of the hair follicle: the basics." Semin Cutan Med Surg **25**(1): 2-10.

Kretzschmar, M., F. Liu, A. Hata, J. Doody and J. Massague (1997). "The TGF-beta family mediator Smad1 is phosphorylated directly and activated functionally by the BMP receptor kinase." Genes Dev **11**(8): 984-995.

Kurek, D., G. A. Garinis, J. H. van Doorninck, J. van der Wees and F. G. Grosveld (2007). "Transcriptome and phenotypic analysis reveals Gata3-dependent signalling pathways in murine hair follicles." Development **134**(2): 261-272.

Lai, K. P., W. F. Leong, J. F. Chau, D. Jia, L. Zeng, H. Liu, L. He, A. Hao, H. Zhang, D. Meek, C. Velagapudi, S. L. Habib and B. Li (2010). "S6K1 is a multifaceted regulator of Mdm2 that connects nutrient status and DNA damage response." EMBO J **29**(17): 2994-3006.

Lan, S., F. Liu, G. Zhao, T. Zhou, C. Wu, J. Kou, R. Fan, X. Qi, Y. Li, Y. Jiang, T. Bai, P.

doi:10.6342/NTU201800580

Li, L. Liu, D. Hao, L. Zhang, Y. Li and J. Y. Liu (2015). "Cyclosporine A increases hair follicle growth by suppressing apoptosis-inducing factor nuclear translocation: a new mechanism." Fundam Clin Pharmacol **29**(2): 191-203.

Langenfeld, E. M., Y. Kong and J. Langenfeld (2005). "Bone morphogenetic protein-2-induced transformation involves the activation of mammalian target of rapamycin." Mol Cancer Res **3**(12): 679-684.

Leblond, C. P. (1951). "Histological structure of hair, with a brief comparison to other epidermal appendages and epidermis itself." Ann N Y Acad Sci **53**(3): 464-475.

LeBoeuf, M., A. Terrell, S. Trivedi, S. Sinha, J. A. Epstein, E. N. Olson, E. E. Morrisey and S. E. Millar (2010). "Hdac1 and Hdac2 act redundantly to control p63 and p53 functions in epidermal progenitor cells." Dev Cell **19**(6): 807-818.

Li, H., J. Lee, C. He, M. H. Zou and Z. Xie (2014). "Suppression of the mTORC1/STAT3/Notch1 pathway by activated AMPK prevents hepatic insulin resistance induced by excess amino acids." Am J Physiol Endocrinol Metab **306**(2): E197-209.

Li, L. and H. Clevers (2010). "Coexistence of quiescent and active adult stem cells in mammals." Science **327**(5965): 542-545.

Li, S., R. L. Thangapazham, J. A. Wang, S. Rajesh, T. C. Kao, L. Sperling, J. Moss and

doi:10.6342/NTU201800580

T. N. Darling (2011). "Human TSC2-null fibroblast-like cells induce hair follicle neogenesis and hamartoma morphogenesis." Nat Commun **2**: 235.

Lien, W. H., X. Guo, L. Polak, L. N. Lawton, R. A. Young, D. Zheng and E. Fuchs (2011). "Genome-wide maps of histone modifications unwind in vivo chromatin states of the hair follicle lineage." Cell Stem Cell **9**(3): 219-232.

Lin, S. J., J. Foley, T. X. Jiang, C. Y. Yeh, P. Wu, A. Foley, C. M. Yen, Y. C. Huang, H. C. Cheng, C. F. Chen, B. Reeder, S. H. Jee, R. B. Widelitz and C. M. Chuong (2013). "Topology of feather melanocyte progenitor niche allows complex pigment patterns to emerge." Science **340**(6139): 1442-1445.

Luong, M. X., C. M. van der Meijden, D. Xing, R. Hesselton, E. S. Monuki, S. N. Jones, J. B. Lian, J. L. Stein, G. S. Stein, E. J. Neufeld and A. J. van Wijnen (2002). "Genetic ablation of the CDP/Cux protein C terminus results in hair cycle defects and reduced male fertility." Mol Cell Biol **22**(5): 1424-1437.

Ma, L., J. Liu, T. Wu, M. Plikus, T. X. Jiang, Q. Bi, Y. H. Liu, S. Muller-Rover, H. Peters, J. P. Sundberg, R. Maxson, R. L. Maas and C. M. Chuong (2003). "'Cyclic alopecia' in Msx2 mutants: defects in hair cycling and hair shaft differentiation." Development **130**(2): 379-389.

Magnuson, B., B. Ekim and D. C. Fingar (2012). "Regulation and function of ribosomal

doi:10.6342/NTU201800580

protein S6 kinase (S6K) within mTOR signalling networks." Biochem J **441**(1): 1-21.

Malkinson, F. D., M. L. Griem and R. Marianovic (1973). "Effects of hydroxyurea and radiation on hair matrix cells." Cell Tissue Kinet **6**(4): 395-405.

Malkinson, F. D. and J. T. Keane (1981). "Radiobiology of the skin: review of some effects on epidermis and hair." J Invest Dermatol **77**(1): 133-138.

Matsumura, H., Y. Mohri, N. T. Binh, H. Morinaga, M. Fukuda, M. Ito, S. Kurata, J. Hoeijmakers and E. K. Nishimura (2016). "Hair follicle aging is driven by transepidermal elimination of stem cells via COL17A1 proteolysis." Science **351**(6273): aad4395.

Metri, K., H. Bhargav, P. Chowdhury and P. S. Koka (2013). "Ayurveda for chemo-radiotherapy induced side effects in cancer patients." J Stem Cells **8**(2): 115-129.

Mills, A. A., B. Zheng, X. J. Wang, H. Vogel, D. R. Roop and A. Bradley (1999). "p63 is a p53 homologue required for limb and epidermal morphogenesis." Nature **398**(6729): 708-713.

Mills, J. R., Y. Hippo, F. Robert, S. M. Chen, A. Malina, C. J. Lin, U. Trojahn, H. G. Wendel, A. Charest, R. T. Bronson, S. C. Kogan, R. Nadon, D. E. Housman, S. W. Lowe and J. Pelletier (2008). "mTORC1 promotes survival through translational control of Mcl-1." Proc Natl Acad Sci U S A **105**(31): 10853-10858.

doi:10.6342/NTU201800580

Moore, K. A. and I. R. Lemischka (2006). "Stem cells and their niches." Science **311**(5769): 1880-1885.

Morris, R. J., Y. Liu, L. Marles, Z. Yang, C. Trempus, S. Li, J. S. Lin, J. A. Sawicki and G. Cotsarelis (2004). "Capturing and profiling adult hair follicle stem cells." Nat Biotechnol **22**(4): 411-417.

Muller-Rover, S., B. Handjiski, C. van der Veen, S. Eichmuller, K. Foitzik, I. A. McKay, K. S. Stenn and R. Paus (2001). "A comprehensive guide for the accurate classification of murine hair follicles in distinct hair cycle stages." J Invest Dermatol **117**(1): 3-15.

Murakami, M., T. Ichisaka, M. Maeda, N. Oshiro, K. Hara, F. Edenhofer, H. Kiyama, K. Yonezawa and S. Yamanaka (2004). "mTOR is essential for growth and proliferation in early mouse embryos and embryonic stem cells." Mol Cell Biol **24**(15): 6710-6718.

Nakatsumi, H., M. Matsumoto and K. I. Nakayama (2017). "Noncanonical Pathway for Regulation of CCL2 Expression by an mTORC1-FOXK1 Axis Promotes Recruitment of Tumor-Associated Macrophages." Cell Rep **21**(9): 2471-2486.

Nguyen, H., B. J. Merrill, L. Polak, M. Nikolova, M. Rendl, T. M. Shaver, H. A. Pasolli and E. Fuchs (2009). "Tcf3 and Tcf4 are essential for long-term homeostasis of skin epithelia." Nat Genet **41**(10): 1068-1075.

Nowak, J. A., L. Polak, H. A. Pasolli and E. Fuchs (2008). "Hair follicle stem cells are

doi:10.6342/NTU201800580

specified and function in early skin morphogenesis." Cell Stem Cell **3**(1): 33-43.

Ohyama, M., A. Terunuma, C. L. Tock, M. F. Radonovich, C. A. Pise-Masison, S. B. Hopping, J. N. Brady, M. C. Udey and J. C. Vogel (2006). "Characterization and isolation of stem cell-enriched human hair follicle bulge cells." J Clin Invest **116**(1): 249-260.

Olsen, J. V., B. Blagoev, F. Gnad, B. Macek, C. Kumar, P. Mortensen and M. Mann (2006). "Global, in vivo, and site-specific phosphorylation dynamics in signaling networks." Cell **127**(3): 635-648.

Oshimori, N. and E. Fuchs (2012). "Paracrine TGF-beta signaling counterbalances BMP-mediated repression in hair follicle stem cell activation." Cell Stem Cell **10**(1): 63-75.

Panteleyev, A. A., N. V. Botchkareva, J. P. Sundberg, A. M. Christiano and R. Paus (1999). "The role of the hairless (hr) gene in the regulation of hair follicle catagen transformation." Am J Pathol **155**(1): 159-171.

Paus, R. (1998). "Principles of hair cycle control." J Dermatol **25**(12): 793-802.

Paus, R. and K. Foitzik (2004). "In search of the "hair cycle clock": a guided tour." Differentiation **72**(9-10): 489-511.

Paus, R., I. S. Haslam, A. A. Sharov and V. A. Botchkarev (2013). "Pathobiology of

doi:10.6342/NTU201800580

chemotherapy-induced hair loss." Lancet Oncol **14**(2): e50-59.

Perez-Riverol, Y., R. Wang, H. Hermjakob, M. Muller, V. Vesada and J. A. Vizcaino (2014). "Open source libraries and frameworks for mass spectrometry based proteomics: a developer's perspective." Biochim Biophys Acta **1844**(1 Pt A): 63-76.

Plikus, M. V. and C. M. Chuong (2008). "Complex hair cycle domain patterns and regenerative hair waves in living rodents." J Invest Dermatol **128**(5): 1071-1080.

Polak, P., N. Cybulski, J. N. Feige, J. Auwerx, M. A. Ruegg and M. N. Hall (2008). "Adipose-specific knockout of raptor results in lean mice with enhanced mitochondrial respiration." Cell Metab **8**(5): 399-410.

Rauniyar, N. and J. R. Yates, 3rd (2014). "Isobaric labeling-based relative quantification in shotgun proteomics." J Proteome Res **13**(12): 5293-5309.

Rendl, M., L. Lewis and E. Fuchs (2005). "Molecular dissection of mesenchymal-epithelial interactions in the hair follicle." PLoS Biol **3**(11): e331.

Renninger, S. L., H. B. Schonthaler, S. C. Neuhauss and R. Dahm (2011). "Investigating the genetics of visual processing, function and behaviour in zebrafish." Neurogenetics **12**(2): 97-116.

Rhee, H., L. Polak and E. Fuchs (2006). "Lhx2 maintains stem cell character in hair follicles." Science **312**(5782): 1946-1949.

doi:10.6342/NTU201800580

Richardson, R. J., J. Dixon, S. Malhotra, M. J. Hardman, L. Knowles, R. P. Boot-Handford, P. Shore, A. Whitmarsh and M. J. Dixon (2006). "Irf6 is a key determinant of the keratinocyte proliferation-differentiation switch." Nat Genet **38**(11): 1329-1334.

Rompolas, P., E. R. Deschene, G. Zito, D. G. Gonzalez, I. Saotome, A. M. Haberman and V. Greco (2012). "Live imaging of stem cell and progeny behaviour in physiological hair-follicle regeneration." Nature **487**(7408): 496-499.

Rompolas, P., K. R. Mesa and V. Greco (2013). "Spatial organization within a niche as a determinant of stem-cell fate." Nature **502**(7472): 513-518.

Ruzankina, Y., C. Pinzon-Guzman, A. Asare, T. Ong, L. Pontano, G. Cotsarelis, V. P. Zediak, M. Velez, A. Bhandoola and E. J. Brown (2007). "Deletion of the developmentally essential gene ATR in adult mice leads to age-related phenotypes and stem cell loss." Cell Stem Cell **1**(1): 113-126.

Saxton, R. A. and D. M. Sabatini (2017). "mTOR Signaling in Growth, Metabolism, and Disease." Cell **168**(6): 960-976.

Schwartz, D., M. F. Chou and G. M. Church (2009). "Predicting protein post-translational modifications using meta-analysis of proteome scale data sets." Mol Cell Proteomics **8**(2): 365-379.

doi:10.6342/NTU201800580

Sharov, A. A., G. Z. Li, T. N. Palkina, T. Y. Sharova, B. A. Gilchrest and V. A. Botchkarev (2003). "Fas and c-kit are involved in the control of hair follicle melanocyte apoptosis and migration in chemotherapy-induced hair loss." J Invest Dermatol **120**(1): 27-35.

Shimizu, H. and B. A. Morgan (2004). "Wnt signaling through the beta-catenin pathway is sufficient to maintain, but not restore, anagen-phase characteristics of dermal papilla cells." J Invest Dermatol **122**(2): 239-245.

Shortt, J., B. P. Martin, A. Newbold, K. M. Hannan, J. R. Devlin, A. J. Baker, R. Ralli, C. Cullinane, C. A. Schmitt, M. Reimann, M. N. Hall, M. Wall, R. D. Hannan, R. B. Pearson, G. A. McArthur and R. W. Johnstone (2013). "Combined inhibition of PI3K-related DNA damage response kinases and mTORC1 induces apoptosis in MYC-driven B-cell lymphomas." Blood **121**(15): 2964-2974.

Stenn, K. S. and R. Paus (2001). "Controls of hair follicle cycling." Physiol Rev **81**(1): 449-494.

Stenn, K. S. and R. Paus (2001). "Controls of hair follicle cycling." Physiological Reviews **81**(1): 449-494.

Szklarczyk, D., J. H. Morris, H. Cook, M. Kuhn, S. Wyder, M. Simonovic, A. Santos, N. T. Doncheva, A. Roth, P. Bork, L. J. Jensen and C. von Mering (2017). "The STRING

doi:10.6342/NTU201800580

database in 2017: quality-controlled protein-protein association networks, made broadly accessible." Nucleic Acids Res **45**(D1): D362-D368.

Tominaga, H., S. Kodama, N. Matsuda, K. Suzuki and M. Watanabe (2004). "Involvement of reactive oxygen species (ROS) in the induction of genetic instability by radiation." J Radiat Res **45**(2): 181-188.

Trempus, C. S., R. J. Morris, C. D. Bortner, G. Cotsarelis, R. S. Faircloth, J. M. Reece and R. W. Tennant (2003). "Enrichment for living murine keratinocytes from the hair follicle bulge with the cell surface marker CD34." J Invest Dermatol **120**(4): 501-511.

Tsai, M., R. H. Chen, S. Y. Tam, J. Blenis and S. J. Galli (1993). "Activation of MAP kinases, pp90rsk and pp70-S6 kinases in mouse mast cells by signaling through the c-kit receptor tyrosine kinase or Fc epsilon RI: rapamycin inhibits activation of pp70-S6 kinase and proliferation in mouse mast cells." Eur J Immunol **23**(12): 3286-3291.

Tumbar, T., G. Guasch, V. Greco, C. Blanpain, W. E. Lowry, M. Rendl and E. Fuchs (2004). "Defining the epithelial stem cell niche in skin." Science **303**(5656): 359-363.

van der Poel, H. G. (2004). "Mammalian target of rapamycin and 3-phosphatidylinositol 3-kinase pathway inhibition enhances growth inhibition of transforming growth factor-beta1 in prostate cancer cells." J Urol **172**(4 Pt 1): 1333-1337.

Van Hoof, D., J. Munoz, S. R. Braam, M. W. Pinkse, R. Linding, A. J. Heck, C. L.

doi:10.6342/NTU201800580

Mummery and J. Krijgsveld (2009). "Phosphorylation dynamics during early differentiation of human embryonic stem cells." Cell Stem Cell **5**(2): 214-226.

Van Mater, D., F. T. Kolligs, A. A. Dlugosz and E. R. Fearon (2003). "Transient activation of beta -catenin signaling in cutaneous keratinocytes is sufficient to trigger the active growth phase of the hair cycle in mice." Genes Dev **17**(10): 1219-1224.

Vanhoutteghem, A., B. Delhomme, F. Herve, I. Nondier, J. M. Petit, M. Araki, K. Araki and P. Djian (2016). "The importance of basonuclin 2 in adult mice and its relation to basonuclin 1." Mech Dev **140**: 53-73.

Vanscott, E. J., T. M. Ekel and R. Auerbach (1963). "Determinants of Rate and Kinetics of Cell Division in Scalp Hair." J Invest Dermatol **41**: 269-273.

Vignard, J., G. Mirey and B. Salles (2013). "Ionizing-radiation induced DNA double-strand breaks: a direct and indirect lighting up." Radiother Oncol **108**(3): 362-369.

Wagers, A. J. and I. L. Weissman (2004). "Plasticity of adult stem cells." Cell **116**(5): 639-648.

Wang, W., X. Li, M. Lee, S. Jun, K. E. Aziz, L. Feng, M. K. Tran, N. Li, P. D. McCrea, J. I. Park and J. Chen (2015). "FOXKs promote Wnt/beta-catenin signaling by translocating DVL into the nucleus." Dev Cell **32**(6): 707-718.

doi:10.6342/NTU201800580

Wilanowski, T., J. Caddy, S. B. Ting, N. R. Hislop, L. Cerruti, A. Auden, L. L. Zhao, S. Asquith, S. Ellis, R. Sinclair, J. M. Cunningham and S. M. Jane (2008). "Perturbed desmosomal cadherin expression in grainy head-like 1-null mice." EMBO J **27**(6): 886-897.

Wu, X., Q. T. Shen, D. S. Oristian, C. P. Lu, Q. Zheng, H. W. Wang and E. Fuchs (2011). "Skin stem cells orchestrate directional migration by regulating microtubule-ACF7 connections through GSK3beta." Cell **144**(3): 341-352.

Xu, L., Y. G. Chen and J. Massague (2000). "The nuclear import function of Smad2 is masked by SARA and unmasked by TGFbeta-dependent phosphorylation." Nat Cell Biol **2**(8): 559-562.

Xue, Y., J. Ren, X. Gao, C. Jin, L. Wen and X. Yao (2008). "GPS 2.0, a tool to predict kinase-specific phosphorylation sites in hierarchy." Mol Cell Proteomics **7**(9): 1598-1608.

Zhang, H., H. A. Pasolli and E. Fuchs (2011). "Yes-associated protein (YAP) transcriptional coactivator functions in balancing growth and differentiation in skin." Proc Natl Acad Sci U S A **108**(6): 2270-2275.

Zhu, K., C. Xu, M. Liu and J. Zhang (2017). "Hairless controls hair fate decision via Wnt/beta-catenin signaling." Biochem Biophys Res Commun **491**(3): 567-570.

doi:10.6342/NTU201800580

Zuckermann, A., E. Osorio-Jamillio and A. Z. Aliabadi-Zuckermann (2018). "mTOR Inhibition and Clinical Transplantation: Heart." Transplantation **102**(2S Suppl 1): S27-S29.

doi:10.6342/NTU201800580